DEVELOPMENT OF COMPACT PULSED POWER SYSTEM AND STUDY ITS PERFORMANCE

By

Surender Kumar Sharma

Enrolment No: ENGG01200904045

Bhabha Atomic Research Centre, India

A thesis submitted to the

Board of Studies in Engineering Sciences

In partial fulfillment of requirements

For the Degree of

DOCTOR OF PHILOSOPHY

of

HOMI BHABHA NATIONAL INSTITUTE

January, 2014

Homi Bhabha National Institute

Recommendations of the Viva Voce Board

As members of the Viva Voce Board, we certify that we have read the dissertation prepared by **Surender Kumar Sharma** entitled "Development of compact pulsed power system and study its performance" and recommend that it may be accepted as fulfilling the dissertation requirement for the Degree of Doctor of Philosophy.

Manmohan Singh **Date:** 16/1/14

Chairman: **Prof. M. S. Bhatia**

Archana **Date:** 16/1/14

Guide / Convener: **Prof. Archana Sharma**

Anurag Shyam **Date:** 16/1/14

Technical Advisor: **Prof. Anurag Shyam**

Badodkar **Date:** 16.1.2014.

Member: **Prof. D. N. Badodkar**

Date: 16/01/2014

Examiner: **Prof. T.C. Kaushik**

K.V. Nagesh **Date:** 16/1/2014

Examiner: **Dr. K. V. Nagesh**

Final approval and acceptance of this dissertation is contingent upon the candidate's submission of the final copies of the dissertation to HBNI.

I hereby certify that I have read this dissertation prepared under my direction and recommend that it may be accepted as fulfilling the dissertation requirement.

Archana

Date: 16/01/2014 **Prof. Archana Sharma**

Place: Mumbai **(Guide)**

CERTIFICATE

I, hereby declare that the queries raised by the examiners of the thesis have been incorporated as suggested.

Archana

(Prof. Archana Sharma)

(Guide)

STATEMENT BY AUTHOR

This dissertation has been submitted in partial fulfilment of requirements for an advanced degree at Homi Bhabha National Institute (HBNI) and is deposited in the Library to be made available to borrowers under rules of the HBNI.

Brief quotations from this dissertation are allowable without special permission, provided that accurate acknowledgement of source is made. Requests for permission for extended quotation from or reproduction of this manuscript in whole or in part may be granted by the Competent Authority of HBNI when in his or her judgment the proposed use of the material is in the interests of scholarship. In all other instances, however, permission must be obtained from the author.

Surender

Surender Kumar Sharma

DECLARATION

I hereby declare that the investigation presented in this thesis has been carried out by me. The work is original and has not been submitted earlier as a whole or in part for a degree/diploma at this or any other Institution or University.

Surender

Surender Kumar Sharma

DEDICATIONS

I dedicate this thesis to

My father

Late Shri Jagdish Prasad Sharma

ACKNOWLEDGEMENTS

I express my sincere gratitude to my guide, Prof. Archana Sharma and technical advisor, Prof. Anurag Shyam for their valuable support and guidance. Their persistent encouragement, motivation and valuable technical input have benefited me a lot. I am also thankful to Shri G. P Srivastava, Ex- Director, E&I Group, BARC, Mumbai for his support and encouragement. I take this opportunity to thank Shri. S. Bhattacharya, Ex AD (T) E&I Group, BARC, Mumbai for motivation and support during the early phase of my PhD work.

I am grateful to Prof. M.S Bhatia and Prof. D. N. Bododkar for their advice and monitoring the yearly progress of the research work. I thank Prof. B. K Dutta, Dean-Academic, BARC for the words of support and advice. I also thank Shri P. Lahri, Regional Director, Vizag for his continuous support and encouragement. I would like to acknowledge the support and company of my colleagues Pankaj Deb, Rohit Shukla, Partha Banerjee, Prabaharan, Biswajit Adhikary, Dr. Rajesh Kumar and Dr. Rishi Verma for brilliant support during different stages of the research work.

I am grateful to my father, Late Shri Jagdish Prasad Sharma and my mother, Smt. Amrit Sharma for their relentless support, love and encouragement. They have always been a constant source of inspiration to me. I am also thankful to my wife, Dr. Shveta Sharma my son, Chaitanya and my daughter, Sameeksha for the inspiration, belief and being very supportive, without that I could not have done this work. In addition I express my gratitude to all persons who have not been listed here but helped to complete this work.

Surender Kumar Sharma

CONTENTS

ABSTRACT

Nowadays, compact pulsed power technology that is robust and repetitive is driven by size, weight and volume constraints in recent times. In both the military and commercial applications, there is an overwhelming need to provide more and more capability in ever smaller and lighter packages. Certain applications require technology that can be deployed in smaller volume under stressful environments. The need for higher energy densities, power densities and efficiency is the driving force in this field. Remarkable advances in high energy density materials for capacitor development and new solid-state high power devices have enabled pulsed power systems to achieve reduction in size and weight. The research issues are still open on studying and utilizing new materials-dielectrics, insulators, metals, and interface in the design of sub-systems of the compact pulsed power systems. This development requires combined efforts at three levels: efficient and robust devices at component levels, novel circuits and architecture at the system level, and effective technique to deliver fast pulses at the application levels. Fundamental studies on compact pulse forming lines with high dielectric constant ceramics and alternative engineering topologies are investigated in the thesis. The research focus was on the studies on development of compact pulse forming lines using composite mixture of high dielectric constant ceramics such as barium titanate, and also investigating new engineering topologies using helical inner conductor to reduce the size of the pulse forming line that is used as intermediate energy storage in pulsed power system. This thesis describes the development of compact pulsed power system and its performance. The transmission line characteristics of the pulse forming line, which generates longer duration rectangular pulses, is also investigated and a novel technique for fast repetitive double pulse generation with very short inter pulse interval is also described.

SYNOPSIS

Pulsed power is a technology to compress the energy and release it in shorter duration of time to generate peak instantaneous power levels. The roots of pulsed power can be traced to the development of high voltage technology prior to World War II for use in radar. Nowadays the pulsed power field is driven by size, weight, and volume constraints; there is an overwhelming need to provide more and more capability in ever smaller and lighter packages. Our appetite for small, lightweight devices extends well beyond the domestic purposes to include defense, industry, medicine and research. The demand is increasing for compact pulsed power to serve ever smaller applications with lightweight power sources and the response has been a sustained trend toward compactness. The interest in the compactness is not limited to achievement of a minimum size and weight but rather the investigation of a system that has lesser components than its predecessor. New compact pulse forming lines were developed during the research using solid composite dielectric and novel system engineering techniques discussed in the thesis. The fast repetitive pulsed power system has limitation due to switches, power supplies and load characteristics, During the research on pulse forming line it was found that the transmission line characteristics of the pulse forming line can also be used to generate fast double pulse with extremely short repetition interval and is discussed in the thesis.

The recent advancements in high energy density capacitors and high power solid-state devices have enabled pulsed power systems to achieve considerable reduction in size. Fundamental studies on pulsed power component development, new material and novel engineering techniques to reduce the size and mass of the pulsed power components are needed to be investigated. An effective research effort in any of these component systems will require a combination of theory, experiment and modelling. This area of research focuses on the primary and intermediate energy storage system, modelling of high voltage generator for compact geometry, investigation of novel pulse forming techniques using solid and liquid dielectric for pulse compression. The transmission line circuits offer the possibility of realizing fast rectangular pulses while connecting energy storage elements to loads. For making compact systems, new dynamic strategies are needed besides compaction of individual elements. This aspect was the main motivation of this thesis. For this goal, focus was on new pulse compression techniques. Combined research efforts were required at component levels, system architecture and application level to develop compact pulsed power technology.

Ferroelectric materials such as barium titanate possess high degrees of functionality, with highly exploitable electrical, mechanical and optical properties. As the most studied ferroelectrics are transition metal oxides with perovskite crystal structure their integration into heterostructure devices with other transition metal oxides with different but equally exciting properties (magnetism and superconductivity) is a direction that shows enormous potential for both exciting physics and breakthrough devices.

Coaxial pulse forming lines are widely used for pulse compression in pulsed power system. The research effort also includes investigation of alternative engineering topologies by using helical inner conductor for longer duration pulse generation in compact geometry. Water is also extensively used for pulse compression in pulsed power system. The effect of reduction in temperature of water on the pulse width looked promising and was investigated for developing compact systems. Finally, fast repetitive systems have limitation due to circuit inductance and capacitance, power supplies, and switch. Investigation and study in this area was also planned and done, leading to development of fast repetitive pulses using the transmission line characteristic of the pulse forming line. With all these inclusions, compact pulsed power system was developed, sub systems analyzed and performance evaluated on the matched load.

The work reported in this thesis is aimed towards the development of subsystems of the pulsed power system for the compact geometry. The research involves solving the engineering problems related to design of system components, their characteristics and then assembly of the complete system. The modelling of the sub system was also done for the optimization of the subsystem system and the validation of the experimental finding using simulation software.

Chapter 1 is the introduction to this thesis, with pulsed power system description and its applications. The research area on developing compact pulse forming line was defined based on the review of available literature. The detailed in-depth literature survey led us to focus on the following problems:

1. Ceramic has very high relative permittivity but it is not widely used in pulsed power technology due to its piezoelectric properties, so a composite dielectric with high permittivity ceramic material such as barium titanate was chosen and investigated for intermediate energy storage for pulse compression. This increased the system capacitance thereby realizing the possibility of operating at reduced system volumes. The study of non linear effect of electric field on the relative permittivity of the composite dielectric was also chosen for experimental investigation.

2. The compactness in system architecture level using alternative engineering technique of helical inner conductor inside water coaxial pulse forming line was investigated for the generation of longer duration rectangular pulse in compact size.

3. Deionised water is extensively used as intermediate energy storage for pulse compression in pulsed power system. The effect of reduction in water temperature inside the pulse forming line, on the pulse width was identified for investigation.

4. With all these subsystem developments, a compact pulsed power system was developed and its testing and performance evaluated on the matched load.

5. The transmission line characteristics of pulse forming line, which is used for generation of longer duration rectangular pulses, was also investigated for the development of fast repetitive pulse system using novel system architecture techniques.

During the course of the research, compact pulse forming lines were developed using ceramic material which has higher capacitance, high energy density and reduced volume. The relative permittivity of the medium plays very important role to increase the capacitance and energy density to make compact system so this aspect was studied. The increase in relative permittivity was also found by reducing the temperature of the water which is used for pulse compression. The alternative engineering topology developed using helical inner conductor to increase the transit time in smaller length of the pulse forming line was shown to achieve compaction. A novel technique was also developed using the transmission line characteristics of the helical pulse forming line to generate very fast repetitive pulses with very small repetition interval. It overcomes the limitations caused by the circuit inductance and capacitances, power supplies and the switch. Thus the goals set for were effectively met through design, development and testing stages.

Chapter 2 presents the detailed literature survey and description of important research issues for the development of compact pulsed power system. The development of compact pulsed power technology requires combined efforts at three levels: efficient and robust devices at component levels, novel circuits and architecture at the system level, and effective technique to deliver fast pulses at the application levels. Capacitors continue to be major components of pulsed power systems, especially as primary energy storage and pulse discharge devices. Capacitors are frequently a limiting factor for pulse power technologist in terms of size, cost, lifetime and reliability. On-going research and development at international level in capacitor technology and dielectric materials has resulted in significant expansion in several dimensions of the film capacitor operating envelope. Pulse generators are frequently used for pulse charging of the pulse forming lines. Pulse transformer driven circuits are designed to operate as Tesla or double resonance circuit has an added advantages over Marx generator due to its compact size, low input voltage on primary side, low driving energy requirement, Only one single switch for energy transfer and capacity to run on high repetition rates is necessary. The pulse transformers that are used in the microsecond range cannot be used for the transformation of high-voltage pulses of nanosecond duration because of higher inductances and capacitances so the pulse forming lines are required. The pulse forming line uses solid, liquid or other medium for pulse compression. The high voltage breakdown research issues in these dielectrics are discussed. Finally, the switch is an important component for pulse shaping and delivery of the peak power to the load. The limitations in inductance, rise time and repetitive operation of these switches are also discussed.

Chapter 3 describes the details of the experimental set up, its subsystem development and the diagnostics used in the experiments. The experimental set up consists of an in-house developed 25 kV high voltage power supply, which charges the primary energy storage capacitor bank. The capacitor bank discharges into the primary of pulse transformer through a triggered sparkgap switch. The high voltage generated across the secondary of the pulse transformer charges the pulse forming, which then discharges to load through a self breakdown sparkgap switch. A compact conical high voltage pulse transformer was modelled, designed and developed for the pulse charging of pulse forming line. A tapered construction (with the larger diameter at the bottom) was used for the secondary coil. A tapered construction was used for the secondary coils to avoid any break-down at the high voltage end of the secondary winding. The high voltage will appear at the upper end and the greater space around the high voltage terminal will prevent the possibility of any high-voltage break down. The secondary winding was placed inside the delrin mandrel used to support the primary winding. The diameter and the length of the pulse transformer are 240mm and 300mm. The pulse transformer charges the pulse forming line up to 200 kV. The design and development of compact pulse forming lines are discussed in chapter 4. The sparkgap switch was also designed and developed for pulse sharpening and delivering peak power to the load. The inductance and rise time of the switch was 20 nH and 14 ns respectively. The diagnostics used for the measurements of voltages with high voltage probes and oscilloscope, Measurements of circuit parameters such as inductances and capacitance with LCR meter is also discussed.

Chapter 4 describes the design and development of compact pulse forming lines. The research and investigation on development of high permittivity materials is one area which can help in designing compact systems. The ceramic material was investigated for developing compact pulse forming lines. Ceramic dielectric material has very high relative permittivity so it could be used for making compact pulse forming lines. Ceramic dielectric material has not been widely studied for pulsed power applications as they have piezoelectric effects and hence stresses are developed at high electric fields. The composite dielectric was made using ceramic materials which have relatively higher permittivity. Barium Titanate ($BaTiO_3$) has high relative permittivity (~1200) and also it has piezoelectric effect. During high voltages discharges local stresses are developed which breaks the material. To overcome these stress we have made a composite mixture of barium titanate and neoprene rubber as rubber was an elastic material and experimentally investigated it. When local stresses are developed in barium titanate due to its piezoelectric properties the rubber will expand and contract to absorb the stress and regain its original shape after the discharges. A Coaxial pulse forming line of inner diameter 120 mm, outer diameter 240 mm was designed and studied. The volume between the two cylinders was filled with composite mixture of barium titanate and neoprene rubber. The composite mixture was prepared by mixing barium titanate of 1-3 micron size with neoprene rubber in the ratio of 1:10. The mixing ratio of 1:10 was taken as at higher ratio it increases the quantity of Barium titanate so the piezo-electric effect will dominate and at lower ratio it will not show significant compactness. Other additives Magnesium oxide (MgO), Zinc Oxide (ZnO), Steric acid & mineral oil in traces are added for the curing of rubber.

Water coaxial pulse forming lines are widely studied and used for pulse compression in pulsed power systems. The novel engineering techniques using helical inner conductor was investigated for making compact pulse forming line. The helical transmission line has higher inductance as compared to coaxial transmission lines. The increase in inductance will increase the transit time, which increases the pulse width across the load. A compact pulse forming line was also designed and developed using helical inner conductor for pulse compression. The helical pulse forming line inner conductor was made of SS-304 strip rolled on delrin cylinder and outer conductor was made of SS-304 cylinder. The length of the pulse forming line was 800 mm. The conductor inner strip was 0.5 mm thick and 39.5 mm wide rolled on the 168 mm delrin cylinder. 13 turns are wounded on delrin cylinder and the inter turn gap was 20.5 mm. The outer cylinder was 2mm thick and has internal diameter of 232 mm. The volume between the inner strip and outer cylinder was filled with deionised water circulated through a pump and deionizer unit. The conductivity of the deionised water was less than 0.2 µSemen/cm.

Chapter 5 describes the experimental testing and studies in compact pulse forming lines. The composite dielectric break down strength and its relative permittivity was experimentally calculated. The composite dielectric pulse forming line was pulse charged to 120 kV and a voltage pulse of 70 kV, pulse width of 21 ns has been measured across 5 Ω load. The relative permittivity of the ceramic material changes with applied electric field. The effect of electric field on composite mixture was experimentally investigated up to 25 kV/cm and found no significant change in the pulse width measure across the load. The composite dielectric has successfully withstood voltages up to 35 kV/cm. It was found that the compactness in the pulse forming line was achieved by mixing of barium titanate in neoprene rubber which reduces the length of the pulse forming line by a factor of 3.8. The pulse forming line was charged and discharged for few shots (~10) and no significant effect into its performance degradation was seen. It was found that the pulse forming line using barium titanate and neoprene rubber was compact in size and does not require maintenance compared to oil, water line as it was of all solid material.

The performance of water based helical pulse forming line was also evaluated. The helical pulse forming line was charged to 200 kV peak using a pulse transformer in 3.5 μs and discharged into the matched 22 Ω resistive load through a self breakdown pressurized sparkgap switch. The flat top rectangular voltage pulse of 100 kV, 260 ns (FWHM) was measured across the load. The electric field and potential distribution inside the helical pulse forming line was also simulated. The circuit simulation modelling of the system was done to validate the experimental results. The effective reduction in length by a factor of 5.5 as compared to coaxial pulse forming line was seen. The effect of reduction in water temperature on pulse width was also investigated. The deionised water was circulated through water chilling unit and the pulse width across the load was experimentally measured from the water temperature range of 5 ^{0}C to 25 ^{0}C. It was found that the relative permittivity of the water increases with the reduction in the temperature of the water. We could find from the experimental investigation that the pulse width generated across the load increases up to 6% more when the temperature of the water was reduced from 25 ^{0}C to 5 ^{0}C. It was concluded that the length of the pulse forming line can further be reduced with the circulation of cold water inside the pulse forming line.

Chapter 6 describes the novel engineering technique for fast double pulse generation using the transmission line characteristics of the pulse forming line. The transmission line characteristic of the pulse forming lines was investigated for generation of fast double pulses with extremely short repetition interval for compact pulsed power repetitive system. The water helical pulse forming line was used as it was investigated that it can generate longer duration pulse in smaller length. The initial two turn of the helical pulse forming line are wound with ethylene propylene rubber tape (ε_r ~ 3). The helical pulse forming line was charged to 200 kV peak and discharged through sparkgap switch in to 22 Ω resistive load and this generated the double pulse of 100 kV, 100ns with an interval of 30 ns. The electrostatic modelling of the input side of the helical pulse forming line was done and it was found that when the pulse forming line was charged to 200 kV, the maximum potential appears across the ethylene propylene rubber and above that the water capacitor is charged to lesser extent, after the two turns the water capacitor was fully charged, so while discharging the pulse forming line generates two flat top rectangular pulses of 100 kV, 100 ns duration with the 30 ns interval between the pulses. It was further investigated that the system can generate two flat top rectangular pulses of desired pulse width and of the desired interval between the pulses. The pulse width and the interval between the pulses depend on the length of the ethylene propylene rubber wound on the inner conductor of the pulse forming line.

Chapter 7 Summarises the findings and proposes lines of future work that will be of important to this technology.

The following is the summary of the work reported in the thesis.

1. The composite dielectric with ceramic has higher dielectric constant and it can increase system capacitance with the possibility of operating at reduced system volumes for few shot applications. Compact PFL was developed using composite material of barium

titanate and neoprene rubber and tested up to 120 kV. It was also found that the dielectric constant of the composite mixture remains unchanged under high electric field (< 20 kV/cm).

2. An alternative technique was investigated and developed using helical inner conductor inside the PFL. The helical conductor increases the transit time, so longer duration pulse can be generated in compact geometry. A 200 kV, 0.5 GW, 260 ns pulsed power system was designed and developed using helical PFL and was tested on matched load.

3. It was found that higher energy can be stored and more compact systems can be developed using chilled water circulation inside the PFL, it increase the pulse width by a factor of 6%, when the temperature of water was reduced from 25 ^{0}C to 5 ^{0}C .

4. A novel technique was developed using the transmission line characteristic of PFL and also using different dielectric constant material to store energy inside the PFL to generate fast repetitive double pulse with small repetition interval.

In many cases novel propositions along with experimental or theoretical modelling have been made for better understanding to solve the difficulties encountered for developing compact pulsed power subsystem. Further the research issues related to study of new materials-dielectrics, insulators, metals, and interfaces in the design of components of the compact pulsed power systems are enumerated. In the future the advanced component technologies can be applied to pulsed power problems using a suite of integrated design tools and micromachining techniques. New developments in materials research, combined with electrostatic design tools, will set a pathway for revolutionary advancements in compact pulsed power technology.

LIST OF ABBREAVIATIONS

BDV	Breakdown Voltage
CES	Capacitive Energy Storage
ESR	Equivalent Series Resistance
EMI	Electromagnetic Interference
FRDPS	Fast Repetitive Double Pulse System
FWHM	Full Width at Half Maximum
HPM	High Power Microwave
IES	Inductive Energy Storage
ITER	International Thermonuclear Experimental Reactor
KALI	Kilo Ampere Linear Injector
PFL	Pulse Forming Line
PFN	Pulse Forming Network
RF	Radio Frequency
SS	Stainless Steel
UWB	Ultra Wide Band

LIST OF SYMBOLS

c	Velocity of light	3 x 10^8 ms^{-1}
e	Charge on electron	1.6 x 10^{-19} C
ε_0	Permittivity of free space	8.85 x 10^{-12} C $V^{-1}m^{-1}$
ε_r	Relative permittivity of the medium	
ε_s	Static permittivity at zero frequency	
ε_∞	Relative permittivity at infinite frequency	
μ_0	Permeability of free space	4π x 10^{-7} H m^{-1}
μ_r	Relative permeability of the medium	
m_e	Electron mass	9.109 x 10^{-31} kg
1 eV	Energy in electron volts	1.6 x 10^{-19} Joule
n_e	Electron density	
w	Energy density	
π	3.14285	
α	Propagation constant	
β	Phase constant	
γ	Attenuation constant	
ρ_0	Load reflection coefficient	
τ	Pulse duration	
V_{pp}	Velocity of propagation	
Z_0	Characteristic impedance	
E	Electric field intensity kg m s^{-3} A^{-1}	
E_t	Tangential component of electric field intensity	
E_n	Normal component of electric field intensity	

E_b	Electric breakdown strength
R	Resistance (ohms)
L	Inductance (Henry)
C	Capacitance (Farad)
G	Conductance (S)
S_c	Closing switch
S_o	Opening switch
τ_c	Time constant of R-C circuit
τ_L	Time constant of L-R circuit
τ_d	Debye relaxation time
M	Mutual inductance (Henry)
k	Coupling coefficient

LIST OF FIGURES

LIST OF TABLES

LIST OF PUBLICATIONS

1. "Compact pulsed power driver for double pulse effect studies in nanosecond laser ablation"

   Surender Kumar Sharma, P. Deb, R. Kumar, Archana Sharma and A. Shyam

   IEEE Transaction on Plasma Sciences, Volume 41, Issue 10, 2609 (2013)

2. "Fast double pulse system using the transmission line characterises of the pulse forming line"

   Surender Kumar Sharma, P. Deb, Archana Sharma and A. Shyam

   Review of Scientific Instruments, Volume 83, 115108 (2012)

3. "Compact helical pulse forming line for longer duration rectangular pulse generation"

   Surender Kumar Sharma, P. Deb, Archana Sharma, R. Shukla, T. Prabaharan, B. Adhikary and A. Shyam

   Review of Scientific Instruments, Volume 83, 066103 (2012)

4. "Compact pulsed electron beam system for high power microwave generation"

   Surender Kumar Sharma, P. Deb, R. Shukla, P. Banerjee, T. Prabaharan, B. Adhikary, R. Verma, A. Sharma and A. Shyam

   Journal of Physics: Conference Series 390, 012035 (2012)

5. "Compact pulse forming line using barium titanate ceramic material"

   Surender Kumar Sharma, P Deb, R Shukla, T Prabaharan and A Shyam.

   Review of Scientific Instruments, Volume 82, 115102 (2011)

6. “Design and modelling of capacitor bank power supply for fast charging”

Surender Kumar Sharma, P Deb, R Shukla, P Banerjee, T Prabaharan, R Das, B Das, B Adhikary and A Shyam.

Journal of Korean Physical Society, Volume 59, No. 6, 3468 (2011)

7**.** “Explosive detection system using pulsed 14 MeV neutron source”

Surender Kumar Sharma, SC Jakhar, R Shukla, CVS Rao and A Shyam.

Fusion Engineering and Design Volume 85, pp 1562-1564 (2010)

8. “Compact electron beam accelerator using helical forming line for microwave generation”

S K Sharma, R Shukla, P Deb and A Shyam

Journal of Nepal Physical Society Volume 26 No 1, Pages 17-21 (2010)

CHAPTER 1

INTRODUCTION

1.1 Pulsed power

Pulsed power is a technology to compress the duration of time to generate peak instantaneous power levels. A natural source of pulsed power is clouds, which get electrically charged over a period of tens of minutes or even more due to several mechanisms inside the cloud. When the voltage due to charging (commonly negative at the cloud bottom) is adequately high, a discharge occurs to earth delivering a huge current and energy over a short duration (milli-seconds). The roots of pulsed power can be traced to the developments of high voltage technology and nuclear physics prior to World War II. Pulsed power itself was first developed during World War II for use in radar. A massive development program was undertaken to develop pulsed radar, requiring very short high power pulses. After the war, development in pulsed power technology continued for various other applications that led to the development of novel pulsed power machines [1-2]. In 2001, the U.S. Department of Defence initiated multidisciplinary university research initiative program to study fundamental issues for development of compact pulsed power for military applications [3]. Pulsed power generates very short electrical pulses (nanoseconds to milliseconds) with the possibilities of:

- Currents up to several hundreds of mega-amperes.
- Voltages up to several mega-volts.
- Energy releases up to several hundreds of terra-joules per second.
- Power densities of several hundreds of mega-watts per square centimeter
- Pressures of hundreds of kg/cm^2.
- Temperatures of millions of degrees Kelvin.

Pulsed power science and technology deals with physical and technical foundations for production and application of high voltages pulses with very high power (> 100 MW) and energies (> 1 kJ). Pulsed power is a broad technical field that is united by a common activity of the transformation of electrical energy in to high-peak power pulses. It is the technology of accumulating energy over a relatively longer duration of time and then releasing it in a shorter duration thus increasing the instantaneous power levels [4]. For example, 1 kJ of energy stored within a capacitor, and then released into a load over one second will deliver 1 kW of the peak power to the load. However, if all of the stored energy were released within one microsecond, the peak power would be 1 GW.

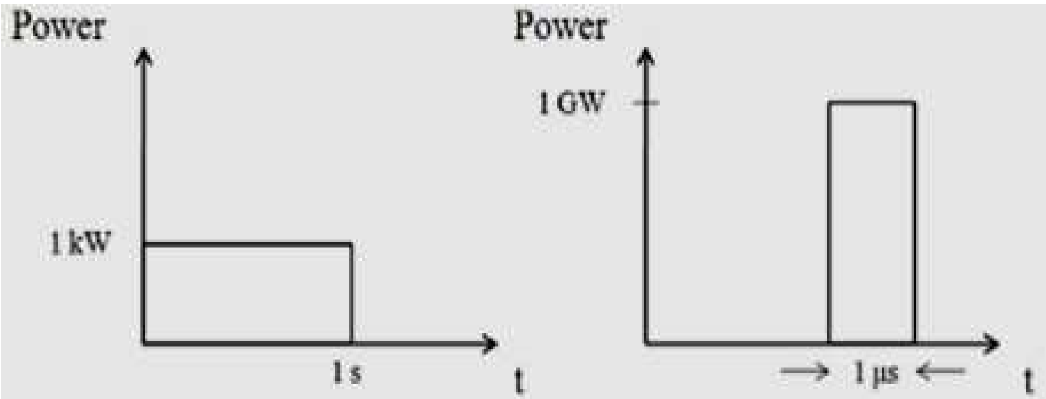

Figure 1.01 Low power-long pulse converted to high power-short pulse

A pulsed power system converts a low power-long time pulse to high power-short time pulse (Figure 1.01). The average power for pulsed power system is low to moderate (watts to kilowatts), however the peak power levels are very high (megawatts to terawatts), typically producing megavolts and megamperes, but for short times on the order of ~ 100 ns. The block diagram of a pulsed power system is shown in Figure 1.02. A pulsed power system is consists of low power accumulation subsystem which has a conventional primary energy source (ac. mains or batteries) that supplies the energy in longer duration of time to the energy storage system (capacitor, inductor). The high power accumulation subsystem has a high voltage generator (pulse transformer or Marx generator), pulse forming line and a switch, which shapes the pulse released from the energy storage element and transfer to the load. The loads in pulsed power system in initial days used to be particle beam diodes, imploding plasma and military applications (rail gun, HPM, UWB). Nowadays the loads include biological samples, drinking water, and effluent treatment plants. The pulsed power has evolved to not only play an important role in defence but has made inroads in environmental and biomedical applications.

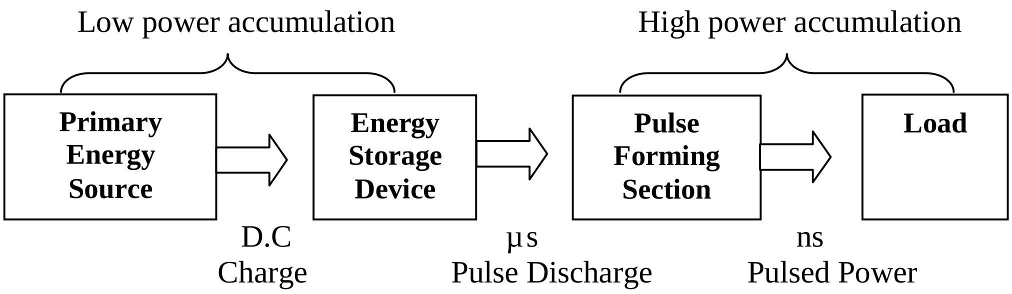

Figure 1.02 Block diagram of a pulsed power system

Pulsed power system is specified by the power levels delivered to the load, energy stored in the system, duration of the pulse, number of times the pulses are repeated and size of the energy storage medium etc. The typical ranges of electrical parameters frequently encountered in high power pulse system specifications are shown in Table 1.01

Energy	10 J – 100 MJ
Power	1 MW – 1 TW
Voltage	1 kV – 10 MV
Current	100 A – 10 MA
Pulse width	100ps - 100µs

Table 1.01 Typical ranges of electrical parameters of pulsed power system

The high power pulse is also characterized by its shape, *i.e.* rise time, fall time, duration and flatness of its plateau region. The overall duration of the high power pulses lies typically in between the range of sub-nanoseconds to microsecond's regime. The typical pulse shape parameters of a high power pulse are shown in Figure1.03.

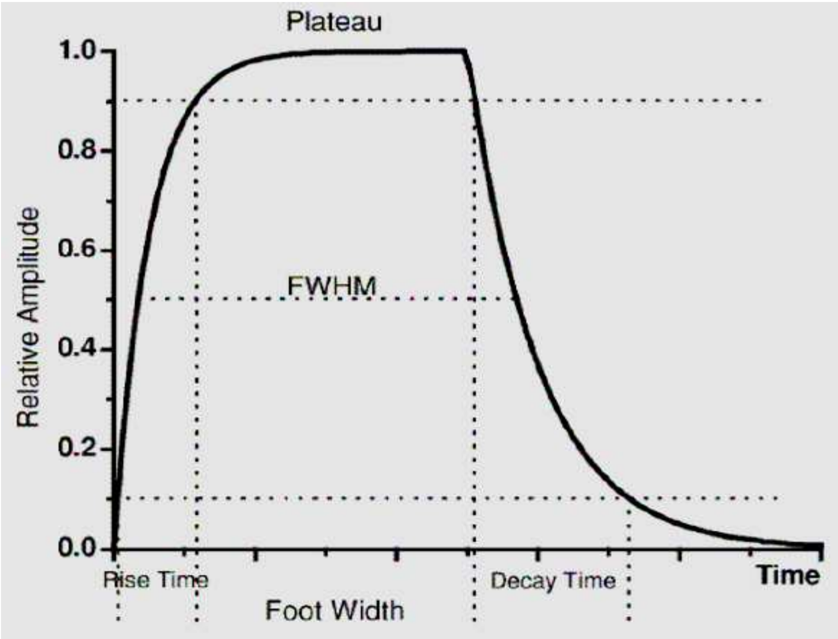

Figure 1.03 Typical pulse shape parameter [5]

The pulse rise time is the time taken by the voltage to rise from 10% to 90% of its peak amplitude. The fall, or decay, time in also defined in the similar way. Both the fall and the rise time of a pulse depend on the evolution of the load impedance, which in most cases varies with time. There is no unique definition of the pulse duration in the literature. Sometimes it is understood as the full width at half maximum (FWHM) of the pulse. However, for some applications, it is better to define it as the duration at 90% of the peak amplitude. Flatness of the plateau region is an important requirement for driving some loads for *e.g.* pockels cells and electron beam diodes [5].

1.2 Repetitive pulsed power

The technology for repetitive pulsed power was originally developed to support the defence program, As the technology matured, its potential use in industrial applications were explored based on its inherent strength of high average power, high repetition rate, cost efficient scaling with power for long life performance. The development of compact repetitive pulsed power system is the current trend in pulsed power technology to increase the average power output which has applications in defence and industrial areas. Fast repetitive double pulse with extremely short interval can also be used to study the double pulse effect in nanosecond laser ablation for the study of laser induced breakdown spectroscopy [6]. The trend in repetitive-pulse-power system design is toward higher energies, larger average power levels, and faster pulse-repetition rates. There is a great demand of repetitive pulsed power system, but there are few technical problems that need to be investigated and resolved. Switches are an important component of a pulsed power system and for its repetitive operation it is required to recover its insulation between the pulses. Compact repetitive pulsed power systems can be developed by enhancing the peak and average power output, by increasing the pulse repetition frequency (PRF) and reducing the equipment size to meet the demands of ever increasing applications. Improvements can be made in components and sub systems of the pulsed power system. Successful introduction of pulsed power technologies in industries depends to a great extent on the availability of highly efficient and reliable cost-effective sources. All these possibilities are under investigation in various laboratories worldwide. Pulsed power system using semiconductor devices have become more and more popular in industrial applications because of their compactness, light weight, repetition rate, low cost and high efficiency. Repetitive pulsed power technology has a lot of potential for future growth.

1.3 Application of pulsed power

Pulsed power technology enables the generation of extremely high temperatures, brilliant flashes of light and powerful bursts of sound. It accelerates particles to great velocities, produces tremendous forces, detects objects at a great distance, and creates many other extreme conditions that are not possible to sustain continuously. As a primarily enabling technology, pulsed power circuits are used in many cutting edge applications such as the generation of X-rays [7] and high power microwaves [8]. It is used in pulsed high power laser systems, and also the generation of shockwaves to dissolve kidney stones (lithotripsy) [9]. It is a unique way to generate dense plasmas in plasma focus [10], and also produces a burst of neutrons, which can be used for detection of explosives and illicit materials [11]. Pulsed power is also a key technology in the research on particle beam (KALI 5000) [12], inertial confinement fusion (Z-Machine) [13] and for magnetic confinement fusion (ITER) [14].

A growing interest in pulsed power technologies can also be found for industrial, medical, biological and environmental applications. Electro-mechanical forming and Electro-hydro forming are techniques for welding or cutting the materials at high velocity. In this technique the energy in the form of short pulse is concentrated on the work piece, which results in high temperature and softening locally in the material known as adiabatic softening. Energy can be applied to the work piece mechanically, hydraulically or electromagnetically. In hydraulic forming the work piece is placed between a press tool and a chamber that is filled with water (or liquid). Pressure is applied to the water in the chamber, which in turn presses the work piece against the press tool. When electro-hydraulic discharge is used, an underwater electric discharge creates a pressure shockwave that shapes the work piece by pressing it against the tool. The pressure in the shockwave is in the range of 1000 to 10000 kg/cm^2 [15]. By forming the material at very high velocity improves the ductility drastically, adiabatic heating is also advantageous for cutting where the work pieces are cut off by short impact and pieces are cut with high accuracy.

Pulsed electrical discharges can also be designed to create non-thermal plasma 'streamers'. This non-thermal plasma has the ability to attack biological and chemical agents and is in particular promising for decontamination and purification of water [16]. High electric pulse is used for the treatment of food [17]. Another emerging application is the manipulation of mammalian cells with pulsed electric fields [18-19]. One of the most appealing results so far is that they can trigger apoptosis in cancer cells and can be used to fight tumours. The use of streamers and pulsed electric fields on cells and tissues are cornerstones of a new era in biomedical engineering.

The recent advancement in pulsed power technology has made it possible to apply the technology to commercial and industrial environment. The *International Society on Pulsed Power Applications* was founded in Gelsenkirchen Germany in 1997, specifically to support the commercial side of pulsed power applications. The military application is particularly interested in compact, reliable pulsed power for radars, electromagnetic launchers, HPM generation and UWB generation.

1.4 Area of research

High-voltage rectangular pulses of very short duration (few 10’s of nanoseconds – few 100’s of microseconds) are required in many pulsed power applications. These short pulses give a peak power multiplication of more than 10^6 over the average power. The generation of high-voltage pulses is usually obtained until some tens kV by conventional circuits. These voltages achieve kA of discharge currents thereby enabling high peak powers mentioned above. The transmission line circuits offer the possibility of realizing fast rectangular pulses while connecting energy storage elements to loads. For making compact systems, new dynamic strategies are needed besides compaction of individual elements. This aspect was the main motivation driving this thesis and was investigated in detail. For this goal, focus was on new pulse compression techniques. Combined research efforts were required at component levels, system architecture level and application level to develop compact pulsed power technology.

For example, solid dielectric is generally considered to be non-recoverable in the event of dielectric breakdown but there are single shot pulse power applications where it is useful. This can increase system capacitance with the possibility of operating at increased energy levels or reduced system volumes. However solid insulation failure under pulsed conditions is not fully understood. The pulse compression system has a high voltage generator, pulse forming lines and a switch. The duration of pulse generated from the pulse forming lines depends on the length of the line, relative permittivity of the dielectric medium, temperature and stress on the dielectric medium. Conventional pulse forming lines are made up of plastic, castor oil or other dielectrics whose relative permittivity varies from 2-10. Ceramics offer very high relative permittivity. However, very little work existed in literature related to ceramic used in compact pulsed power applications as it is not widely used due to its piezoelectric properties. This thread was picked up by us.

Ferroelectric materials such as barium titanate possess high degrees of functionality, with highly useful electrical, mechanical and optical properties. As the most studied ferroelectric in transition metal oxides with perovskite crystal structure their integration into heterostructure devices with other transition metal oxides with different but equally exciting properties (magnetism and superconductivity) is a direction that shows enormous potential for both exciting physics and breakthrough devices.

Coaxial pulse forming lines are widely used for pulse compression in pulsed power system. The research effort also includes investigation of alternative engineering topologies by using helical inner conductor for longer duration pulse generation in compact geometry.

Water is also extensively used for pulse compression in pulsed power system. The effect of reduction in temperature of water on the pulse width looked promising and was investigated for developing compact systems.

Finally, fast repetitive pulsation has limitation due to circuit inductance and capacitance, power supplies,and switch. Investigation and study in this area was also planned and done leading to development of fast repetitive pulses using the transmission line characteristic of the pulse forming line.

With all these inclusions, compact pulsed power system was developed, sub systems analyzed and performance evaluated on the matched load.

To summarize, from the literature survey the issues that needed attention were identified. They were; new materials such as ceramics, and novel alternative engineering techniques to reduce the size and mass of pulsed power components and better topology. It was realized that an effective research effort in any of these component systems will require a combination of theory, experiment and modelling. The research efforts focused on investigation of new compact pulse forming lines using composite dielectric of high relative permittivity ceramic, and also using helical geometry conductor to study the performance for few 10's of nano-seconds to 100's of nano-seconds of pulse generation.

1.5 Aim and accomplishment of thesis

As described above, the overall research work was aimed towards the development of compact pulse systems. The research described here involves solving the component level and system architecture level problems to design the compact system, pulse forming lines, their realization, and characterization. The detailed in-depth literature survey led us to focus on the following problems:

1. Ceramic has very high relative permittivity but is not widely used in pulsed power technology due to its piezoelectric properties, so a composite dielectric with high permittivity ceramic material such as barium titanate was chosen and investigated for intermediate energy storage for pulse compression. This increased the system capacitance thereby realizing the possibility of operating at reduced system volumes. The study of non linear effect of electric field on the relative permittivity of the composite dielectric was also chosen for experimental investigation.
2. The compactness in system architecture level using alternative engineering technique of helical inner conductor inside water coaxial pulse forming line was investigated for the generation of longer duration rectangular pulse in compact size.
3. Deionised water is extensively used as intermediate energy storage for pulse compression in pulsed power system. The effect of reduction in water temperature inside the pulse forming line, on the pulse width was identified for investigation.
4. With all these subsystem developments, a compact pulsed power system was developed and its testing and performance evaluated on the matched load.
5. The transmission line characteristics of pulse forming line, which is used for generation of longer duration rectangular pulse, was also investigated for the development of fast repetitive pulse system using novel system architecture techniques.

During the course of research compact pulse forming lines were developed using ceramic material which has higher capacitance, high energy density and reduced volume. As relative permittivity of the medium plays very important role to increase the capacitance and energy density to make compact system this aspect was also studied. The increase in relative permittivity was also found by reducing the temperature of the water which is extensively used for pulse compression. The alternative engineering topology developed using helical inner conductor to increase the transit time in smaller length of the pulse forming line was shown to achieve compaction. During the research on pulse forming lines a novel technique was also developed using the transmission line characteristics of the helical pulse forming line to generate very fast repetitive pulses with very small repetition interval. It overcomes the limitations caused by the circuit inductance and capacitances, power supplies and the switch.

Thus the goals set for were effectively met through design, development and testing stages.

1.6 Outline of thesis

The thesis defines the progress on investigation and development of novel compact pulse forming line for intermediate energy store for pulse compression and its study for single pulse and repetitive pulse generation, the modelling of its sub-systems and development of compact pulsed power system with its evaluation. Chapter 1 is the introduction to this thesis, with description of the pulsed power system, repetitive pulsed power system and its application in defence and commercial areas. It also defines the broad area of the research and the overall aim of the thesis.

Chapter 2 is the literature update on compact pulsed power technology and summarizes the important issues for development of compact pulsed power system at component levels, system architecture level and application level. Energy storage for pulsed power systems using capacitive storage are also discussed as the state of the art for capacitor is relatively well developed. It also discusses the intermediate energy storage system for pulse compression using solid and liquid dielectrics. The switch used for pulse shaping is also discussed.

Chapter 3 describes the development of subsystems that are used for the study and testing of the compact pulse forming line. The design details and fabrication of the primary energy storage capacitor bank and its power supply, high voltage conical pulse transformer and pulse sharpening switch. The diagnostic equipments used in the testing of pulse forming lines are also discussed.

Chapter 4 describes the design and developments of compact pulse forming lines. The compact pulse forming lines can be developed by increasing the dielectric constant, and also the length of the pulse forming line. Two types of pulse forming lines were developed using solid composite dielectric and another one using helical inner conductor. The solid composite dielectric pulse forming line is made up of using composite mixture of barium titanate ceramic and neoprene rubber, which is used as intermediate energy storage system is presented. Another pulse forming line is designed and developed using helical inner conductor inside water coaxial pulse forming line for generation of longer duration rectangular pulse in compact geometry.

Chapter 5 describes the pulsed high voltage testing of solid composite dielectric pulse forming line. The relative permittivity of the composite mixture is calculated. We also report the experimental study on the non linear effect of electric field on the relative permittivity of composite mixture. The water helical pulse forming line is also pulse charged and tested with the matched load. The compactness achieved as compared to coaxial pulse forming line is reported. The effect of reduction in the temperature of deionised water inside the pulse forming line on the pulse width generated across the matched load is also reported. The discussion and analysis of the result for development of compact pulse forming line is also summarized.

Chapter 6 describes the novel technique for the development of fast repetitive double pulse system. The transmission line characteristic of the helical pulse forming line is used to generate fast repetitive double pulse with extremely small repetition interval. High voltage insulation rubber tape is placed on the outer surface of SS strip at the initial few turn of the inner helical conductor, while discharging it generates two fast pulses (~ 100 ns) with very small inter pulse repetitive interval (~10 ns).

Chapter 7 concludes the findings and proposes lines of future work that will be reflective of future attractions in this area.

CHAPTER – 2

LITERATURE SURVEY

2.1 Compact pulsed power

Compact pulsed power technologies are characterized by concentration of energy both in time and size to generate pulses of high intensity. Nowadays the pulsed power field is driven by size, weight, and volume constraints and certain applications require technology that can be deployed in smaller volume under stressful environments. In both the military and commercial applications, there is an overwhelming need to provide more and more capability in ever smaller and lighter packages [20]. The need for higher energy density, power density and efficiency is driving further progress in the field. The pulse conditioning system is an important part of pulsed power system, its general functions are the storage, switching, and scaling (Figure 2.01) [21].

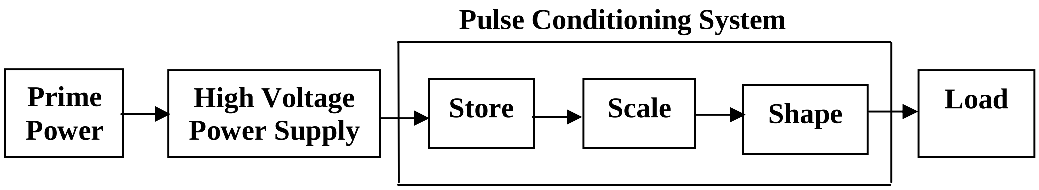

Figure 2.01 Basic pulsed power supply architecture

In order to minimize the weight and volume of the system, two types of system architectures are routinely considered. The first architecture is one that stores all the energy required for multiple pulses and then uses an opening and closing switch to transfer the energy to the load (Figure 2.02). This approach is the simplest in operation, but requires a much larger volume for the energy storage.

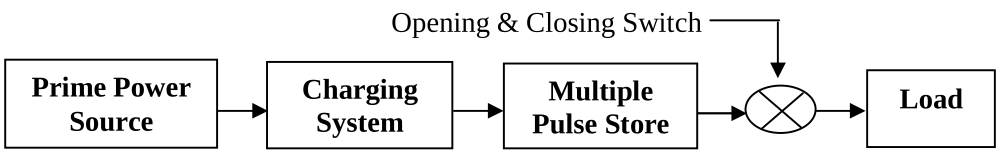

Figure 2.02 Multiple pulse store architecture

The second architecture is a single pulse storage system with repetitive charge system (Figure 2.03).

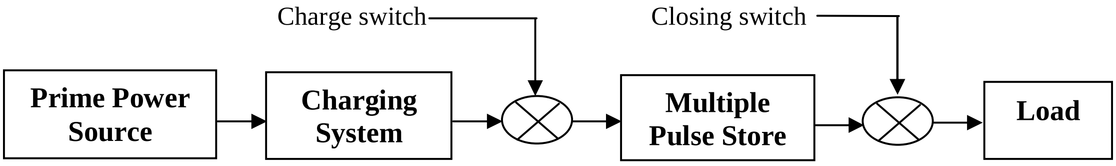

Figure 2.03 Single pulse storage with recharge

The single pulse system will provide the minimum energy storage volume, but requires increased complexity. The minimum system volume and thus weight will be one in which all the operations required to store, scale, and shape the load pulse are performed in the same volume as illustrated in Figure 2.04.

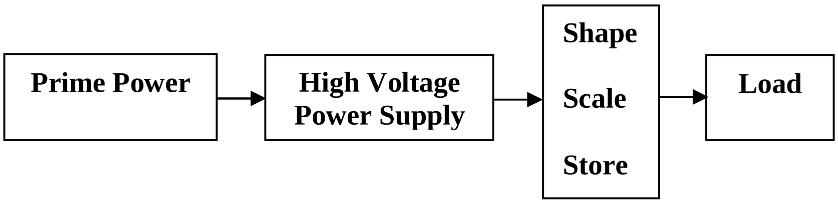

Figure 2.04 Ideal compact pulse power system

The pulsed power has expanded its capabilities in the later half of 20th centaury with the research and development in improved materials and electrical components with high energy and power densities. Multidisciplinary university research initiative program was also started in United States during the starting of 21st century to study the fundamental issues for development of compact pulsed power systems [3]. The recent advancements in high energy density components (capacitors, cores etc), and new solid-state devices have enabled pulsed power systems to undergo reduction in size and weight [22]. Modern electronic products depend on pulsed power to convert ac or battery power, as the pulsed converter become smaller, and occupy an ever smaller portion of the product volume. Computers that were once giants have now shrunk to pocket-size. Our appetite for small, lightweight, yet powerful devices extends well beyond the domestic purpose to include defence, industry, medicine, and research. The demand is increasing for pulsed power to serve ever smaller applications with reliable, efficient, lightweight power sources and the response has been a sustained trend toward compact pulsed power technologies. The compact pulsed power research is more application specific nature than an organized effort [23]. A compact pulsed power technologist absorbs advanced ideas and components from other efforts and knit them together into a unique system that may have little to do with the original component or its intended purpose. For example, a high power solid-state switch, developed for the traction industry, might be combined with a high energy density capacitor, developed for a small computer power supply, and the entire circuit powered by a long-life battery developed for a new generation of cellular phones. While the general demand for compact sources increases, the case by case development of a new source is typically achieved by raw innovation. Many historic examples of compact pulsed power are available in the literature. One such paper illustrates how a commercial switching system becomes smaller with each new generation [24], while others cite examples of compact components, such as capacitors [25], transformers [26], and pulse generators [27].

2.2 Research issues in compact pulsed power technology

The development of compact pulsed power technology requires combined efforts at three levels: efficient and robust devices at component levels, novel circuits and architecture at the system level, and effective technique to deliver fast pulses at the application levels. On-going research and development at international level in capacitor technology and dielectric materials has resulted in significant expansion in several dimensions of the film capacitor operating envelope. Research in high-voltage film capacitors has produced a self-healing feature that extends capacitor life under harsh pulsed power uses. The new dielectrics have produced new high energy density materials that enable capacitors to store more energy in ever smaller packages

[28-29]. The capacitor technology developments have enabled much higher energy densities to be reached over the last few years. This progress shows no indication of levelling off in the near future (Figure 2.05).

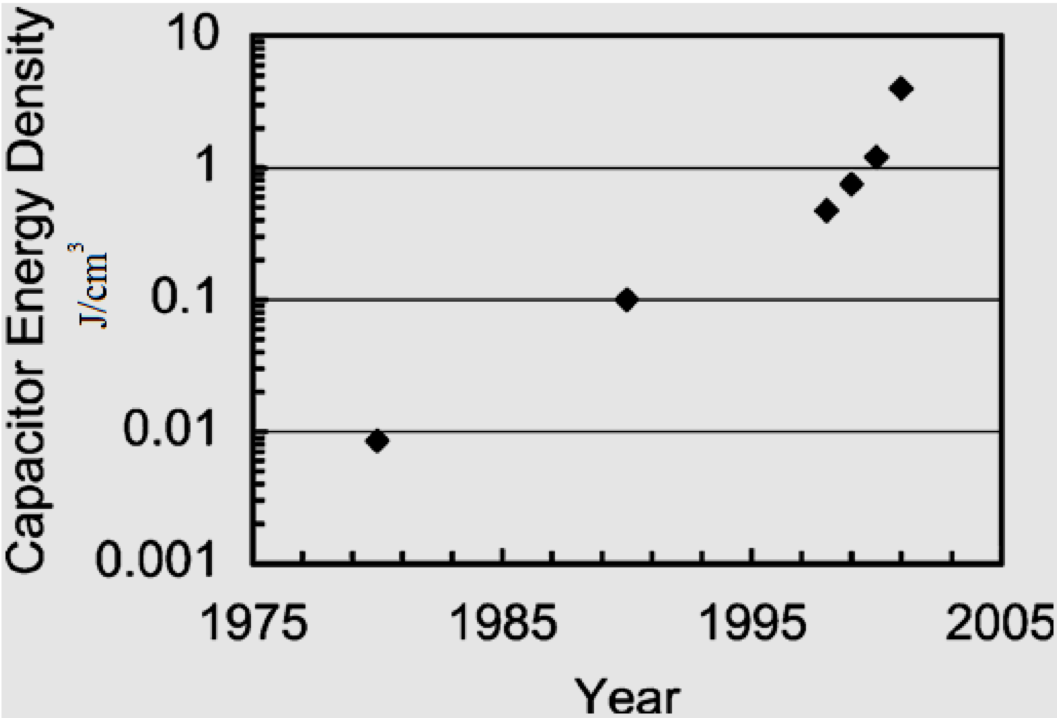

Figure 2.05 Progress in capacitor energy density versus time [23]

Advancement of capacitor construction methods and dielectric quality has resulted in improved stored energy density, pulse life, and DC life. W J Sergeant [30] has reported a review of capacitors used in pulsed power systems. The use of very thin metalized film electrodes is a significant improvement in capacitor construction technology. If an internal breakdown should occur, the metal film is vaporized at the fault site and thereby disconnects the problem area from the remaining capacitor [31].

Ceramic dielectric materials such as dense titania ceramic and nanocrystalline titanium oxide are developed and studied to make transmission lines with higher energy storage capabilities for compact pulsed power applications [32-33]. Very low impedance pulse forming lines can be made with ceramic materials for low impedance load such as z-pinches. From the literature survey it was found that the research on high voltage insulation material is one area which can help in designing very compact systems. This area of research also explores development of high relative permittivity material. But both of this will lead to material science research for the development of new materials. The other reliable solution will be to use the best of the material available in this field and continue development of compact systems. Ceramic materials very high relative permittivity and could be used for making compact pulsed power system but it is not much explored for designing pulsed power system due to its piezoelectric properties. The newer techniques for storing energy could be explored for making compact pulsed power system. Study of pulsed breakdown in liquid dielectric has received considerable attention in recent years due to great demands from pulsed power field for the development of liquid dielectric transmission lines. Liquids dielectric has played a major role as dielectric material in energy storage, pulse forming, and switching in the development of pulsed power technology. The switching utilizes liquid breakdown at high fields, thus going beyond just the insulating property of liquids. However, in energy storage and pulse forming breakdown is detrimental to the proper functioning of a pulsed power system. It is also obvious that the size of a pulsed power system has always been a concern, and the effort of making existing systems even more compact will have to deal with the higher electric fields that come with the inherently smaller distances of a compact system. Though an abundance of experimental data is available for breakdown in various insulating liquids, such as water, cyclohexane, and the noble gases, the basic physics of liquid breakdown has remained unclear. The two classic physical models are the crack propagation, which was recently transferred from solid breakdown, and the older bubble mechanism [34]. The main motivation for the development of liquid dielectrics for pulsed power applications is their structural compatibility with high power pulsed system. There are a large variety of liquids that can be used but for practical usage, mineral oil and water is widely used in pulsed power systems. Mineral oil has high dielectric strength and small dielectric constant so it is suitable for making low impedance systems. Water is attractive due to its high dielectric constant, high dielectric strength and efficient energy storage capability.

The longer duration rectangular pulse has also attracted more and more interest in the development of pulse power technology. In development of compact pulsed power system, a general research issue is to improve the system architecture. For example, study the geometry-driven issues in pulse forming line. A paper discussed the edge effect of the water blumlein for short pulse widths through computational modelling, and optimized the line design based on three dimensional simulations [35]. Another paper investigated the effects of folds on dielectric breakdown and the voltage waveform at the load in a folded blumlein [36]. Alternative topologies and novel engineering techniques should be investigated and the optimization of the geometry can be done using any electromagnetic software.

An important current trend also in pulsed power technology is the development of compact repetitive pulsed power systems, which have many important applications in defence and other industrial areas. The trend in repetitive-pulse-power system design is toward higher energies, larger average power levels, and faster pulse-repetition rates. There is a great demand of repetitive pulsed power system, but there are few technical problem needs to be investigated and resolved. Repetitive pulsed power generation by compact sources is being developed for industrial applications. Successful introduction of pulsed power technologies in industries depends to a great extent on the availability of highly efficient and reliable cost-effective sources. Compact repetitive pulsed power systems can be improved by enhancing the peak and average power output, increasing the pulse repetition frequency and reducing the equipment size to meet the demands of the increasing applications [37]. Improvements can be made in pulsed power system components. The electrical insulation and dielectric breakdown should be considered as the design criteria of an improved compact repetitive system.

Some issues of fundamental importance are needed to be investigated for compact pulsed power system developments such as new materials for high dielectric strength and high dielectric constant, exploring alternate engineering topologies for compact systems, improvements in switches etc. The research issues are still open on studying and utilizing new materials-dielectrics, insulators, metals, and interface in the design of components of the compact pulsed power systems. Fundamental studies on compact pulsed power system development with new materials and novel engineering techniques are needed to be investigated to reduce the size of the system. The energy density of pulsed power systems is often limited by the storage capabilities of the dielectric subsystem. Advances in pulsed power switches, capacitors, pulse forming line are necessary to develop compact, reliable electrical power on directed energy systems as well as space platforms for military applications. Research is also underway by to gauge the future of compact pulsed power by investigating the fundamental limits of dielectric materials and pulsed power components.

2.3 Primary energy storage system

The primary energy storage systems generally used are capacitive, inductive, chemical and inertial. Electrical energy is typically stored in capacitors as electric field and inductors as magnetic field. It can also be stored as mechanical energy in rotating wheel and flywheel, and in the form of chemical energy in batteries and explosives. Table 2.01 shows the salient features and comparison of these energy storage systems.

Primary energy storage device	Energy density (MJ/m^3)	Energy /Weight (J/Kg)	Typical transfer Time (Seconds)
Capacitors	0.01 – 1	300 – 500	microseconds
Explosives	6000	5 x 10^6	microseconds
Inductors	3 – 40	10^2 – 10^3	micro – milliseconds
Flywheel	400	10^4 - 10^5	seconds
Battery	2000	10^6	hundreds of seconds

Table 2.01 Comparison of energy storage systems

High explosives have the highest energy density and the shortest energy release times, but they are limited to single-shot operation and require auxiliary equipment to convert their chemical energy into electrical energy. A battery has a high energy storage density but a low power delivery capability, and requires both long charge and discharge times. Inertial storage has a high storage density and a moderate power output capability, and capacitors have the highest electrical discharge capability but they have a relatively low energy storage density. Releasing this stored energy over a very short interval to generate peak power by a process called energy compression. Electrical energy stored in a pulsed power system is released in the form of an intense high voltage and high power pulse or repetitive pulses. There has been rapid development in electrical pulsed power systems over the past few decades. Two different means of energy storage utilized in electrical pulsed power systems are capacitive energy storage (CES) and inductive energy storage (IES). The circuits of the inductive storage systems are duals of the corresponding capacitive storage systems (Figure 2.06). The CES has capacitor banks and closing switches while IES has inductive coils and opening switch. In IES the switch must carry the large coil current during the storage time, interrupt the current, and then withstand the high voltage generated by the coil current flowing through the load. The opening switch problem is difficult enough for single-shot operation in many applications [38]. There are two major obstacles to the practical use of inductive storage in pulsed power systems, both of which become obvious when the basic capacitive and inductive energy discharge circuits are compared.

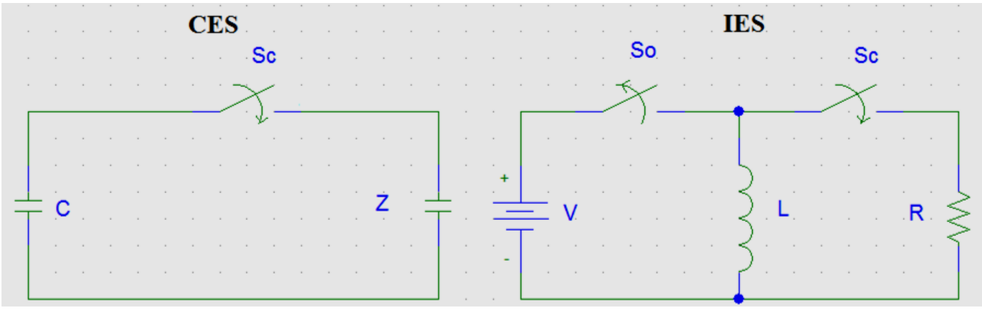

Figure 2.06 Comparison of CES and IES

In the capacitive energy discharge circuit (Figure 2.07) the capacitor C is charged through a resistor R to voltage V. The time constant for the self- discharge of the capacitor is $\tau_c = R_cC$ where R_c is the leakage resistance, may be of the order of tens of minutes. For such capacitors, the charging current can be kept fairly low. In a practical system the capacitor will typically be discharged into the load Z_L by means of the closing switch S_c. The discharge current is usually large compared to the charging current and a capacitive discharge circuit can be considered as a current amplifier.

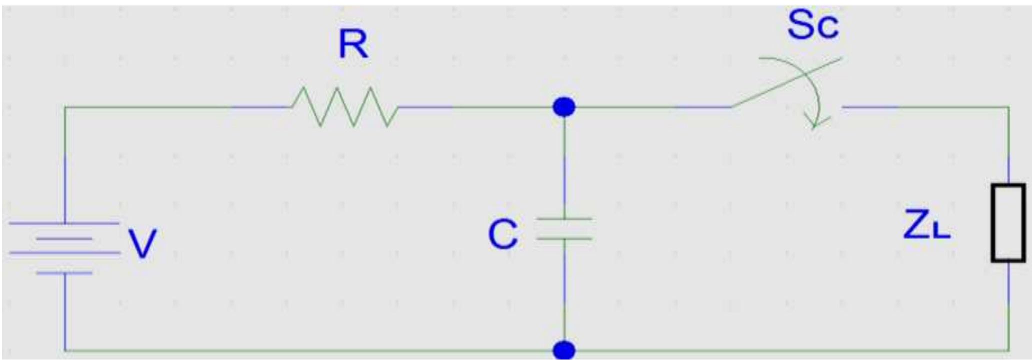

Figure 2.07 Capacitive energy discharge circuit

If dW_C/ dt is the rate of increase of stored energy in the capacitor and dW_R/dt is the rate at which energy is dissipated in the load, then during charging the capacitor we have

$$\frac{\frac{dW_c}{dt}}{\frac{dW_R}{dt}} = \frac{\frac{d}{dt}\left(\frac{1}{2}CV^2\right)}{\left(R\left(C\frac{dV}{dt}\right)^2\right)} = \frac{1}{RC\frac{1}{V}\frac{dV}{dt}} \tag{2.01}$$

Where R is in series with C and V is the voltage across C.

Suppose the capacitor C is charged by a constant current charger (I_t), such that, $V(t) = I_t/C$,

Then equation 2.01 can be written as,

$$\frac{\frac{dW_c}{dt}}{\frac{dW_R}{dt}} = \frac{T}{\tau_c} \tag{2.02}$$

Where T is the charging time of the capacitor and slow charging is best since this gives T >> τ_c and a low loss in the resistor R while the capacitor is charging.

In the inductive energy storage circuit (Figure 2.08), the inductor L is charged to a current I, and the time constant for the L-R circuit is τ_L = L/R, where R is the combined series resistance of the current source, the switch So and the inductor.

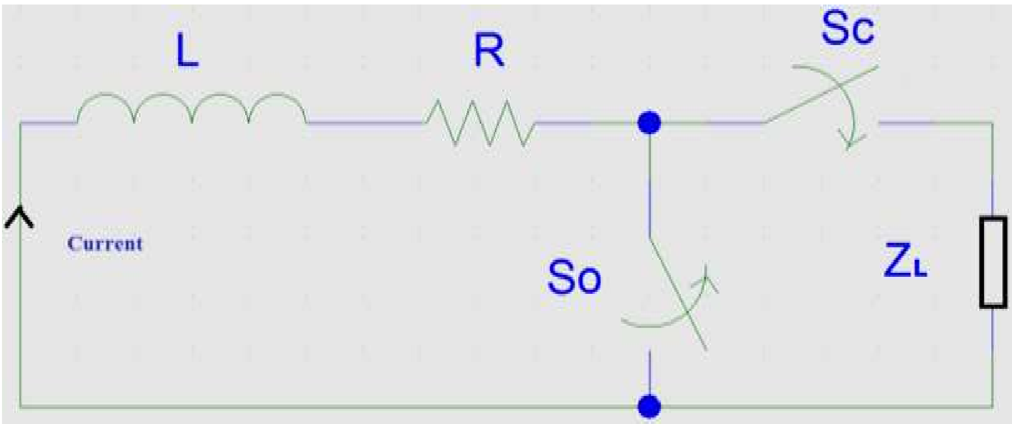

Figure 2.08 Inductive discharge circuit

For inductive energy storage systems, τ_L can be in the order of seconds, which means that inductors have to be charged in relatively short times, and high power primary sources are needed. The energy stored in the inductor is transferred to the load by means of an opening switch S_o, which interrupts the current (I) in the charging circuit and a closing switch S_c, which in turn connects to the load Z_L. Due to the rapid decrease of current, a high voltage of magnitude L(dl/dt) is induced across the opening switch and load, and inductive discharge circuits can, therefore, be considered as voltage amplifiers.

If dW_L/dt is the rate of stored energy in the inductor L and dW_R/dt is the rate at which energy is dissipated in the load the rate of energy in the magnetic field of the inductor, divided by the energy dissipated in the series resistance in the same time is

$$\frac{\frac{dW_L}{dt}}{\frac{dW_R}{dt}} = \frac{\frac{d}{dt}\left(\frac{1}{2}LI^2\right)}{(RI^2)} = \frac{L}{R}\frac{1}{i}\frac{di}{dt} \tag{2.03}$$

Now $di/dt = i/T$, where T is the charging time and $L/R = \tau_L$, the inductor time constant, So for a high charging efficiency, i.e a large $(dW_L/dt)/(dW_R/dt)$, one must ensure that τ_L/T is large, which means charging rapidly with respect to the inductor time constant. It is evident that the two major technical complexities encountered in inductive energy storage systems are the charging circuit, because of the necessary fast charging of the inductor, and the opening switch because of its in built complexities at the currents and voltage involved [39]. Energy storage for pulsed power systems commonly implies capacitive storage for which the state of the art is relatively well developed. The components of capacitor banks, including capacitors and switches, are commercially available and relatively inexpensive. We will be using capacitive energy storage system for primary energy storage in our project. It is very essential to study and investigate different type of capacitors and select best suitable capacitor to make a compact system.

2.31 Capacitors for pulsed power

The recent advancements in energy storage capacitor technologies have enabled reduction in size of pulsed power systems. R. A Cooper et. al. [40] has reported the progress in the reduction of inductance to 50 nH in energy storage capacitor. Improvement in polymer film quality and construction techniques has increased the energy densities [30]. Energy storage capacitors have been developed over a long time and a lot of them got their names from the material used as dielectric and the electrode type. The capacitors used for compact pulsed power application are shown in Figure 2.09. Dielectric is an important component in capacitors to store the electrical energy. Most of the dielectrics used nowadays are ceramics, plastic films, oxide layer on metal (aluminium, tantalum, niobium), natural materials (mica, glass, paper, air, vacuum). All of them store their electrical charge statically within an electric field. The important parameters of these dielectric used in capacitors are mentioned in Table 2.01

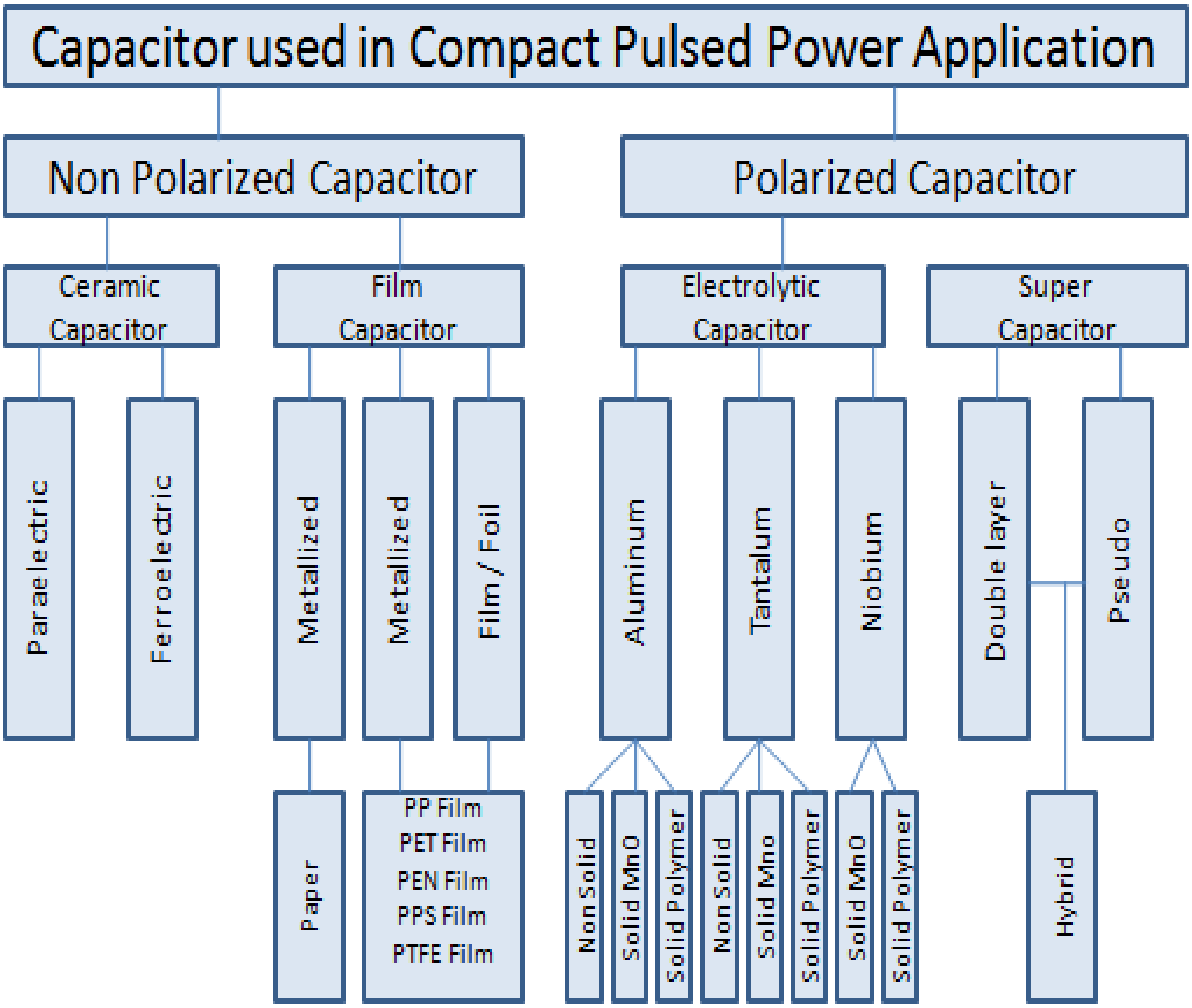

Figure 2.09 Capacitors used in compact pulsed power applications

Capacitor Type	Dielectric Material	Permittivity @ 1 kHz	Max dielectric strength(V/µm)	Min dielectric thickness (µm)
Ceramic	Paraelectric	12 – 40	< 100	1
Ceramic	Ferroelectric	200 - 14000	< 25	0.5
Film	Polypropylene	2.2	650	3.0
Film	Polyester	3.3	580	0.7
Film	Polyphenylene sulfide	3.0	470	1.2
Film	Polyethylene Naphthalate	3.0	500	0.9
Film	Polytetrafluroethylene	2.0	250	5.5
Paper	Paper	3.5 – 5.5	60	5 – 10
Aluminum	Aluminum oxide (Al_2O_3)	9.6	710	< 0.01
Tantalum	Tantalum pentoxide (Ta_2O_5)	26	625	< 0.01
Niobium	Niobium pentoxide (Nb_2O_5)	42	455	< 0.01
Mica	Mica	5 - 8	118	4 - 50

Table 2.02 Parameters of dielectric used in capacitor [41 - 43]

A ceramic capacitor is a non-polarized capacitor made up of ceramic material and metal in which the ceramic material acts as the dielectric and the metal as the electrodes. The ceramic material is composed out of a mixture of finely ground granules paraelectric or ferroelectric materials, modified by mixing oxides, which are necessary to achieve the capacitor’s desired characteristics. Paraelectric ceramic capacitor has high stability and low losses for temperature compensation in resonant circuit application. Ferroelectric ceramic capacitor has high volumetric efficiency for buffer, by-pass and coupling applications. Ceramic capacitor has high current limitations so they are not preferred for fast discharge applications.

Film capacitors are non polarized capacitors with an insulating plastic film as the dielectric. The dielectric films are drawn in a special process to an extremely thin thickness, provided with metallic electrodes and wound into a cylindrical shaped winding. The electrodes of film capacitors may be metalized aluminium or zinc applied to the surface of the plastic film.

Metalized film capacitors possess self-healing properties that is dielectric breakdowns between the electrodes are not leading to the destruction of the capacitor. The metalized type of construction makes it possible to produce wound capacitors with larger capacitance values (up to 100 µF and larger) in smaller cases than within the film/foil construction. Film/foil capacitors or metal foil capacitors are made of two plastic films as the dielectric each covered with a thin metal foil, mostly aluminium, as the electrodes. The advantage of this construction is the easy contractibility of the metal foil electrodes and the excellent current pulse strength. A key advantage of every film capacitor internal construction is direct contact to the electrodes on both ends of the winding. This contact keeps all current paths to the entire electrode very short. The setup behaves like a large number of individual capacitors connected in parallel, thus reducing the internal ohmic losses and the parasitic inductance. The inherent geometry of film capacitor structure results in very low ohmic losses and a very low parasitic inductance, which makes them especially suitable for applications with very high surge currents applications, or for applications at higher frequencies. The plastic films used as dielectric for film capacitors are Polypropylene, Polyester, Polyphenylene Sulphide, Polyethylene Naphthalate and Polytetrafluoroethylene or Teflon .

Kraft paper is impregnated with electrical grade castor oil or similar high dielectric constant fluid with extended foil plates. It is designed for intermittent duty, high current discharge application. The advantage of these capacitors is enhanced tolerance to voltage reversal and its disadvantages are lower energy densities and large size. Dry and oil filled constructions are available using a variety of dielectric materials- polypropylene, kraft and polyester with both foil and metalized electrodes. In recent times the high energy density achieved from metalized, segmented metalized paper and segmented metalized polypropylene has allowed designers to benefit from the higher energy density achieved from this construction.

Electrolytic capacitors have a metallic anode which is covered with an oxidized layer used as dielectric. The second electrode of electrolytic capacitors is a non solid or solid electrolyte. Electrolytic capacitors are polarized electrical components. Three families of electrolytic capacitors used are aluminium electrolytic capacitors with aluminium oxide as dielectric, tantalum electrolytic capacitors with tantalum pentoxide as dielectric, niobium electrolytic capacitors with niobium pentoxide as dielectric [44]. The anode of electrolytic capacitors is highly roughened to extend the surface area which increases the capacitance value. The relatively high permittivity of the oxide layers gives these capacitors the very high capacitance per unit volume compared with film or ceramic capacitors. The electrical parameters of the capacitors are established by the material and composition of the electrolyte, especially by the conductivity. Three types of electrolytes used are non solid electrolyte which has electrical conductivity (~ 10 mS/cm), Solid manganese oxide electrolyte is of high quality and forms long time stable capacitors, its electrical conductivity (~ 100 mS/cm), Solid conductive polymer electrolyte for capacitors with very low ESR values down to values <10 mΩ, its electrical conductivity (~ 10,000 mS/cm). The larger capacitance per unit volume of electrolytic capacitors than other types makes them valuable in relatively high-current and low-frequency electrical circuits.

The supercapacitor is an electrochemical capacitor whose capacitance value is composed of a static capacitance stored in electric field with in double layer and pseudo capacitance stored electrochemically with redox reactions and charge transfer between electrode and electrolyte [45]. The capacitance of double layer capacitor is the charge stored statically in electric fields within the double-layers on the surfaces of the two electrodes. A double layer is a structure that appears on the solid surface of an electrode when it is placed into a liquid. The thickness of this structure acting like a dielectric is on the scale of nanometers so it has the energy density hundreds of times greater compared with conventional electrolytic capacitors. The pseudo capacitors store charges through adsorption, reversible redox reactions and intercalation of ions combined with charge transfer between electrolyte and electrode [46]. Pseudo capacitors can achieve much higher specific capacitance and energy density than double layer capacitors. The energy density of a pseudo capacitor can be as much as 100 times higher than in a double-layer capacitor. In parallel to the research of the pseudocapacitance the conductivity of electrolytes for double-layer capacitors could be reduced. Low ohmic double layer capacitors for high power applications were developed. Hybrid capacitors were developed it has new electrode materials such as Lithium ion to increase the pseudocapacitance.

Capacitors used in pulse power circuits are generally high voltage, fast discharge type designed to have low inductance and low series resistance. Typically they are charged over a relatively long period of time and then discharged via a closing switch in microseconds or milliseconds. The figure of merit used in assessing pulsed power capacitors includes energy density, peak current rating, inductance and reliable lifetime [47]. The rapid charging capacitor bank power supplies using solid state devices available in market. These power supplies are prone to failure in intense electromagnetic environment. Power supplies can be made using simple resistive charging circuit and its resistance is optimized for the fast charging [48].

2.4 High voltage generator for pulse charging

High voltage generation circuits are either based on Marx generator or a pulse transformer. Marx generators offer a common way of generating high voltage impulses that are higher than the available charging supply voltage. Fast rise time, low energy and high peak power Marx generators are developed using ceramic capacitors for applications in UWB [49] and using plastic case capacitors for HPM sources [50]. At lower energy levels (< 5 kJ) pulse transformer driven circuits are designed to operate as Tesla or double resonance circuit that has added advantage over Marx generator due to its compact size, low input voltage on primary side, low driving energy requirement, only one single switch for energy transfer and capacity to run on high repetition rates. The pulse transformer transfers the energy efficiently from energy storage capacitor to another capacitor under matched load condition. For the maximum energy transfer, it is mandatory to have a coupling coefficient between windings of the transformer as 0.6, 0.385 or 0.153 [51 - 52]. The unloaded waveforms of Tesla transformer for coupling coefficients are shown in Figure 2.10.

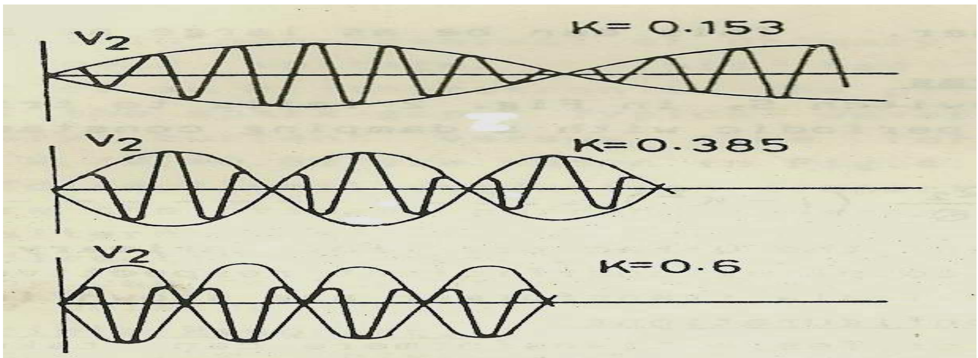

Figure 2.10 Unloaded waveforms of Tesla transformer output [51]

E.A Abramayan et. al. [53 -54] has reported the design and development of micro second duration transformer based accelerator for intense electron beam generation. P Sarkar et. al. [55] has also reported the design of half Mega volt transformer for EMP generation.

2.5 Intermediate energy storage system

The pulse transformers that are used in the microsecond range cannot be used to transform high-voltage pulses of nanosecond duration because of higher inductances and capacitances of the windings that lengthen the pulse rise time and distort the pulse waveform. So, an intermediate energy storage system is needed to deliver peak power to the loads. An intermediate energy storage system accumulates electrical energy over a comparatively long time, and then releases the stored energy in the form of a square pulse of comparatively short duration for various pulsed power applications. They are also known as pulse forming lines (PFL) or pulse forming networks (PFN). A PFN consists of a series of high voltage energy storage capacitors and inductors. These components are interconnected (as a "ladder network") that behaves similarly to a length of transmission line. The component values of the PFN are optimized to synthesize a pulse output with minimum flattop ripple. A PFL or PFN is charged by means of a high voltage power source, and then rapidly discharged into a load via a high voltage switch, such as a sparkgap.

2.51 Pulse forming lines

Pulse forming line is simplest of all pulse conditioning techniques, it starts with slow charging process and gets tens of nanoseconds output pulses with flat top amplitude. It can be made by off the shelf available coaxial cable or putting two-three concentric cylinders. Coaxial PFL is the simplest both in terms of structure and operation. It is simple to construct and easy to operate, however, the drawback is that the output voltage is half of the charging voltage. A brief comparison of various types of PFL's is mentioned in Table 2.03. The electrical energy is stored in the dielectric medium of the intermediate energy storage system for very short duration (micro-seconds to milliseconds). Solid and liquid dielectrics are used for pulsed energy storage in the PFL. The compactness of the system depends up on the dielectric constant of the medium.

S.No	Characteristics	Coaxial PFL	Blumlein PFL	Strip forming line
1	Characteristic Impedance	High	Very high	Low
2	Size	Medium	Large	Compact
3	Electric Field	Low	Low	High
4	Output Voltage	Half of charging	Equal to charging	Half of charging
5	Operating Voltage	Medium	High	Low

Table 2.03 Comparison of various PFLs

2.511 Pulse forming line using solid dielectric

Solid dielectrics materials have higher breakdown strength compared to liquid and gases dielectrics. A good solid dielectric should have low dielectric loss, high mechanical strength, should be free from gaseous inclusions, and moisture, and be resistant to thermal and chemical deterioration. Studies of the electrical breakdown in solid dielectrics are of extreme importance in pulsed power applications. When breakdown occurs, the solid dielectric get permanently damaged, while gases fully and liquids partly recover their dielectric strength after the applied electric field is removed. The conductivity of solid dielectric is not negligible when the electric field exceeds more than 100 kV/cm, it increases rapidly with electric field. The conductivity in solid dielectric at higher fields is due to field emission from electrodes, field aided thermionic emission and field enhanced ionization of impurities. The breakdown strength can be improved by ultimately reducing or inhibiting these effects. The main factors that influence the solid breakdown strength are dielectric type and properties, thermodynamic and mechanical states, structural defects and impurities, electrode material and surface conditions, applied voltage, gap geometry, other environmental effects, etc [57 - 58].

The static and dynamic nature of high voltage testing is used for the testing of solid dielectric insulation. M M Morcas et. al. [59] and D B Watson et. al. [60] has reported a brief overview of the application of statistical methods to establish the insulation strength and life time of solid dielectrics. The short term solid dielectric breakdown studies is also reported by weibull statistical analysis [61- 63]. Solid dielectric is generally considered to be non-recoverable in the event of dielectric breakdown but there are single shot pulsed power applications where its use is warranted. This can result in increased system capacitance with the possibility of operating at increased energy levels or reduced system volumes. However solid insulation failure under pulsed power conditions is not fully understood. Solid dielectric materials have been used as intermediate energy store for pulse compression using high voltage cables [64]. The investigation on high dielectric strength with high dielectric constant materials is one area which can help in designing very compact and sophisticated systems. Ceramic materials has very high relative permittivity and could be explored for making compact pulsed power system, but it is not much used in pulsed power system due to its piezoelectric properties [4]. Ceramic mixed with epoxies are tried and considerable increase in dielectric constant was seen [4]. Ceramic tiles have been made and it has been possible to charge them up to 60 kV [33].

2.512 Pulse forming line using liquid dielectric

Liquid dielectric is used in high voltage systems to serve the dual purpose of insulation and heat conduction. The advantage of liquid dielectric is that a breakdown path is self healing and the temporary failures due to overvoltage are reinsulated quickly by fluid flow to the attached area. Efforts to understand breakdown mechanisms in a variety of liquid dielectric are continued for longer time. There is no single theory that has been unanimously accepted for breakdown in liquid dielectric unlike in gases and solid because of complex and not regular molecular structure of liquid. The effect of short- and long-term electric strengths of dielectrics as functions of various influencing factors is studied and reported [65]. Methods of improving working field strengths and calculating the static, volt-second and statistical characteristics of the electric strength of insulation and the insulation service lifetime and reliability are also investigated. Factors influencing the electric strength includes dielectric material properties, states (pressure, density, viscosity, temperature, molecular, mechanical stress condition, etc.), electrode material, electrode surface, contaminations, polarity (for dc and impulse), type (for ac, frequency is also a factor), duration (for pulses) of the voltage, insulation gap geometry and other environmental conditions [58]. The increase in hydrostatic pressure will increase the electric strength of liquids for large electrode areas and for long voltage pulses (>1 μs) [66]. For very pure liquids under short-term voltage exposure, the main effect of temperature on electric strength is due to the temperature-dependent density. The electric strength slowly decreases with the increasing temperature and the decrease in voltage duration weakens this effect [67 - 68]. The dependence of electric strength on electrode material is due to the variations in the work function for electrons going from metals to liquids. The electric strength of liquid is mainly affected by the anode material. Degassing of electrode material increases the electric strength of degassed liquids for dc and ac voltages by 15-20%. Shielding the electrode surface by ionic layers and heating the volume of liquid adjacent to micro-tips by high-voltage conduction currents are two means to increase local electrical conductivity and consequently increase the electric strength of gaps with liquid insulation. Coaxial pulse forming lines are widely used for pulse compression. T.H Martin [69] has reported oil based helical pulse forming line having pulse power system rated 1 MV, 75 Ω, 100 ns with capacitance of 750 pF. The coaxial pulse forming line 60” long, 30” diameter with impedance and transit time of 11 Ω and 15 ns is converted to 1 MV, 260 ns, 75 Ω. An oil sparkgap has been used as output switch with 0.26 MV/cm breakdown strength. V.P Singal et. al [70] has also reported the development of blumlein based helical line storage element for generation of 150 kV, 5 μs pulse. Water helical pulse forming line will also significantly reduce the size of the system. Water free from mechanical impurities and gas is used in pulse power system and reduces the dimension of the system. Water has a breakdown strength ~ 130 kV/cm at pulses with duration of ~ 1 μs and electrode areas of up to tens of square meters, a large relative permittivity (~ 80) and a small loss tangent in the frequency range of 0 – 1 GHz [71 - 72].

2.6 High voltage switch

The switch is an important component of pulsed power system, which controls the flow of current in a circuit and also shapes the pulse. The switch used in pulsed power system to transfer peak power has operating time in range of ~ 1 ns to ~ 10 μs. The switches capable for handling giga-watt power and having very small jitter time (~ few ns) are frequently needed in pulsed power applications [39]. The conventional switches are no longer adequate to meet these requirements so the development of new types of switches becomes necessary. The high power switches are classified according to the mode of its operation as closing switch and opening switch. The closing switch is used to make the electrical circuitry and the current increases from zero to the maximum value with the fall in voltage across the switch. The opening switch is used to open the electrical circuitry and the current fall from the maximum value to zero with the increase in the holding voltage of the switch. These switches are generally trigged by external sources. The rise time of the switch determines its operational limits. The rise time of the switch is governed by three limits [5].

- Rate of carrier generation in the insulating medium of uniform field intensity resulting in critical charge density in a given time.
- Finiteness of propagation time of the electromagnetic wave across the switch
- Circuit model in which the resistive and inductive models determines the rate of rise of voltage pulse.

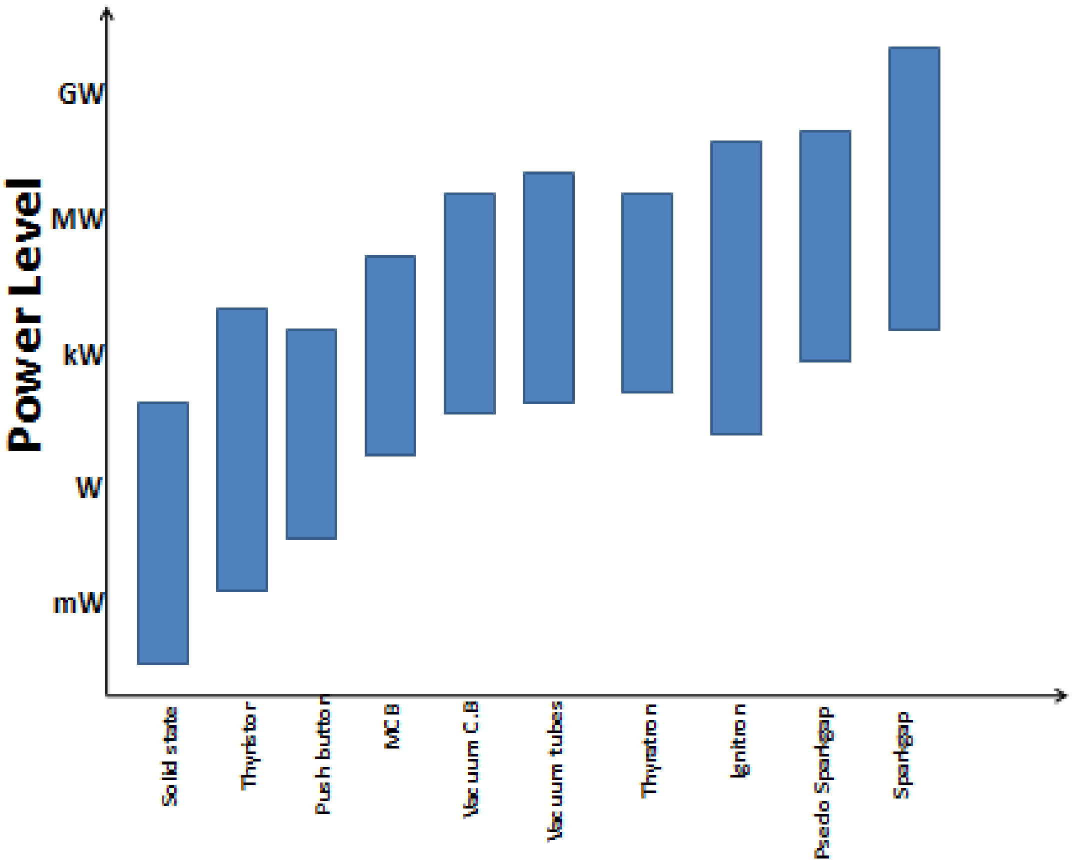

Figure 2.11 Switches used in pulsed power system

The switches used in pulsed power systems are shown in Figure (2.11). Sparkgap switch is used as a closing switch in pulsed power system. It has simple design, low cost, and its outstanding switching characteristics displays an excellent voltage withstand capacity (around a few MV) and a high charge transfer capability. Sparkgap switches have fast nanosecond duration closure time. A gas switch can be considered to be electrically closed when under a high electrical field stress the insulating gas between the electrodes becomes conducting and a plasma channel develops. The gap length between the two electrodes should be kept to a minimum to lower the inductance of the gap. A small gap can however break at an undesirable low voltage, although this can be avoided by pressurization of the gas medium. The breakdown voltage depends on both pressure and length of gap. The plot of breakdown voltage with product of pressure–distance is called paschen curve. The paschen curve for gases is shown in Figure 2.12.

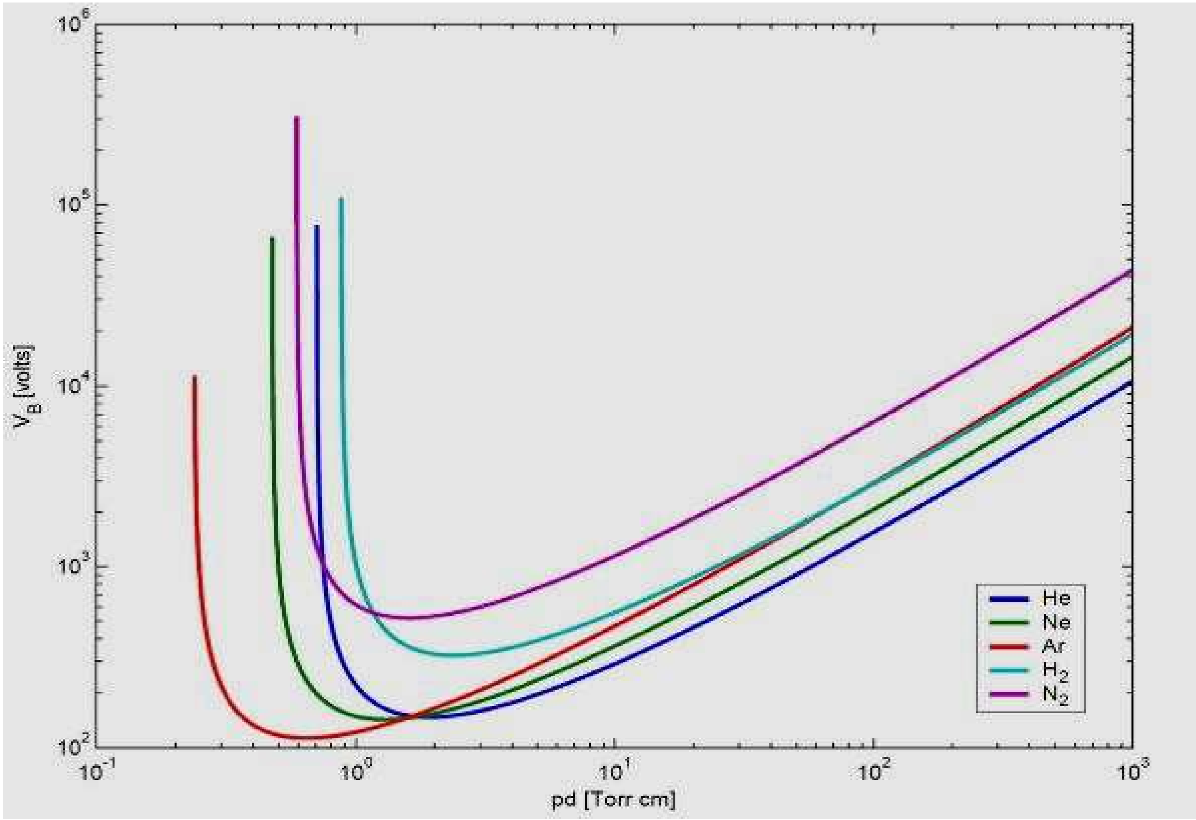

Figure 2.12 Breakdown voltage and Pressure-distance curve for gases

The sparkgap switch is still not replaceable when a compact pulsed power system is required to generate high voltage (> 10 kV) and high current (> 1 kA) with fast rising (sub-nanosecond) electric pulses. The primary limitation lies in lifetime and repeatability, other shortcomings with spark gaps are related to electrode erosion, insulator degradation, high arc inductance, and costly triggering systems [73]. The recovery of the sparkgap between the first and subsequent pulses is a very important phenomenon in repetitive pulsed sparkgaps operation [74]. Pressurized sparkgaps switches with hydrogen gas and pressure up to 120 kg/cm^2 has been used for fast switching up to 100 ps for ultra wide band generation [75]. Moran et. al [76 - 77] describes a high repetition rate hydrogen sparkgap operating at pressures upto 7 MPa and 0.1 mm to 10 mm gap. In a triggatron mode, a recovery time of 100 μs has been obtained. Faster recovery times have been reported when the sparkgap was operated well below the self BDV. Recovery times lower by an order of magnitude can be obtained by operating the sparkgap below fifty percent of self BDV. The recovery time of hydrogen is slower at low pressure by an order of magnitude compared to argon, it is an order of magnitude faster at very high pressure. The recovery of a mixture of hydrogen and argon falls between the curves for separated gases. Experiments of fast recovery of hydrogen gas switch were also conducted on a 600 kV, 10 μs, 5 pulse, and 10 kHz burst mode pulse power system.

Semiconductor switches are used for fast switching fast switching but it is limited by its power handling capacities. These switches have become popular owing to their compactness, better service time, efficiency and reliability over other switches in their operational regime.

2.7 Summary

The literature update and research issues in the development of compact pulsed power technology is discussed. The sub-systems required for the generation of high power pulse are also discussed. To develop compact pulsed power technology, the combined research efforts are required at component levels, system level and application level. The new components of the pulsed power system could be developed using new high energy density materials such as ceramics. The system level research leads to the investigation of novel architectural technique to reduce the size of the pulsed power system.

CHAPTER – 3

EXPERIMENTAL SETUP

The block diagram of the experimental set up for testing of compact pulse forming lines is shown in Figure 3.01. The primary energy storage capacitor bank was charged with high voltage power supply, and then discharged into the primary of pulse transformer through a triggered sparkgap switch. The high voltage generated across the secondary of the pulse transformer charges the compact pulse forming line, which then discharges through a self breakdown switch into the load.

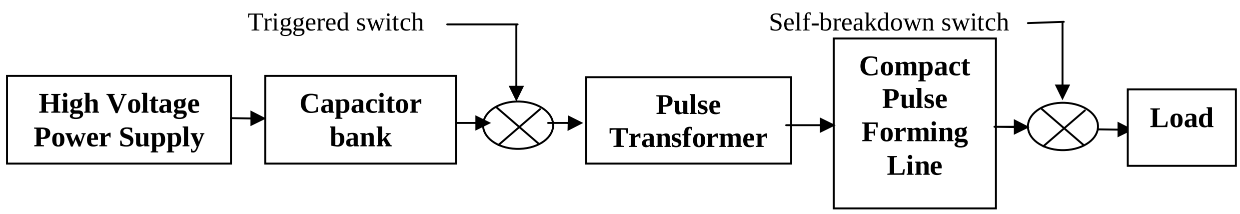

Figure 3.01 Block diagram of experimental setup

The circuit diagram of the compact pulsed power system is shown in Figure 3.02. The supply mains (Vac) is given to input of variac (V_TX), the output of variac is given to the input of step up transformer (TX) to gradually increase the voltage, the secondary of the step up transformer is then connected to the voltage multiplier circuit to generate high voltage. The high voltage power supply is connected to the capacitor bank (C_bank) through a decoupling switch (DC_SW), after charging the capacitor bank to the rated voltage the power supply is disconnected with decoupling switch. The sparkgap switch (SW1) is triggered to discharge into the primary of the air core pulse transformer (Lp). The high voltage generated across the secondary (Ls) will charge the compact pulse forming line. The self breaking sparkgap switch (SW2) break at the set voltage and a high power pulse is transferred to the load (Z).

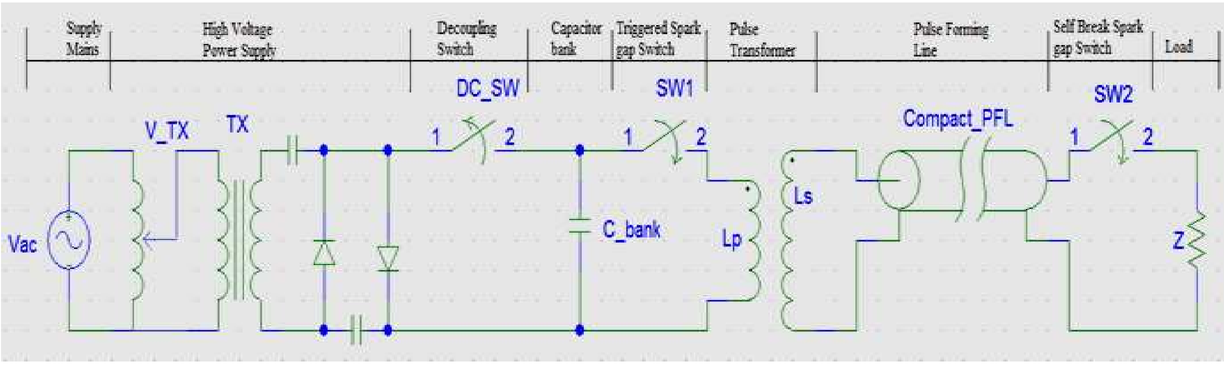

Figure 3.02 Circuit diagram of the pulsed power system

3.1 High voltage power supply

The capacitor bank was charged with a multiplier based in house developed 25 kV high voltage power supply (Figure 3.03). Supply main voltage (230 V, 50 Hz) was given to primary of the variac (0-230 V) to gradually increase the input voltage to the primary of step up transformer (230 V / 5 kV). The secondary of the transformer was connected to a five stage voltage multiplier circuit to charge the capacitor bank. The five stage multiplier circuit was built with El-Ci-Ar make capacitors (5 kV, 0.22µF) and high voltage diode (10kV, 500mA). Higher voltage can be generated by increasing the number of stages in the multiplier circuit. The power supply was decoupled after charging the capacitor bank to the rated voltage by a pneumatically operated decoupling switch.

Figure 3.03 Multiplier based power supply

3.2 Capacitor bank

The primary energy storage capacitor bank consists of the large numbers of low inductance capacitors connected in parallel, its switches and the power supplies. The low inductance capacitors available are selected for designing the primary energy storage system. A primary energy storage capacitor bank was designed and developed, which was used in the primary circuit of the pulse transformer to generate high voltage pulses and charge the pulse forming line. High voltage energy storage capacitor (Yesha Make: 200 J/ 50 kV/0.16µF) was used in the capacitor bank. The inductance of the capacitor bank was 200 nH. The capacitor bank was made up of eight number of 0.16µF capacitor connected in parallel that can be charged up to 50 kV. The capacitor terminals are connected in parallel with the aluminium plate (Figure 3.04). Four numbers of RG 213 cables were used to connect the capacitor bank to the sparkgap switch. The energy stored in the capacitor bank was discharged by triggering the sparkgap switch. The capacitor bank parameters are mentioned in Table 3.02

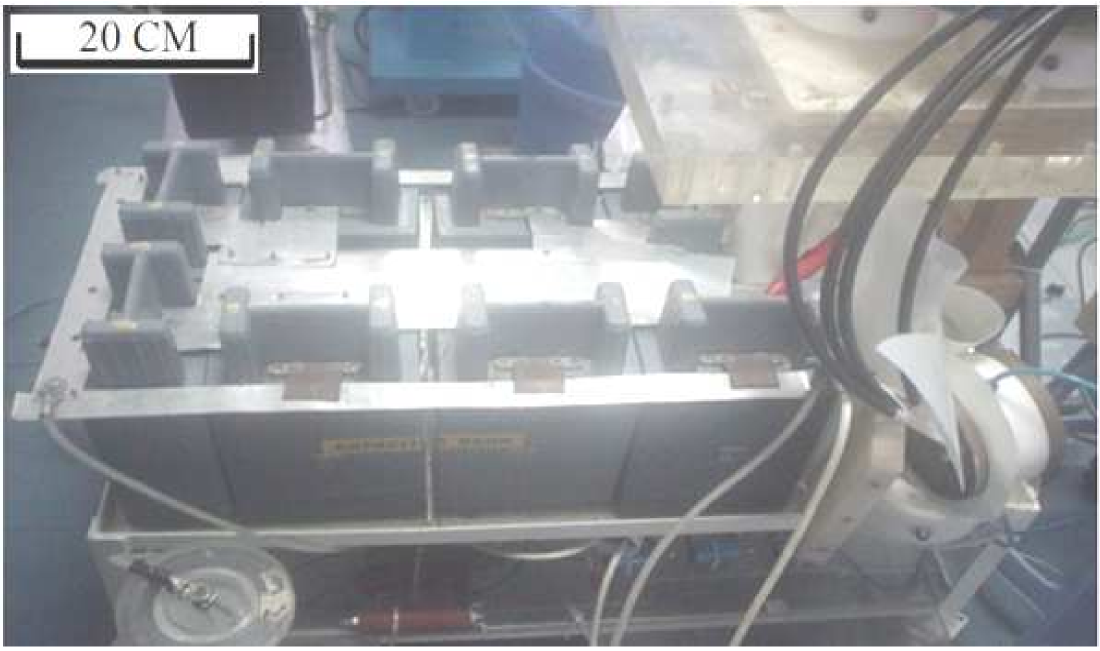

Figure 3.04 Capacitor bank

Stored Energy	1.6 kJ
Peak Charging Voltage	50 kV
Capacitance	1.29 µF
Inductance	200nH
Peak current	125 kA
Size	100 x 60 x 30 cm

Table 3.01 Parameters of capacitor bank

The capacitor bank was connected to the primary of the pulse transformer through a triggered sparkgap switch. After charging the capacitor bank to the rated voltage the power supply was decoupled from the capacitor bank. The sparkgap switch was then triggered to break and the capacitor bank discharges into the primary of the pulse transformer. The sparkgap switch can operate in 8kV to 50kV range by adjusting pressure in the gap. Four numbers of RG 213 coaxial cables of 0.8 meters length were used to keep the inductance low and are connected to the primary of pulse transformer through a triggered sparkgap switch. The inductance of the capacitor bank and the connecting cable was 200 nH and 50 nH. The advantage of using coaxial cables was that they are flexible and therefore they offer shock absorbing capability. These cables are used in parallel to reduce the inductance and to increase the current carrying capacity.

3.3 High voltage pulse transformer

The pulse transformer has two mutually coupled circuits. The primary circuit has high voltage capacitor bank which discharges into low inductive primary winding through a switch. The secondary circuit has a high inductance secondary winding mutually coupled to the primary winding and the load capacitance. Every discharge in the primary circuit magnifies the voltage in the secondary coil. Figure 3.05 shows an air core pulse transformer, with the resonant circuits

(L_1C_1 and L_2C_2) coupled through their mutual inductance M, R_1 and R_2 are the resistance in the primary and secondary circuits. The open circuit resonant frequencies of the two circuits are chosen to be equal for complete energy transfer from the primary circuit to the secondary circuit [78].

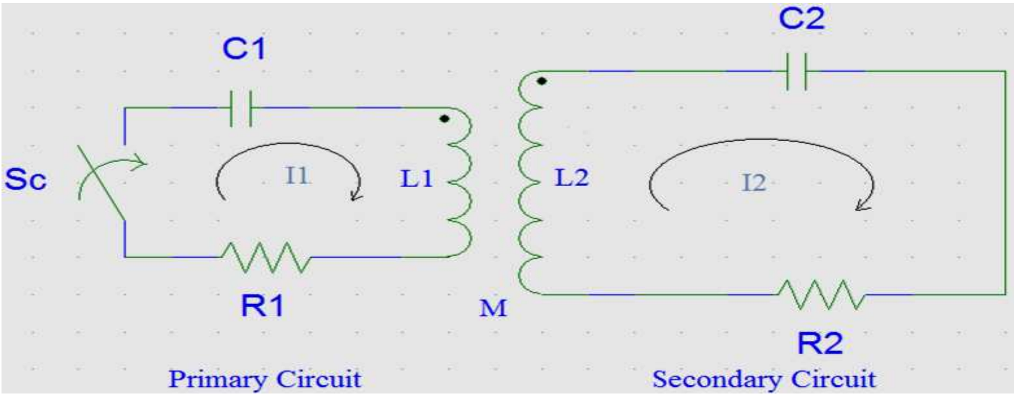

Figure 3.05 Inductively coupled primary and secondary circuits

As the sparkgap (Sc) closes, the energy stored in the primary capacitor C_1 feeds L_1 and the primary circuit oscillates close to its resonance frequency defined by the values of C_1 and L_1. Part of this energy is magnetically coupled into the secondary L_2 that oscillates with its own resonance frequency. The amplitude of the resultant oscillation is at a maximum when these two are in phase. The energy transfers back and forth from one circuit to the other with this frequency until it is entirely dissipated in resistive and RF losses.

The primary capacitor C_1 is initially charged, and when the sparkgap is closed, operation of the transformer is described by the following equations [79 - 80].

For the primary circuit

$$R_1 I_1 + \frac{1}{C_1}\int I_1\, dt + L_1 \frac{dI_1}{dt} + M\frac{dI_2}{dt} = 0 \qquad (3.01)$$

And for the secondary circuit

$$R_2 I_2 + \frac{1}{C_2}\int I_2\, dt + L_2 \frac{dI_2}{dt} + M\frac{dI_1}{dt} = 0 \qquad (3.02)$$

If q_1 and q_2 are the instantaneous charge on the capacitor C_1 and C_2, then

$I_i = \frac{dq_i}{dt}$, i = 1, 2

And equations 2.04 and 2.05 may be written as

$$R_1 \frac{dq_1}{dt} + \frac{1}{C_1} q_1 + L_1 \frac{d^2 q_1}{\mathrm{dt}^2} + M \frac{d^2 q_2}{\mathrm{dt}^2} = 0 \quad (3.03)$$

$$R_2 \frac{dq_2}{dt} + \frac{1}{C_2} q_2 + L_2 \frac{d^2 q_2}{\mathrm{dt}^2} + M \frac{d^2 q_1}{\mathrm{dt}^2} = 0 \quad (3.04)$$

Introducing the differential operator $D \; (= \frac{d}{dt})$ and combining equation 3.03 and 3.04 gives auxiliary equation

$$(1 - k^2)D^4 + \left(\frac{R_2}{L_2} + \frac{R_1}{L_1}\right) D^3 + \left(\omega_2^2 + \omega_1^2 + \frac{R_1}{L_1}\frac{R_2}{L_2}\right) D^2 + \left(\frac{R_1}{L_1}\omega_2^2 + \frac{R_2}{L_2}\omega_1^2\right) D + \omega_1^2 \omega_2^2 = 0 \quad (3.05)$$

Where

$$k = \frac{M}{\sqrt{L_1 L_2}} \quad (3.06)$$

$$\omega_1 = \frac{1}{\sqrt{L_1 C_1}} \quad (3.07)$$

$$\omega_2 = \frac{1}{\sqrt{L_2 C_2}} \quad (3.08)$$

T is the tuning ratio,

$$T = \left(\frac{\omega_1}{\omega_2}\right)^2 = \frac{L_2 C_2}{L_1 C_1} \quad (3.09)$$

Equation 3.05 has four complex roots E_i and its solution can be written in terms of the charge on the capacitors as

$q_2 = \sum_i A_i \exp\,(E_i t)$

$q_1 = \sum_i B_i \exp\,(E_i t)$

Where A_i and B_i are constant (and i = 1..,4), which can be evaluated by using the boundary conditions at t = 0 of

$q_2 = 0, q_1 = q$ (initial charge on C_1) and $dq_1 = dq_2 = 0$

Subsequently, the primary and secondary capacitor voltages can be written as

$$V_1 = \frac{q_1}{C_1} = \frac{1}{C_1} \sum_i B_i \exp(E_i t) \tag{3.09}$$

$$V_2 = \frac{q_2}{C_2} = \frac{1}{C_2} \sum_i A_i \exp(E_i t) \tag{3.10}$$

Solution of equations 3.09 and 3.10, when the primary and secondary resistances are neglected gives the voltage developed across the secondary circuit capacitance C_2 as

$$V_2 = \frac{2kV_1}{\sqrt{(1-T)^2 + 4k^2T}} \sqrt{\frac{L_2}{L_1}} \sin(\frac{\omega_a+\omega_b}{2} t) \sin(\frac{\omega_b-\omega_a}{2} t) \tag{3.11}$$

$$\omega_a = \omega_1 \sqrt{\frac{(1+T)-\sqrt{(1-T)^2+4k^2T}}{2(1-k^2)}} \tag{3.12}$$

$$\omega_b = \omega_2 \sqrt{\frac{(1+T)+\sqrt{(1-T)^2+4k^2T}}{2(1-k^2)}} \tag{3.13}$$

ω_a and ω_b are the resonance frequencies of the primary and secondary circuits when coupled; the physical constraints on the values of k and T ensure that ω_a and ω_b are always real. Equation (3.11) shows that the secondary voltage is a high frequency oscillation $(\omega_b + \omega_a) / 2$ which is amplitude modulated by another low frequency oscillation $(\omega_b - \omega_a) / 2$.

The optimum design of pulse transformer depends upon the coefficient of coupling, turning ratio and dielectric medium [81]. The secondary capacitance of pulse transformer is determined by the capacitance of the pulse forming line and the inter winding capacitance of the secondary of the pulse transformer. A compact high voltage pulse transformer was designed and developed for pulse charging and testing of the pulse forming lines. The primary energy storage capacitance was determined by the availability of the capacitors. The primary capacitance was the capacitance of the energy storage capacitor. The primary of the pulse transformer was energized by discharging a 1.29 μF capacitor bank as discussed in section 3.2. The capacitor bank was discharged through a triggered sparkgap switch. The inductance of the capacitor bank and connecting cable were 200 nH and 50 nH. The inductance of the cables is added in series to the primary inductance of the transformer. The secondary capacitance of the pulse transformer was determined by the capacitance of the pulse forming line used for intermediate energy store. We will be designing a pulse transformer to charge 5nF – 6 nF capacity pulse forming line.

For resonance condition L_1, C_1 should be close to L_2, C_2, so we select the parameters as mentioned Table 3.02.

Primary Capacitance	1.29 µF
Primary Inductance	450 nH
Secondary Capacitance	5.5 nF
Secondary Inductance	110 µH

Table 3.02 Parameter of the pulse transformer required

For the requirement of the project and the testing of the pulse forming line a pulse transformer has to be fabricated with primary and secondary inductance close to 200 nH and 110 µH.

3.31 Fabrication of the pulse transformer

A pulse transformer was fabricated with primary inductance of 200 nH and secondary inductance of 110 µH. A single turn copper sheet was used to make the primary of the pulse transformer and RG 213 cable with braid removed was used as the secondary of the pulse transformer.

3.311 Cylindrical primary winding

A 0.5 mm copper sheet was used to make the primary of the pulse transformer. The internal diameter and height of the primary coil was 240 mm and 300 mm. The primary coil was placed on the polyvinyl chloride cylinder to support it. Four numbers of RG 213 cables (0.8 meters) are used to connect the primary coil to the capacitor bank through a sparkgap switch (Figure 3.06).

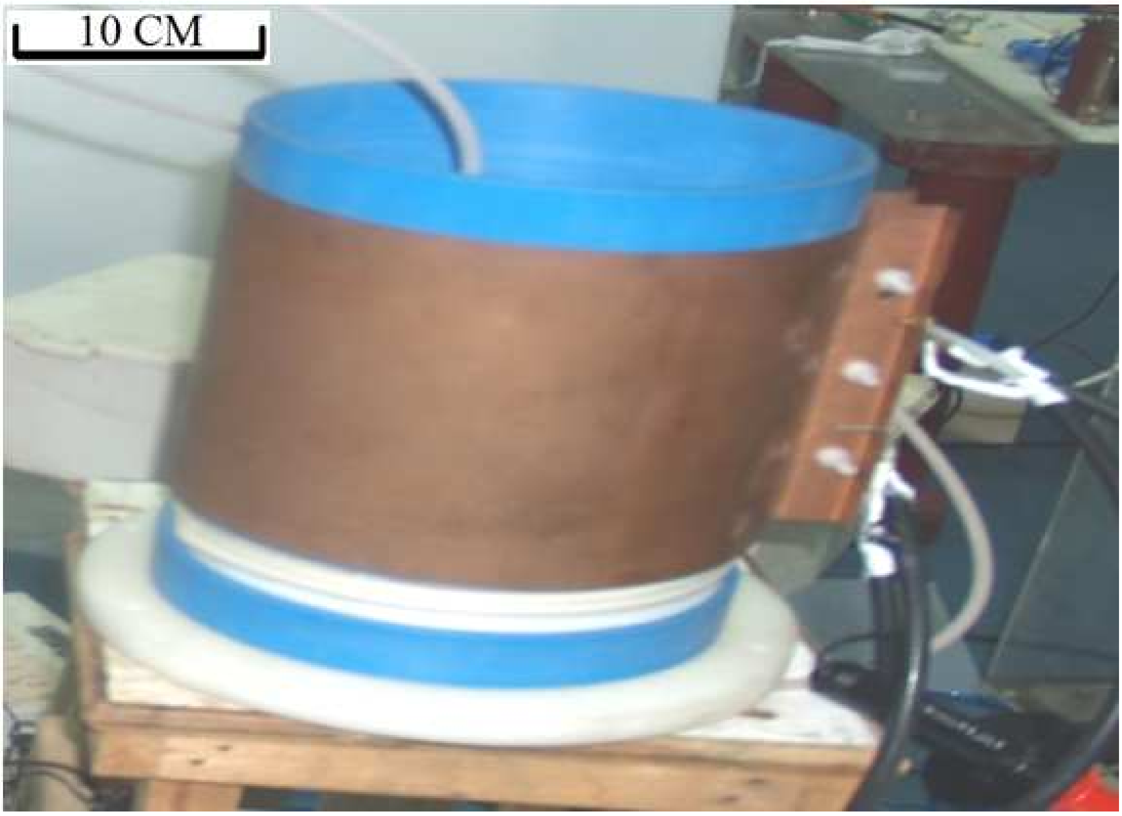

Figure 3.06 Primary winding of the pulse transformer

3.312 Conical secondary winding

A tapered construction (with the larger diameter at the bottom) was used for the secondary coils to avoid any break-down at the high voltage end of the secondary winding. The high voltage appears at the upper end (as the lower end is grounded) and the greater space around the high voltage terminal prevents the possibility of any high-voltage break down. The secondary winding was placed inside the deldrin mandrel used to support the primary winding. The secondary winding was formed by 28 turns of commercially available stripped RG 213 cable in diameter wrapped around a conical mandrel with a lower diameter of 170 mm, an upper diameter of 140 mm. The diameter of wire with 3mm and the pitch of winding is 7.2 mm (Figure 3.07). The secondary of the pulse transformer was connected to the inner and outer conductor of the pulse forming line.

Figure 3.07 Secondary winding of pulse transformer

3.32 Filamentary modelling of conical pulse transformer

The filamentary modelling of the high voltage pulse transformer is done to calculate the inductance of the primary winding, secondary winding and the mutual inductance between them. In the filamentary modelling the given assembly of conductors is divided into an assembly of filaments in the direction of the current paths through the conductor. The filaments must be sufficiently small for the current distribution in their cross section to be regarded as uniform and the dimensions should be much less than the equivalent skin depth. The number of filaments required to describe accurately their properties under transient conditions is obtained by calculating the parameters for a relatively small numbers of filaments and then repeating the calculations for a progressively increased number until the differences between successive calculations are less than about 1% [82].

By assuming a uniform current distribution across the cross section of the filaments the self inductances and mutual inductance between every possible pair of filaments can readily be calculated from the well known formulae (Appendix 1). Thereby the electromagnetic problem was reduced to a simple circuit problem in which the solid conductors are represented by an assembly of current filaments. The currents in each branch are defined as state variables and the circuit equations were written as set of linear first order differential equations that have to be solved for the circuit currents. A typical set of equations will appear in matrix form as

$$\frac{d}{dt}\begin{bmatrix} L_1 & M_{1,2} & \dots & M_{1,N} \\ M_{2,1} & L_2 & \dots & M_{2,N} \\ - & - & \dots & - \\ - & - & \dots & - \\ - & - & \dots & - \\ M_{N,1} & M_{N,2} & \dots & L_N \end{bmatrix}\begin{bmatrix} I_1 \\ I_2 \\ . \\ . \\ . \\ I_N \end{bmatrix}=\begin{bmatrix} V_1 \\ V_2 \\ . \\ . \\ . \\ V_N \end{bmatrix} \tag{3.14}$$

Where N is the number of filament I_i (i=1……N) is the current in the i_{th} filament. V_i(i=1…..N) is the complete inductive voltage term in the circuit containing the i filament and Mi,j (j=1…..N) is the mutual inductance between the i_{th} and j_{th} filaments. When i=j , Mi,j becomes L_i the self inductance of the i_t filament and equation (1) can be written in compact form as

$$\frac{d}{dt}\left(\sum_{j=1}^{N} M_{i,j}\, I_j\right) = V_i(\, i = 1 \,\dots .\, N) \tag{3.15}$$

The set of first order differential equations that corresponds to the filamentary circuits model can be solved using numerical ordinary differential equation with the filamentary currents thus calculated providing the current distribution in the conductors. Most electromagnetic devices encountered in the pulsed power have rotational symmetry about one axis which is termed axial symmetry. Because of this situation the model here is restricted to the cylindrical co-ordinates (r,z,θ) with symmetry about the z axis. Therefore in the most general case, the effect of an arbitrary current path through symmetrical conductors can be defined in terms of combination of z and θ currents.

Once the filamentary currents of any transformer are known, the magnetic energy stored in all the filamentary self and mutual inductances can be calculated at any time during the discharge of the capacitor bank [83 – 84]. The total energy stored in the winding can then be found directly by adding the magnetic energy associated with each filament and the result obtained must be equal to the energy stored in the corresponding element of lumped component model (i.e $LI^2/2$). The self inductance of the single turn primary winding can be written as [83,85]

$$L_p = \frac{\sum_{i=1}^{N_p} \sum_{j=1}^{N_p} M_{i,j} I_i I_j}{\left(\sum_{i=1}^{N_p} I_i\right)^2} \tag{3.16}$$

where N_p is the total numbers of filaments in the primary winding.

The inductance of the multi-turn secondary winding (represented by N concentric cylinders) is given by [83,85]

$$L_s = \frac{\sum_{i=1}^{N_s} \sum_{j=1}^{N_s} M_{i,j} I_i I_j}{\left(\frac{1}{N} \sum_{i=1}^{N_s} I_j\right)^2} \tag{3.17}$$

Where N_s is the total number of filaments in the secondary winding

Similarly the mutual inductance between the primary and secondary windings is [83,85]

$$M_{p-s} = \frac{\sum_{i=1}^{N_p} \sum_{j=1}^{N_p} M_{i,j} I_i I_j}{\sum_{i=1}^{N_p} I_i \left(\frac{1}{N} \sum_{j=1}^{N_s} I_j\right)} \tag{3.18}$$

Equations (3.16), (3.17) and (3.18) can be evaluated, with the turns divided into a number of filaments their effective self and mutual inductances can be calculated. The filamentary modelling of the pulse transformer was done to calculate the primary inductance, secondary inductance and the mutual inductance between the winding. The equation used in the programming is described in Appendix-1.

3.33 Parameters of pulse transformer

The parameters of the pulse transformer were simulated and also measured with LCR meter and mentioned in Table 3.03. The LCR meter can measure the inductance in the range of 100 pH to 100 MH The accuracy in measurement of inductance is 0.2 % in the range of 1 µH to 10 H, and up to 2.5 % in the range of 10 nH to < 1 µH and > 10 H to 1 kH. The simulated and experimental results of secondary of pulse transformer charging the pulse forming line is shown in Figure 3.08. The variation in experimental and simulation result was less than 2% for second peak.

Parameter	Simulated	Calculated
Inductance of Primary winding	215.7 nH	200 nH
Inductance of Secondary winding	109.5 µH	110 µH
Mutual Inductance	3.55 µH	3.5 µH
Coefficient of coupling	0.73	0.74

Table 3.03 Parameters of the pulse transformer calculated

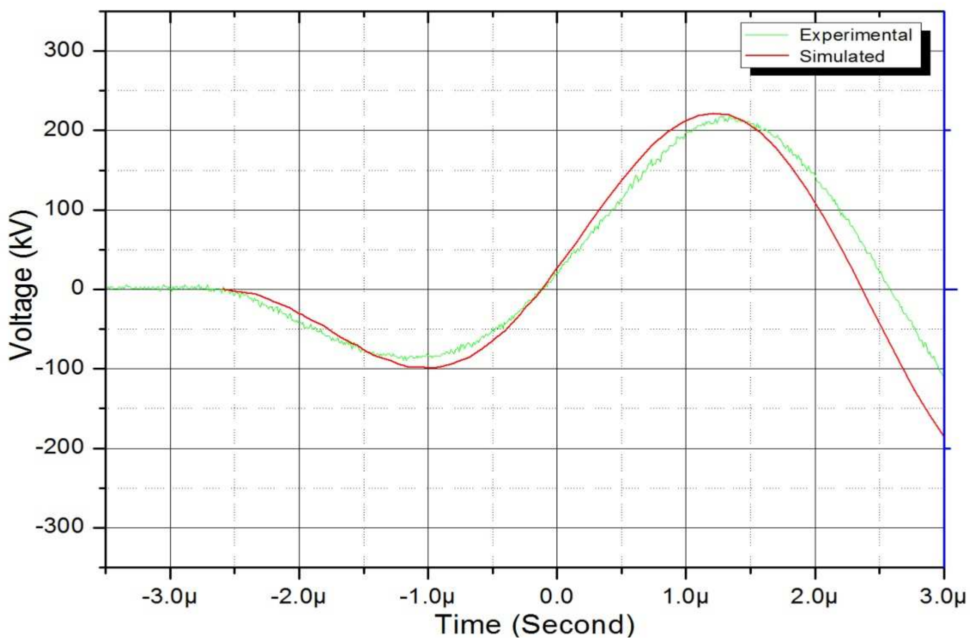

Figure 3.08 Experimental and simulation results of secondary of pulse transformer charging PFL

3.4 Compact pulse forming lines

Pulse forming lines essentially consists of a transmission line, that is charged as a lumped capacitor (which forms the secondary capacitance of the pulse transformer) to store electrical energy and a high voltage switch to discharge this energy in the transmission line to the load. Newer concepts of pulse forming lines were explored using high dielectric constant ceramics and novel engineering techniques. The design details and development of these compact pulse forming lines are discussed in chapter 4.

3.5 High voltage switch

A high voltage self breakdown sparkgap switch was designed and developed for pulse sharpening to operate at ~ 100 kV - 200 kV. Nitrogen gas was used as the dielectric medium inside the switch. To achieve reliable closing and smaller switching time, operating voltage should be nearly 80% - 90% of the static breakdown voltage. So static breakdown voltage of 200 kV is taken and recalling from the paschen curve for obtaining the value of pd (Figure 2.10). The schematic of sparkgap switch is shown in Figure 3.09.

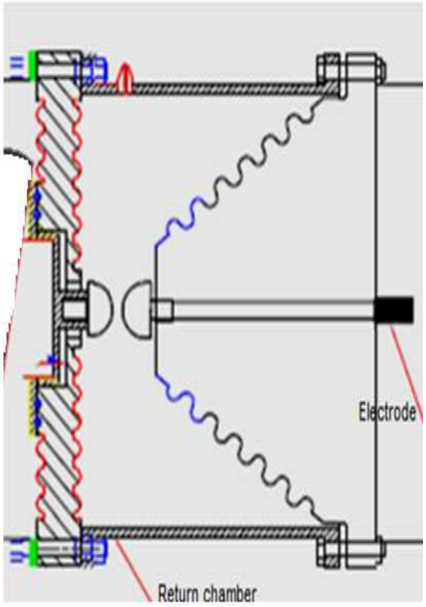

Figure 3.09 Schematic of sparkgap switch

The working pressure inside the switch was taken at 4.5 kg/cm^{2}for operating at 200 kV, so the distance between the sparkgap electrodes required was 1.48 cm recalling from the paschen curve. Brass was used as electrode material (Figure 3.10). The diameter of the sparkgap electrode (D) should be greater than the spacing between the electrodes (d) for the uniform electric field inside the sparkgap switch (D > 2d).

The emperical formulae for the calculation of the inductance and rise time of the sparkgap switch was calculated by J. C Martin and his group [86]

Inductance of the switch (L) is given by [86],

$$L = 14 \times d \ \text{(nH)} \tag{3.19}$$

Where, d is the distance between the sparkgap electrodes (in cms)

The sparkgap switch rise (t_s) consist of the resistive phase rise time (t_r) and the inductive phase rise time (t_l) [86]

$$t_s = 2.2\sqrt{{t_r}^2 + {t_l}^2} \tag{3.20}$$

$$t_r = 88\,\frac{\left(\frac{\rho}{\rho_0}\right)^{\frac{1}{2}}}{Z^{\frac{1}{2}} + E^{\frac{4}{3}}} \tag{3.21}$$

$$t_l = \frac{L}{Z} \tag{3.22}$$

Where,

ρ is the gas density and ρ_0 is the gas density at NTP

E is the electric field inside the gap (kV/mm)

L is the inductance of the switch (nH)

Z = 22 Ω, is the impedance of the system

Inductance of the switch is, L = 20.72 nH

The rise time (t_s) of the switch is 13.7 ns

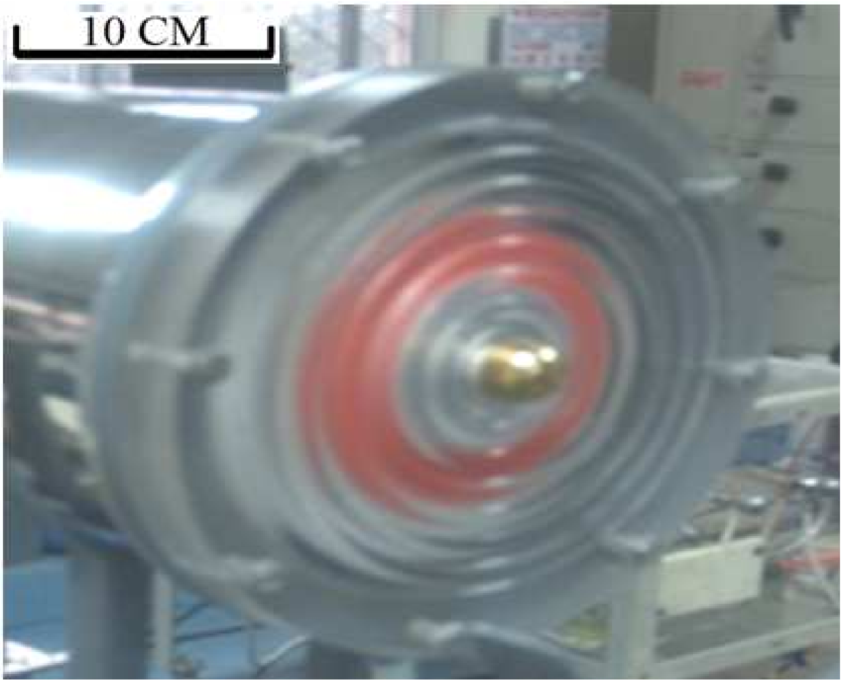

Figure 3.10 Brass electrode of sparkgap switch

The performance of the sparkgap switch was also calculated for 1000 shots operation at 200 kV. It will transfer 10 kA current for the duration of 260 ns. So, the charge transfer during single shot operation is 2.60 mC.

The erosion rate of brass electrode is 40 x 10^{-6} cm^3/C [87]. So, in a single shot operation 0.104 x 10^{-6} cm^3 of brass material will be eroded from the electrodes. In 1000 shots the volume of brass material eroded will be 104 x 10^{-6} cm^3 from both the electrodes. The length of eroded brass from the sparkgap is 2.3 x 10^{-2} cm, which is 1.5% of the distance between the electrodes, which will not affect the performance of the spar gap switch to a large extent.

There is another important issue of breakdown along the surface of insulator used to hold the electrodes. Most commonly used insulators are epoxy resins, polycarbonate resins, nylon, fiber glass, delrin etc. As a rule of thumb surface flashover may be considered at 10 kV/cm, so that the sparkgap breaks in the main dielectric instead through the surface of the insulator. The surface length may be increased by carving grooves over it.

3.6 Diagnostics used in experimental setup

The voltage across the compact pulse forming line was measured with RC voltage divider (VD-100) and the voltage across the load was measured with RC voltage divider (PVM-5). The accuracy of VD-100 and PVM 5 above 1 MHz signal frequency is < 4% and < 2% respectively. The specifications of these standard voltage dividers are mentioned in Appendix- 2. The output signal of these dividers is transferred through RG 58 cable to oscilloscope. The attenuation factor of RG 58 cable is 0.4 db/100 feet at signal frequency of 1 MHz, The attenuation factor increases to 3.3 db/100 feet at 10 MHz and up to 22db/100 feet at 1 GHz signal frequency. The inductance and capacitance of RG 58 cable is 250 nH per meter and 100 pF per meter respectively. The power handling capacity of RG 58 cable is 500 watts at 10 MHz frequency. The voltage divider output waveforms are recorded in oscilloscope. It has a bandwidth of 1 GHz, sampling rate of 4 GSa/s and memory depth of 8 Mpts. The vertical gain and time base accuracy of the oscilloscope is ± 2% and ± 2.5% respectively. The accuracy in measurement of PFL charging voltage is ± 3% and the load voltage is ± 4.5%. The capacitor bank charging voltage is measured with high voltage probe connected to the multimeter meter. The high voltage probe has high input impedance, provide attenuation of 1000: 1 and it measure ac/dc high voltages up to 40 kV. The dc accuracy of the probe is ± 2% for the measuring range of 0 - < 20 kV and ± 1 % for the measuring range of 20 kV to 35 kV. The multimeter can measure dc voltages from 30 mV to 1000 V with an accuracy of ± 0.0225%. The accuracy in measurement of capacitor bank voltage is ± 2.5%. The circuit parameter such as resistance, inductance and capacitance are measured with LCR meter. It can measure the resistance in the range of 10 μΩ to 100 GΩ, inductance in the range of 100 pH to 100 MH and capacitances in the range of 1 pF to 1 F respectively. The accuracy in measurement of resistance is 0.2 % in the range of 0.5 Ω to 1 MΩ, and up to 2.5 %

in the range of 50 mΩ to < 0.5 Ω and > 1 MΩ to 50 MH. The accuracy in measurement of inductance is 0.2 % in the range of 1 µH to 10 H, and up to 2.5 % in the range of 10 nH to < 1 µH and > 10 H to 1 kH. The accuracy in measurement of capacitance is 0.2 % in the range of 100 pF to 1 mF, and up to 2.5 % in the range of 1 pF to < 100 pF and > 1mF to 100 mF respectively.

3.7 Summary

The subsystem used for the testing of compact pulse forming lines were designed and developed. The capacitor bank discharged into the primary of the pulse transformer, the secondary of the pulse transformer pulse charges the pulse forming line and it discharges to the load through a spark gap switch. The in-house developed multiplier based power supply was used to charge the capacitor bank. The primary energy storage capacitor bank was made by using available capacitors. The high voltage pulse transformer was designed and developed for pulse charging of the pulse forming lines. The design and development of pulse forming line are discussed in the chapter 4.

CHAPTER – 4

DESIGN AND DEVELOPMENT OF COMPACT PULSE FORMING LINES

Pulse forming line (PFL) is an important sub system of a pulsed power system. It is one of the basic elements of a pulsed power system for producing very fast rise time pulses of the desired pulse width. The impedance of high voltage generator is generally high and the loads of pulsed power devices are of generally lower impedances, so the PFL is used in intermediate stages, which is charged in few microseconds of durations and discharges in few tens to hundreds of nano seconds of durations into the loads. It is also used for matching the source impedance with the load impedance to deliver peak power.

Transmission lines are widely used in the production and transformation of fast rise time voltage and current pulses. A transmission line is a set of conductors used for transmitting electrical signals with frequencies reaching the microwave frequency bands. The principle properties of the transmission lines that are useful are time delay, impedance and reflection of pulses. With proper switching, transmission lines can be used to re-shape the form of the incoming pulse with the pulse width determined by the length of the transmission line. When they are used for this purpose, they are referred to as pulse forming lines (PFL). Often, there is no clear-cut distinction between a transmission line and an ordinary electric circuit. Whether the two conductors should be treated as a transmission line or as an electric circuit depends on the ratio of the length of the conductors and the wavelength of the applied voltage. If the wave length is very long compared to the length of the conductors, it can be treated as an electric circuit. Otherwise it should be considered as a transmission line. Transmission line when used as intermediate store, for pulse compression from the main energy storage such as a Marx generator or the pulse transformer are usually placed between the primary energy storage element and the load.

4.1 Circuit analysis of transmission lines

The standard circuit theory cannot be employed on an electrical network at microwave frequencies so an alternative analysis is applied to the system [81]. Transmission line theory is a tool which bridges the gap between circuit theory and a complete field analysis. Transmission lines lie between a fraction of a wavelength and many wavelengths in size. Conversely, in circuit analysis, the physical dimensions of the network are much smaller than the wavelength. A transmission line is considered a distributed parameter network as opposed to a circuit which consists of lumped elements. Consequently, the voltages and currents associated with a propagating wave in a transmission line can vary in both phase and magnitude over the length of the line. A uniform transmission line is a distributed circuit that can be describe as a cascade of identical cells with infinitesimal length (Figure 4.01). The conductors used to realize the line has a certain series inductance (L), series resistance (R) and shunt capacitance (C). In addition, there is a shunt conductance (G) if the medium insulating the wires is not perfect. The uniform transmission line is represented as the distributed circuit (general lossy line).

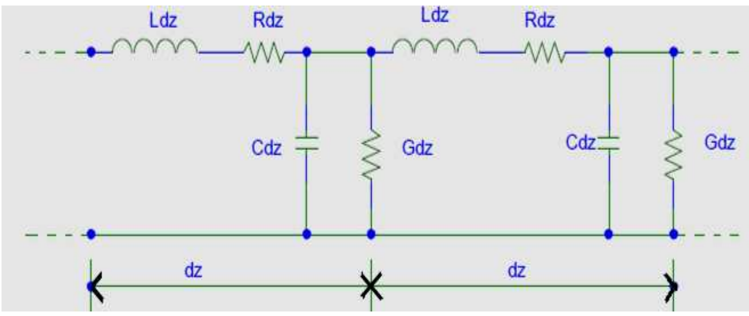

Figure 4.01 Transmission line with distributed circuit

Each cell of the distributed circuit will have impedance elements with values: Ldz, Rdz, Cdz and Gdz are the infinitesimal length of the cells. If we can determine the differential behaviour of an elementary cell of the distributed circuit in terms of voltage and current, we can find a global differential equation that describes the entire transmission line. The solution for a uniform lossy transmission line can be obtained with using the equivalent circuit for the elementary cell shown in the Figure. 4.02.

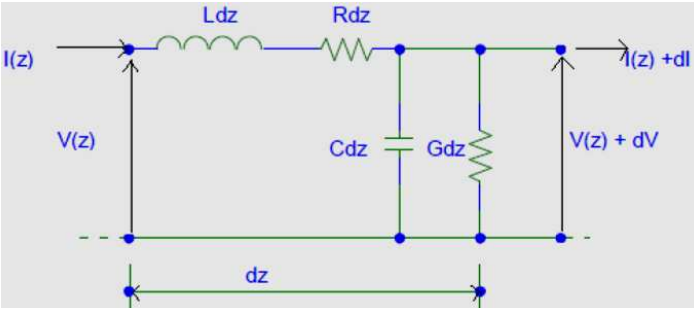

Figure 4.02 Equivalent circuit of lossy transmission line

The series impedance determines the variation of the voltage from input to output of the cell, according to the sub-circuit (Figure 4.03) the corresponding circuit equation is

$$(V + dV) - V = -(j\omega Ldz + Rdz)I \tag{4.01}$$

From which we obtain a first order differential equation for the voltage

$$\frac{dV}{dz} = -(j\omega L + R)\, I \tag{4.02}$$

The current flowing through the shunt admittance determines the input-output variation of the current, according to the sub-circuit Figure 4.04 The corresponding circuit equation is

$$\begin{aligned} dI &= -\,(j\omega C\; dz + G\; dz)(V + dV) \\ &= -(j\omega C + G\,)\, V\, dz - (j\omega C + G) dV\, dz \end{aligned} \tag{4.03}$$

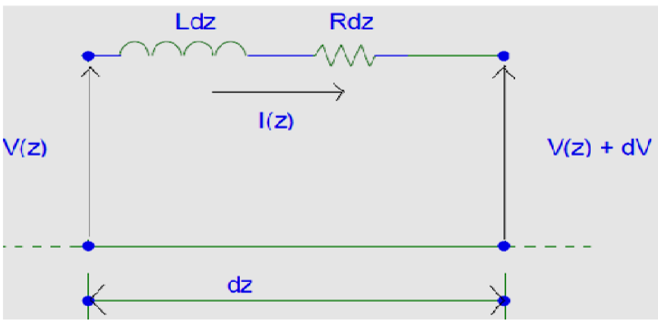

Figure 4.03 Series impedance

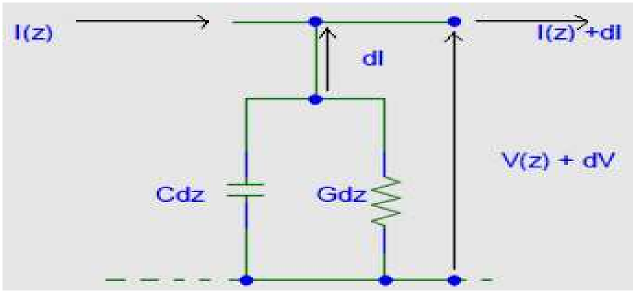

Figure 4.04 Shunt admittance

The second term (dV dz) can be ignored, giving a first order differential equation for the current

$$\frac{dI}{dz} = -(j\omega C + G)\,V \qquad (4.04)$$

We have again a system of coupled first order differential equations that describe the behaviour of voltage and current on the lossy transmission line

$$\frac{dV}{dz} = -(\,j\omega L + R)\,I \qquad (4.05)$$

$$\frac{dI}{dz} = -(j\omega C + G)\,V \qquad (4.06)$$

These equations (4.05, 4.06) are the "telegraphers' equations" for the lossy transmission line. One can easily obtain a set of uncoupled equations by differentiating with respect to the coordinate z as done earlier

$$\frac{d^2V}{dz^2} = -(\,j\omega L + R)\frac{dI}{dz} = (\,j\omega L + R)(\,j\omega C + G)V \qquad (4.07)$$

$$\frac{d^2I}{dz^2} = -(\,j\omega C + G)\frac{dV}{dz} = (\,j\omega C + G)(\,j\omega L + R)I \qquad (4.08)$$

These equations (4.07, 4.08) are the "telephonists' equations" for the lossy line.

The telephonists' equations for the lossy transmission line are uncoupled second order differential equations and are again wave equations. The general solution for the voltage equation is

$$V(z) = V^{+}e^{-\gamma z} + V^{-}e^{\gamma z} = V_{+}\,e^{-\alpha z}\,e^{-j\beta z} + V^{-}e^{\alpha z}\,e^{j\beta z} \qquad (4.09)$$

Where the wave propagation constant is now the complex quantity

$$\gamma=\sqrt{(j\omega L+R)(j\omega C+G)}=\alpha+j\beta \tag{4.10}$$

The real part α of the propagation constant ɤ describes the attenuation of the signal due to resistive losses. The imaginary part β describes the propagation properties of the signal waves as in loss-less lines. The exponential terms including α are "real", therefore, they only affect the "magnitude" of the voltage phase. The exponential terms including β have unitary magnitude and purely "imaginary" argument, affecting only the "phase" of the waves in space.

The current distribution on a lossy transmission line can be readily obtained by differentiation of the result for the voltage

$$\frac{dV}{dz}=-(j\omega L+R)I=-\gamma V^{+}e^{-\gamma z}+\gamma V^{-}e^{\gamma z}$$

This gives

$$I(z)=\sqrt{\frac{(j\omega C+G)}{(j\omega L+R)}}(V^{+}e^{-\gamma z}-V^{-}e^{\gamma z}) \tag{4.11}$$

$$=\frac{1}{Z_o}(V^{+}e^{-\gamma z}-V^{-}e^{\gamma z})$$

$$Z_o=\sqrt{\frac{(j\omega L+R)}{(j\omega C+G)}} \tag{4.12}$$

For loss-less transmission line, R = G = 0, equation 4.13 becomes

$$Z_0=\sqrt{\frac{L}{C}} \tag{4.13}$$

For both loss-less and lossy transmission lines the characteristic impedance does not depend on the line length but only on the metal of the conductors, the dielectric material surrounding the conductors and the geometry of the line cross-section, which determine *L*, *R*, *C*, and *G*.

4.2 Coaxial Pulse forming line

Transmission line based pulse forming line can be made by using commercially available coaxial cables or by putting two/three concentric cylinders with suitable dielectric filled between them. A coaxial pulse forming line is frequently used to produce extremely high pulsed power (multi-gigawatt) levels by compressing the pulse duration into nanoseconds.

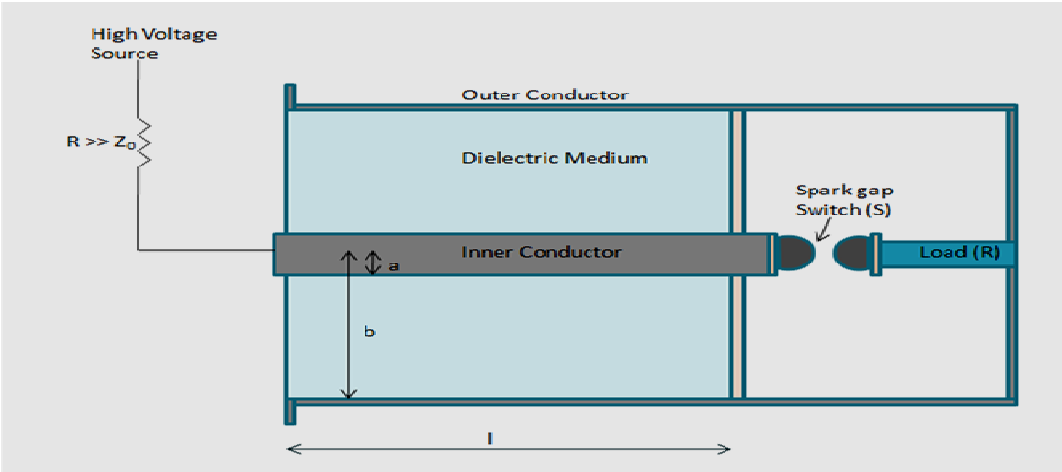

Figure 4.05 Coaxial pulse forming line

The configuration of basic coaxial pulse forming line is shown in Figure 4.05. It comprises of two single length concentric cylinders with suitable dielectric filled between them and a fast switch. The dielectric medium used in coaxial pulse forming line is mentioned in Table 4.01.

Dielectric Medium	Dielectric Constant	Break down Voltage
Deionised Water	81	150 - 300 kV/cm
Ethylene glycol	42	250 kV/cm
Mineral Oil	2-3	150 kV/cm
Castor Oil	4-5	200 kV/cm
Polyethylene	2-2.5	200 kV/cm

Table 4.01 Dielectrics used in PFL

A high voltage source charges the coaxial line, which behaves as a capacitor for a slow charging voltage. After completing the charging of the single line, the closing switch (S) is turned on.

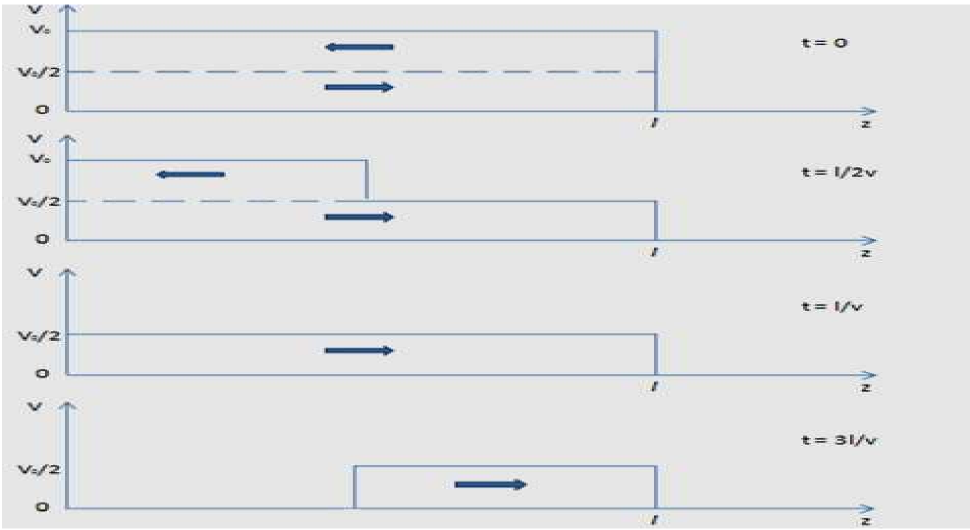

Figure 4.06 Pulsed power generation from a single line.

The charging voltage and the length of the single line are V_0 and l, respectively. The closing switch is turned on at t=0. The waves with a voltage $V_0/2$ and a velocity (v) propagate into two directions, to the load side and to the source side. If the load resistance R is the same as the characteristic impedance of the line Z_0, all the wave energy propagating to the load side is absorbed by the load resistor. The wave propagating to the source side is reflected back to the load side, since the source impedance is usually larger than Z_0. The voltage distributions on the single line at different times are easily obtained as shown in Figure 4.06. The waveform of the output voltage on the load is shown in Figure 4.07. The voltage becomes half of the charging voltage of the single line, and the pulse width becomes two times of l/v.

Figure 4.07 Output Voltage

The design of PFL includes optimization of inner (a) and outer radius (b) of the coaxial cylinder of length (l), dielectric material (ε_r), to get required pulse duration (τ) and source impedance (Z_0). The length of the line will govern the pulse duration which gets altered by the dielectric material used in it by virtue of velocity of wave propagation during the transmission in the medium. The basic design equations are as follows [5, 87];

(i) Velocity of propagation,

$$V_{pp} = \frac{c}{\sqrt{\varepsilon_r}} \quad \text{(in m/s)} \tag{4.14}$$

Where *c* is the speed of light in vacuum

(ii) Pulse duration,

$$\tau = \frac{2l}{V_{pp}} \tag{4.15}$$

(iii) Maximum stress will occur on the outer diameter (2a) of the inner cylinder and given by:

$$E_{max} = \frac{V_{pk}}{a \ln\left(\frac{b}{a}\right)} \tag{4.16}$$

Where V_{pk} is the peak PFL charging voltage

(iv) Inductance per unit of coaxial PFL,

$$L = \frac{\mu_0 \mu_r}{2\pi} \ln\left(\frac{b}{a}\right) \tag{4.17}$$

(v) Capacitance per unit of coaxial PFL,

$$C = \frac{2\pi\varepsilon_0\varepsilon_r}{\ln\left(\frac{b}{a}\right)} \tag{4.18}$$

(vi) Characteristic impedance of the coaxial PFL,

$$Z_0 = \sqrt{\frac{L}{C}} \tag{4.19}$$

(vii) Load reflection coefficient,

$$\rho_0 = \frac{Z_L - Z_0}{Z_L + Z_0} \tag{4.20}$$

The compactness on the PFL depends on the length of the conductor used, dielectric constant of the medium, temperature and stress on the medium. We will be exploring these parameters to develop compact pulse forming lines.

4.3 Development of solid dielectric pulse forming line using ceramic material

Compact pulse forming line can be made using ceramics material as it has large dielectric constant (few hundreds to few thousands) and high bulk breakdown strength (more than 300 kV/cm). Conventionally PFL are made up of castor oil, plastics and other dielectric materials whose relative permittivity varies 2-10 [88]. The length of PFL is increased if these materials are used for generating few hundreds of nanoseconds of pulse width. The length of the PFL, $L \sim 1/\varepsilon^{1/2}$ (here $\varepsilon = \varepsilon_0\varepsilon_r$, ε_0 is the vacuum permittivity). The higher ε can lead to shorter length of the PFL. So, the length of the PFL can be reduced by using high relative permittivity material such as ceramics. Ceramic materials also have low dielectric losses. Ceramics materials can be used to construct very low impedance pulse forming lines for applications to low impedance load such as z-pinches. With the recent development in material technologies, it is now possible to employ the glass ceramic slab or sintered $SrTiO_3$ ceramic with high relative permittivity (ε_r) of up to 300 as energy storage dielectrics in PFL [89-90]. The ceramic material is ideal for energy storage in PFL, but large ceramic bulks are difficult to manufacture. The energy density (w) in the PFL is determined by both ε and breakdown strength (E_b). The energy density is more important because $w \sim E_b{}^2$. However, the E_b of conventional ceramic dielectrics is usually limited by the presence of porosity which acts as the source of local electrical stress concentration. Some pioneer work has been done by using sintered ceramic bulk as dielectric during recent years [91 - 92]. The focus of the former work is fabricating larger ceramic bulk with low porosity to increase the output voltage of PFLs, which is quite difficult and greatly limited by the level of material technology. It is also reported that barium titanate tiles has been made and by milling grooves into the sides of the tiles it has been possible to charge them up to 60 kV without breakdown [33].

In an effort to develop transmission line with high energy storage capabilities for compact pulsed power system for single shot applications, ceramic dielectrics and their electrical breakdown strength are needed to be studied. The composite dielectric can be made using ceramic materials. Ceramic material was mixed with epoxy resins and higher dielectric constant has been reported [4,36,89]. Ceramic material such as barium titanate and barium strontium titanate has very high relative permittivity so very high capacitances and compact PFL can be made using these materials. We have investigated composite dielectric material using barium titanate and neoprene rubber for making compact PFL as rubber has better elastic properties compared to epoxies. Barium tiatnate was not widely used in pulsed power systems due to its piezoelectric properties [93]. During high voltages discharges local stresses are developed in barium titanate, which breaks the material. To overcome these stresses barium titanate was mixed with neoprene rubber, as rubber was an elastic material. When local stresses are developed in barium titanate due to its piezoelectric properties during the high voltage discharges the rubber will expand and contract to absorb the stress and regain its original shape after the discharges.

4.31 Physical properties of barium titanate

Barium Titanate has a very high relative permittivity (~ 1200 - 5000) so it was used for making compact pulse forming line. The chemical formula of barium titanate is $BaTiO_3$. It is an inorganic compound. Barium titanate is a white powder and transparent for larger crystals. Barium titanate is a ferroelectric ceramic material, with a photorefractive effect and piezoelectric properties. The physical properties of barium titanate are mentioned in Table 4.02. The barium titanate solid exists in five phases, listing from high temperature to low temperature are hexagonal, cubic, tetragonal, orthorhombic, and rhombohedral crystal structure. All of the phases exhibit the ferroelectric effect except the cubic phase. The high temperature cubic phase is easiest to describe, consisting of octahedral TiO_6 centers that define a cube with Ti vertices and Ti-O-Ti edges. In the cubic phase, Ba^{2+} is located at the center of the cube, with a nominal coordination number of 12. Lower symmetry phases are stabilized at lower temperatures, associated with the movement of the Ba^{2+} to off-center position. The remarkable properties of this material arise from the cooperative behaviour of the Ba^{2+} centres.

Formulae	$BaTiO_3$
Composition	Ba – 58.9, O – 20.6, Ti – 20.5
Purity	99.9%
Particle Size	1 – 3.0 microns
Dielectric constant	1200 - 5000
Boiling Point	1640 ^{0}C
Density	6.08 gm/cm^3
Electric Resistivity	50 μΩ.cm
Crystal Structure	Tetragonal

Table 4.02 Physical properties of Barium Titanate [94]

Barium titanate is manufactured by heating barium carbonate and titanium dioxide. The reaction proceeds via liquid phase sintering. Single crystals can be grown around 1100 °C from molten potassium fluoride. Barium titanate is a dielectric ceramic used for capacitors. It is a piezoelectric material for microphones and other transducers. As a piezoelectric material, it was largely replaced by lead zirconate titanate, also known as PZT. Polycrystalline barium titanate displays positive temperature coefficient, making it a useful material for thermistors and self-regulating electric heating systems.

4.32 Physical properties of neoprene rubber

Neoprene rubber is an elastic material so it was used to absorb the mechanical stresses that are developed during high voltage charge and discharge inside the pulse forming line. Neoprene is a family of synthetic rubbers that are produced by polymerization of chloroprene. Table 4.03 shows the physical properties of the Neoprene rubber. Neoprene exhibits good chemical stability, and maintains flexibility over a wide temperature range. It is used in a wide variety of applications, such as electrical insulation, liquid and sheet applied elastomeric membranes or flashings, and automotive fan belts. Neoprene is produced by free-radical polymerization of 2-chlorobutadiene. The polymerization is conducted in an aqueous emulsion, using diverse emulsifying agents such as alkyl sulfonates.

Common Name	Neoprene
Composition	Chloroprene
Material Designation (ASTM D-2000)	BC, BE
Temperature range	- 30 F / 212 F
Tensile Strength, (PSI)	1000-3000
Elongation %	200-500
Hardness Range (Durometer Shore A)	15 to 95
Specific Gravity (Base Material)	1.23
General Properties	Weathering Resistance, Flame retarding,

Table 4.03 Physical properties of Neoprene Rubber [95]

4.4 Fabrication of barium titanate – rubber pulse forming Line

A simple coaxial pulse forming line was made as discussed in section 4.2. It has two coaxial cylinders and the dielectric medium filled between the cylinders. A coaxial pulse forming line was made using two coaxial SS 304 cylinders (Figure 4.08).The diameter of the inner cylinder was 120 mm, and the diameter of the outer cylinder wais 240 mm. The thickness of outer cylinder was 2mm. The length of the PFL was 350 mm.

Figure 4.08 Barium titanate rubber pulse forming line

The volume between the two cylinders was filled with composite mixture of barium titanate and neoprene rubber. The mixing ratio was selected after preparing few samples of composite mixture at different ratios and it was found that, as the quantity of barium titanate was increased in the composite mixture (> 1:10) the uniformity and homogeneity of composite mixture was drastically reduced and it becomes very hard. At lower ratio it was mixed properly and uniformity is seen. So, the composite mixture was prepared by mixing barium titanate of 1-3 micron size with neoprene rubber in the ratio of 1:10 and studied. Also, for higher mixing ratio it increases the quantity of barium titanate, so the piezio-electric effect will dominate and leads to reduction in electrical breakdown strength. At lower ratio of barium titanate the dielectric constant will be relatively low so it will not show significant compactness achieved. Other additives Magnesium oxide (MgO), Zinc oxide (ZnO), Steric acid and mineral oil in traces are added for the curing of the rubber. These materials are added with barium titanate and neoprene rubber and mixed in rolling mill for an hour then it is filled between the cylinder by heating the mixture to 120 ^{0}C and then gradually cooling it to room temperature. A solid dielectric pulse forming line was made with the composite mixture of barium titanate and rubber and its parameters are calculated using equation 4.14 to 4.20. The relative permittivity of the composite dielectric was measured and found to be 85. It is discussed in chapter 5.

Inductance of the PFL, L = 48 nH

Capacitance of the PFL, C = 2.4 nF

Impedance of the PFL, Z = 4.5 Ω

Transit time, T = 21 ns

The high voltage testing and the effect of applied electric field on the non linear behaviour of relative permittivity of the composite dielectric are discussed in chapter 5.

4.5 Development of water helical pulse forming line

Pulse power system generally use deionised water as intermediate energy storage. Deionised water is used as liquid dielectric medium in pulsed power system because of its high dielectric constant, high dielectric strength and efficient energy storage capability, which allows designing compact and efficient low impedance pulse forming lines. In a PFL made of conventional coaxial line it is hard to produce longer duration high voltage pulse in smaller size. An increase in the pulse width requires the length of the coaxial pulse forming line be increased. So the length of the coaxial PFL required becomes significantly long for the generation of longer duration rectangular pulses. An alternative topology was investigated to increase the pulse width in compact geometry. The pulse width was also increased by using helical inner conductor, without physically increasing the length of the PFL. The helical pulse forming line produces longer pulse compared with conventional coaxial transmission line as it has higher inductance and increases the transit time. This helical pulse forming line also increases the impedance and the width of the pulses formed without increasing the length of the PFL. The transmission line characteristic of helical inner conductor is used for generating longer duration rectangular high voltage pulse. We have designed and investigated helical water pulse forming line for the generation of longer duration rectangular pulse to deliver peak power to the loads. The effect of reduction in water temperature on relative permittivity is also investigated for increase in pulse width, which can further reduce the length of the PFL and can make compact systems.

4.51 Relative permittivity of water

The relative permittivity of water (ε_r) is a complex quantity and depends on the frequency. The relative permittivity is given by

$$\varepsilon_r = \varepsilon_\infty + (\varepsilon_s - \varepsilon_\infty) / (1+j\omega\tau_D) \qquad (4.21)$$

Where ε_∞, is the relative permittivity at infinite frequency (the square root of the index of refraction for visible light)

ε_s, is the static relative permittivity at zero frequency.

τ_D, is the Debye relaxation time and is the measure of the time required for the molecular dipoles to reorient in a changing field.

The ratio of the imaginary part of ε_r, to the real part is termed the loss tangent. It is apparent that for $\omega\tau_D << 1$, $\varepsilon_r = \varepsilon_s$. For polar liquids $\varepsilon_\infty << \varepsilon_s$ and can often be neglected.

Table 4.04 lists reported relative permittivity and loss tangents of water as a function of frequency and temperature. It shows that the high ε_r values are operative to time scales of 1 ns. The loss tangent values at low frequencies are suspected to be due to ohmic impurities rather than actual properties of the pure substance.

The Debye relaxation time for water is extremely small, being of order 10 ps at 25^0C and shows exponential increase with decreasing temperature due to increasing viscosity. However, τ_D remains below a nanosecond and hence is not of great concern in high-energy pulse-power applications [66]. A useful empirical formula for the temperature dependence of the static relative permittivity of water is [71]

$$\varepsilon_s = 78.54\,(1 - 4.579 \times 10^{-3}\, T_1) + 1.17 \times 10^{-5}\, T_1^2 - 2.8 \times 10^{-8} T_1^3 \qquad (4.22)$$

Where $T_1 = T_0 - 25$ is the centigrade temperature.

As T rises, the ε_s value falls slowly, decreasing from 88.1 at 0 ^{0}C to 78.2 at 25 ^{0}C

The decrease in ε_s with increasing temperature results from the increased thermal agitation of the molecular dipoles.

T (^{0}C)	*f* (Hz)	1 x 10^5	1 x 10^6	1 x 10^7	1 x 10^8	3 x 10^8	3 x 10^9	1 x 10^{10}
1.5	ε_r	87.0	87.0	87.0	87.0	86.5	80.5	38
	tan δ	0.1900	0.0190	0.0020	0.0070	0.0320	0.3100	1.0300
5	ε_r	-	85.5	-	-	85.2	80.2	41
	tan δ	-	0.0220	-	-	0.0273	0.2750	.09500
15	ε_r	-	81.7	-	-	81.0	78.8	49
	tan δ	-	0.0310	-	-	0.0210	0.2050	0.7000
25	ε_r	78.2	78.2	78.2	78	77.5	76.7	55
	tan δ	1.4000	0.0400	0.0046	0.0050	0.0160	0.1570	0.5400
35	ε_r	-	74.8	-	-	74.0	74.0	58
	tan δ	-	0.0485	-	-	0.0125	0.1270	0.400
45	ε_r	-	71.5	-	-	71.0	70.7	59
	tan δ	-	0.0590	-	-	0.0105	0.1060	0.4000
55	ε_r	-	68.2	-	-	68	67.5	60
	tan δ	-	0.0720	-	-	0.0092	0.0890	0.3600
65	ε_r	-	64.8	-	-	64.5	64.0	59
	tan δ	-	0.0865	-	-	0.0084	0.0765	0.3200
75	ε_r	-	61.5	-	-	61	60.5	57
	tan δ	-	0.103	-	-	0.0077	0.0660	0.2800
85	ε_r	58	58	58	58	57	57	56.5
	tan δ	1.24	0.124	0.0125	0.0030	0.0073	0.0660	0.2800

Table 4.04 Relative permittivity and loss tangent as a function of frequency for water [96]

4.52 Electrical breakdown in water

Electrical breakdown in water has to be avoided inside the pulse forming line. The physical mechanisms of electrical breakdown in liquids are not completely understood. It is generally thought that for short sub-microsecond time scales, breakdown is due to ionization, while for time scales greater than few microsecond the, breakdown is in part due to the thermal effects causing bubbles. Gas evolution due to electrolysis may also be important [97]. Other proposed mechanisms of electrical breakdown in water concern the ionization and migration of water molecules [67]. Electrical breakdown in water occur through a statistical probability governing the initiation of the breakdown process, followed by the propagation of a streamer, and then a resistive-inductive circuit response as the current builds up in the newly formed ionization channel.

The empirical relation for liquid breakdown was given by J. C. Martin and his group [86]. After performing a large number of dielectric breakdown (E_b) measurements for various liquids as a function of electrode area A (cm^2) and effective stress time t, (in ps), where t_e is the time from 63 percent V_{max} to V_{max} for a voltage pulse $V(t) = V_{max}(l - \cos \omega t)$ [86].

$$E_b t_e^{\frac{1}{3}} A^{\frac{1}{10}} = C \ (Constant) \tag{4.23}$$

Where,

C = 0.5 for transformer oil, methyl alcohol, ethyl alcohol

C = 0.7 for Glycerine, Caster oil

C = 0.3 for water positive electrode breakdown

C = 0.6 for water negative electrode breakdown

For sub-microsecond time scales it was found the breakdown strength E_b (MV/cm) of water is polarity dependent. Breakdowns in water usually originates from the positive electrode in parallel plate electrodes geometry. For differently shaped electrodes such as for coaxial cylindrical electrodes, the sharper electrode is usually kept negative to allow higher voltage operation. These results are normally independent of the smoothness of the electrodes as long as gross roughness is avoided.

4.6 Fabrication of water helical pulse forming line

Water helical PFL was designed and fabricated (Figure 4.09). The helical PFL inner conductor was made up of SS-304 strip rolled on the delrin cylinder. The outer cylinder was made up of SS-304. The length of the PFL was 800 mm. The volume between the inner strip and outer cylinder was filled with deionised water circulated through a pump and deionizer unit. The conductivity of the deionised water was less than 0.2µS/cm.

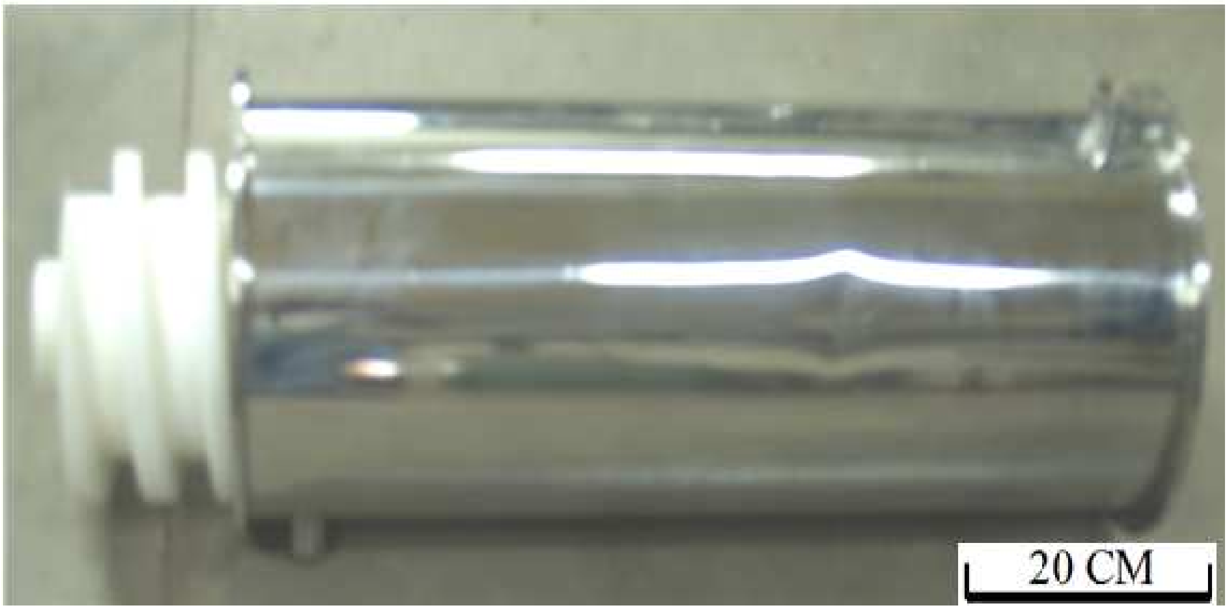

Figure 4.09 Water helical pulse forming line

The capacitance per unit length of helical line is given by [98]

$$C_h = C_0\,[1 + (\varepsilon_r - 1)\,.\,D(\gamma a)].\,[1 - K_c^2\,(\gamma a, \gamma b)]^{-1} \qquad (4.24)$$

The inductance per unit length of helical line is given by [84, 98]

$$L_h = L_0\,[1 - K_L^2\,(\gamma a, \gamma b)] \qquad (4.25)$$

Where, C_0 and L_0 is capacitance and inductance per unit length of helical line without a dielectric and a metal shield, K_c (γa, γb) and K_L (γa, γb) is the capacitive coupling coefficient and inductive coupling coefficient between the helical line and the metal shield and D(γa) is the modified coefficient of the dielectric [98].

$$C_0 = 2\pi\varepsilon_0 / I_0(\gamma a) \,.\, K_0(\gamma a) \quad (4.26)$$

$$L_0 = \mu_0 \beta^2 .\, \cot^2 \psi \,.\, I_1(\gamma a) \,.\, K_L(\gamma a) / 2\pi\gamma^2 \quad (4.27)$$

$$K_c^2 = I_0(\gamma a) \,.\, K_0(\gamma b) / I_0(\gamma b) \,.\, K_0(\gamma a) \quad (4.28)$$

$$K_L^2 = I_1(\gamma a) \,.\, K_L(\gamma b) / I_1(\gamma b) \,.\, K_L(\gamma a) \quad (4.29)$$

$$D(\gamma a) = \gamma a \,.\, I_0(\gamma a) \,.\, K_L(\gamma a) \quad (4.30)$$

Here, a is the radius of the inner helical line, b is the radius of the outer cylinder, ψ is the helix angle. I_n and K_n , with n = 0,1 are the modified Bessel function and modified Hankel function, γ , β and k are propagating constant of electromagnetic field along the radial direction, axial direction and in free space.

The impedance of pulse forming line is given by [5],

$$Z = \sqrt{\frac{L_h}{C_h}} \quad (4.31)$$

Pulse duration across the load is given by [5],

$$T = 2\sqrt{L_h C_h} \quad (4.32)$$

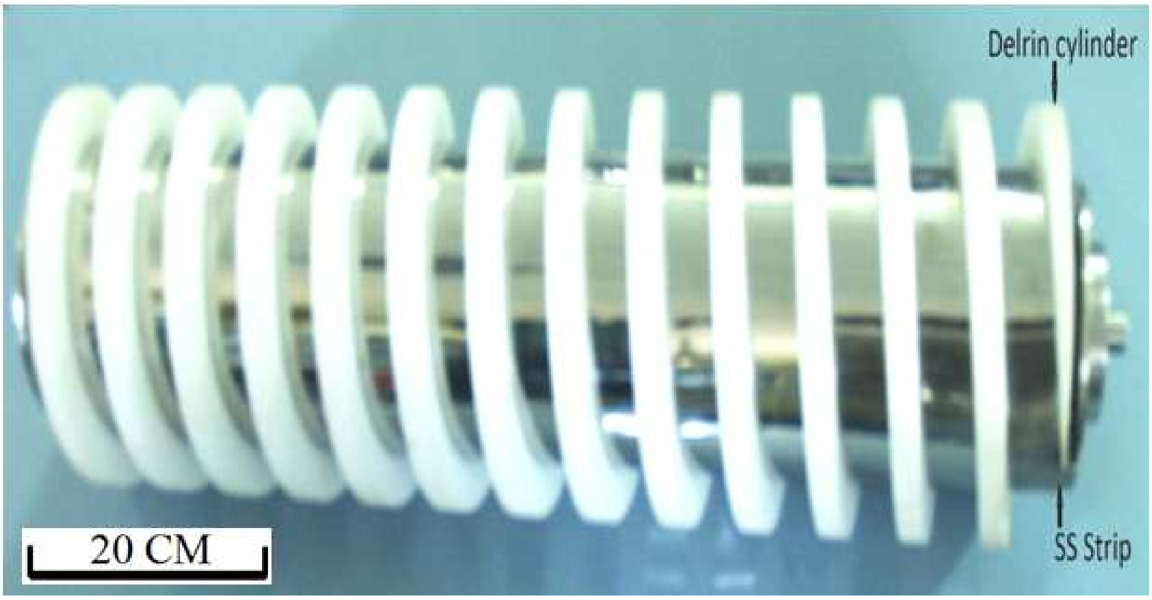

Figure 4.10 Inner helical conductor

The Helical pulse forming line was fabricated with following parameters (Figure 4.10).

Diameter of inner helical line conductor, a = 168 mm

Diameter of outer cylinder, b = 236 mm

Thickness of outer cylinder, t = 2 mm

Number of turns = 13

Width of SS conductor strip = 39.5 mm

Thickness of SS conductor strip = 0.5 mm

Pitch of the SS strip = 20 mm

Length of the PFL = 800 mm

Capacitance of helical pulse forming line, C = 5.9 nF

Inductance of helical pulse forming line, L = 3 μH

Impedance of helical pulse forming line, Z_0 = 22 Ω

Pulse width = 260 ns

The helical pulse forming line was pulse charged with a high voltage pulse transformer and discharges into the load through a high voltage self breakdown pressurized sparkgap switch. The testing and experimental results are discussed in chapter 5.

4.7 Summary

The compact pulse forming line can be developed using high dielectric constant medium inside the PFL and also by increasing the length of the PFL. A compact solid dielectric pulse forming line was designed and developed using a composite mixture of barium titanate ceramic and neoprene rubber. Barium titanate is piezoelectric material and stresses are produced in it during high voltages discharges. The neoprene rubber was mixed with barium titanate as it will absorb the stress produced during charging and discharging of the PFL. Another compact pulse forming line using transmission line characteristic of helical inner conductor was designed and developed. Deionised water was used as dielectric medium inside the PFL. The high voltage testing and result analysis of these compact pulse forming lines are discussed in chapter 5.

CHAPTER – 5

EXPERIMENTAL RESULTS AND ANALYSIS OF COMPACT PULSE FORMING LINES

5.1 Testing of the solid composite dielectric of barium titanate and rubber

The high voltage performance of the composite dielectric material can be predicted by the behaviour of the composite dielectric as a whole. The following considerations determine the performance as a whole:

- The stress distribution at different parts of the material is distorted due to the different dielectric constant and conductivities.
- The breakdown characteristics at the surface are affected by the insulation boundaries of other dielectric.
- The internal or partial discharge products of one dielectric invariably affect the other dielectric.
- The chemical ageing products of one dielectric also affect the performance of other dielectric.

The end point of the solid insulation is normally reached through puncture, thermal runaway, electrochemical breakdown, or mechanical failure leading to complete electrical breakdown.

The high voltage breakdown testing of the composite dielectric material was done and its relative permittivity was also calculated. The composite dielectric PFL was pulse charged and its performance was seen. The relative permittivity of ceramic behaves nonlinear to different applied electric field. The composite dielectric material was subjected to different electric field and its non linear behaviour was experimentally investigated and reported in the following section.

5.11 High voltage breakdown testing of the composite dielectric material

The breakdown strength of a material is examined generally by two methods: static tests in which a number of identical samples are stressed at a constant electric field and the time to breakdown of each sample is measured; or dynamic tests in which the electrical stress applied to an equivalent sample set as a function of time and the magnitude of electric field and the breakdown of each sample recorded**.** The dynamic testing is generally preferred, because the variation in the measured results is less than that for equivalent static testing [99]. Furthermore, static testing, particularly over extended periods of time, requires critical control of the electric field, as small variations in field can give rise to significant variations in the breakdown time. Static tests are useful in the determination of a figure of merit and life of the sample [59].

The schematic diagram of the high voltage testing of composite dielectric material is shown in Figure 5.01. The composite dielectric material was cut precisely in the size of 1 cm x 1 cm x 1 cm to prepare the test sample. The test sample was placed between the two spherical electrodes connected to a sinusoidal high voltage source. The voltage was manually increased to generate high voltage and applied across the sample. A 50 Hz sinusoidal high voltage pulse was applied across the sample and the peak breakdown voltage was recorded.

.

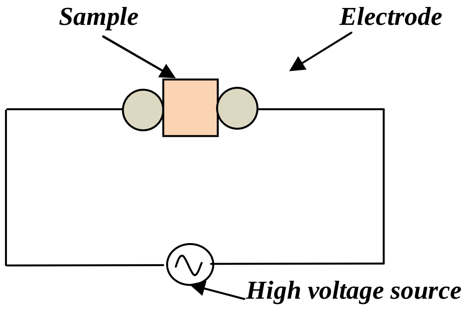

Figure 5.01 Schematic of high voltage testing of the composite dielectric

The breakdown voltage of dielectric was measured by taking identical sample of composite dielectric and measuring its breakdown voltage. We have prepared 20 samples and 18 samples were tested. The breakdown voltages of the samples are recorded. Figure 5.02 show the plot of number of samples breakdown at specific voltage.

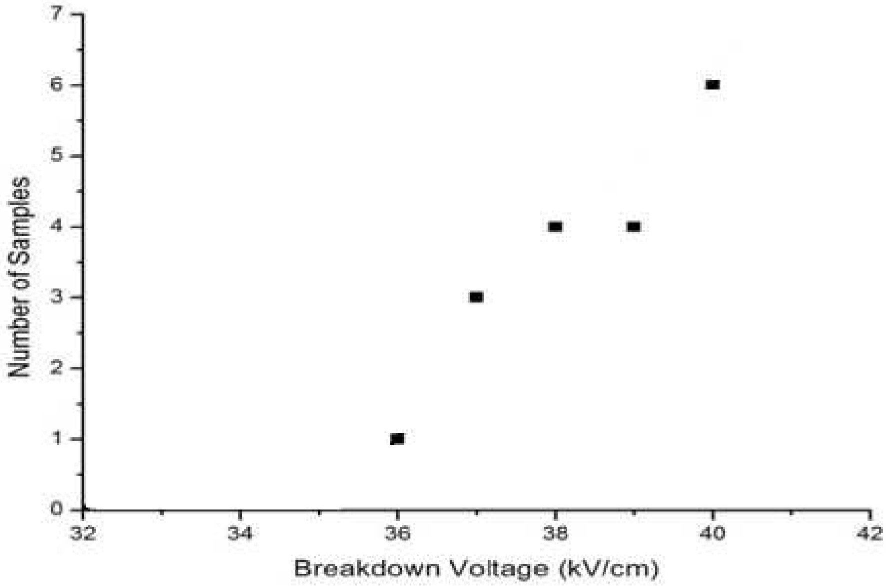

Figure 5.02 Numbers of samples breaks at rated voltage

We could see from the Figure 5.02 that none of the sample breaks below 35 kV and voltage breakdown occurs above 35 kV. It was confirmed that the breakdown is not due to surface flashover and it is due to internal breakdown in the sample by placing the disc between the electrodes. The breakdown strength of composite dielectric is lower than the bulk breakdown strength of the individual material. This can be explained by the stress concentration at the interfaces between the barium titanate and the neoprene rubber in the composite dielectric. When the high dielectric constant material such as barium titanate is added into the rubber, the electrical field in the rubber around the barium titanate is much larger than that in the bulk. The most stressed part is close to the barium titanate ceramic tips or the edge. These stresses also increase with increase in barium titanate aspect ratio. Breakdown is more likely to be initiated at these highly stressed regions than in the bulk material, so a reduction in the overall breakdown strength is expected. The reduction in breakdown strength was attributed to the stress concentration at the interfaces between the ceramic and the neoprene rubber. So, it was concluded that the composite mixture could width stand the voltage up to 35 kV.

5.12 Measurement of relative permittivity of the composite dielectric

The schematic diagram for the measurement of relative permittivity is shown in Figure 5.03. The relative permittivity of the composite dielectric material made up of barium titanate and neoprene rubber was measured by cutting a disk shape of the composite dielectric material and measuring its capacitance. The composite dielectric material disk was placed between the two circular electrodes of 90 mm diameter and its capacitance was measured with LCR meter. The accuracy in measurement of capacitance is 0.2 % in the range of 100 pF to 1 mF, and up to 2.5 % in the range of 1 pF to < 100 pF and > 1mF to 100 mF respectively.

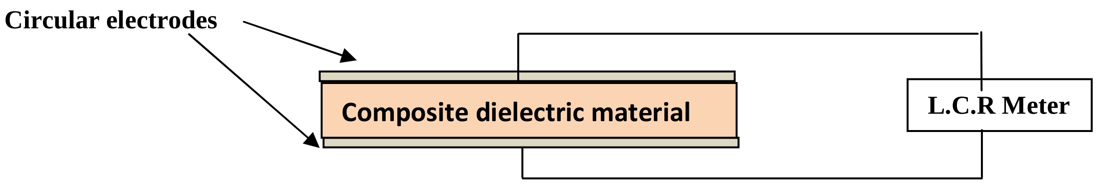

Figure 5.03 Schematic diagram of relative permittivity measurement

The diameter and the thickness of the composite dielectric material disc are 90 mm and 10 mm (Figure 5.04).

Figure 5.04 Disk of composite dielectric

The relative permittivity (ε_r) of the composite dielectric material is given by

$$\varepsilon_r = \frac{C.d}{\varepsilon_0.A} \tag{5.01}$$

Where

C is the capacitance measured

A is the area of the circular electrode

d is the thickness of the disk

The capacitance was measured to be 475 pF. The relative permittivity of the composite dielectric was calculated and found to be 85.

5.2 Testing of barium titanate – rubber pulse forming line

The schematic diagram for testing of composite dielectric of barium titanate - rubber PFL is shown in Figure 5.05. The testing setup consists of a high voltage pulse transformer [100], which pulse charges the composite dielectric PFL. The self breakdown sparkgap switch after the PFL breaks at set voltage and the PFL was then discharged into a 5 Ω resistive load. The distance between the electrodes and the pressured inside the sparkgap switch can be adjusted, so that it breaks at set voltage. The gap and pressure inside the sparkgap switch was kept such that it breaks at 120 kV.

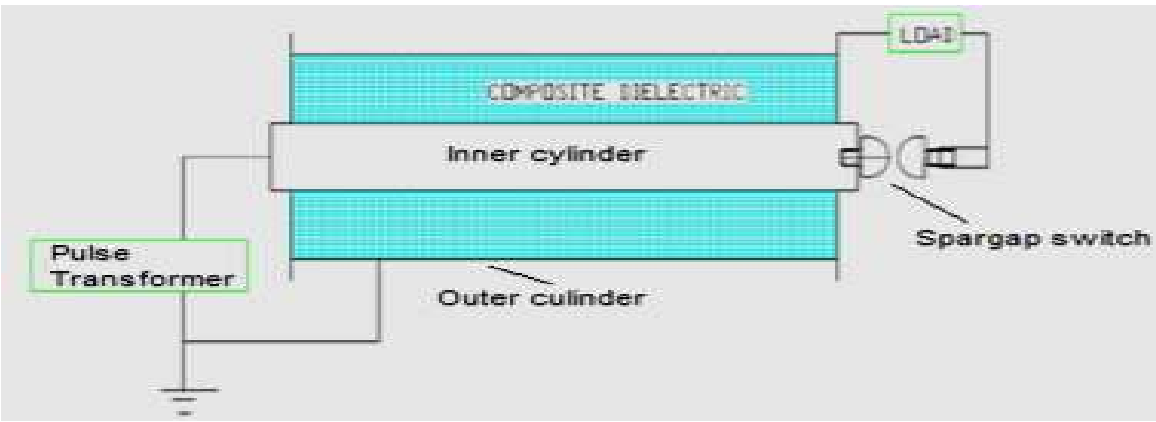

Figure 5.05 Experimental set up

5.21 Experimental results

The voltage across the composite dielectric PFL was measured with voltage divider (VD-100) and the voltage across the load was measured with voltage divider (PVM-5). The accuracy of VD-100 and PVM 5 above 1 MHz signal frequency is < 4% and < 2% respectively. The specifications of these standard voltage dividers are mentioned in Appendix-2. The pulse transformer charge the composite dielectric PFL to 120 kV peak in 200 ns, the sparkgap switch after the PFL breaks and the PFL discharge into the 5 Ω resistive load. A high voltage pulse of 70 kV, 21 ns pulse was measured across the load. The composite dielectric PFL charging voltage and the voltage across the load measured is shown in Figure 5.06.

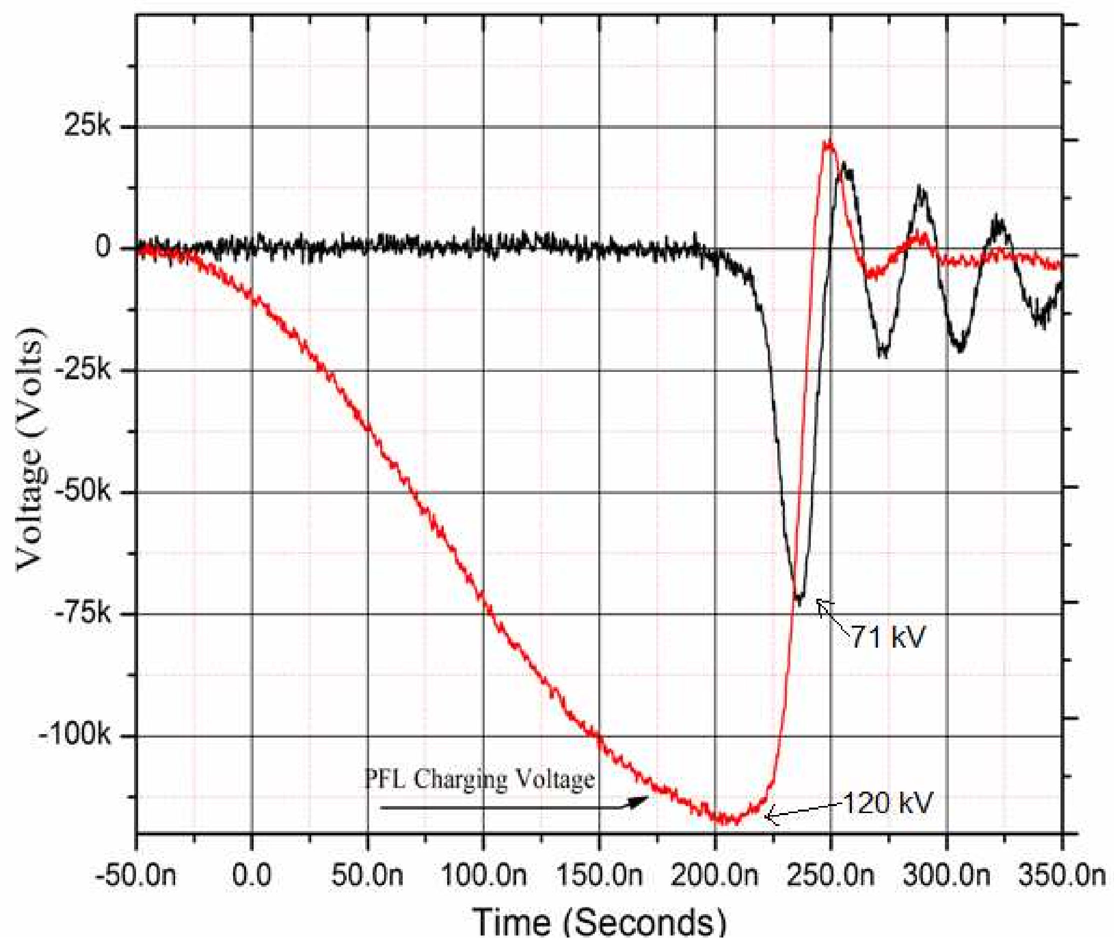

Figure 5.06 PFL charging voltage and load voltage

The voltage pulse duration (T) generated across the load is given by

$$T = 2\,\frac{\sqrt{\varepsilon_r \mu_r}}{c}\,l \qquad (5.02)$$

ε_r is the relative permittivity of the medium

μ_r is the relative permeability of the medium

c, is the speed of the light

l is the length of the PFL

To generate a pulse width of 21 ns only with neoprene rubber (ε_r = 6, μ_r,= 1), 1320 mm of length of PFL is required and to generate a pulse width of 21 ns with this composite mixture (ε_r = 85, μ_r,= 1), 350 mm of length of PFL was used.

The compactness in length of the PFL was achieved by mixing of barium titanate in neoprene rubber, which reduces the length of the PFL by a factor of 3.8. The pulse duration can further be increased by increasing the length of the PFL.

5.3 Investigation of non linear effect of electric field on composite dielectric

The ceramic materials behave non-linearly with different applied electric field [101 - 102]. It is also well known that the dielectric constant of barium titanate is non linear and it falls with applied electric field stress. Barium titanate ceramic belong to an important class of ferroelectric dielectric which exhibit very large dielectric constant due to the spontaneous alignment or polarization of electric dipoles [103]. Barium titanate has spontaneous electrical polarization associated with an ionic displacement. In the barium titanate dipole originates from the displacement of the Ti ion within the oxygen cage (Figure 5.07). These dipoles are formed in ferroelectric materials which have a non-centro symmetric polar lattice at temperatures below critical temperature. In barium titanate, an off-centre displacement of a titanium ion within an octahedral cage of oxygen ions leads to such a polar lattice. The electric dipoles which result from this displacement can be ordered parallel to each other, within the crystal regions known as domains. When an electric field is applied to the material these domains can switch from one direction of spontaneous alignment to another giving rise to very large changes in polarisation and dielectric constant. At very high electric fields all of the domains are aligned in parallel and consequently no further polarisability is possible and the dielectric constant falls. This results in the non-linear behaviour of the dielectric constant with applied electric field.

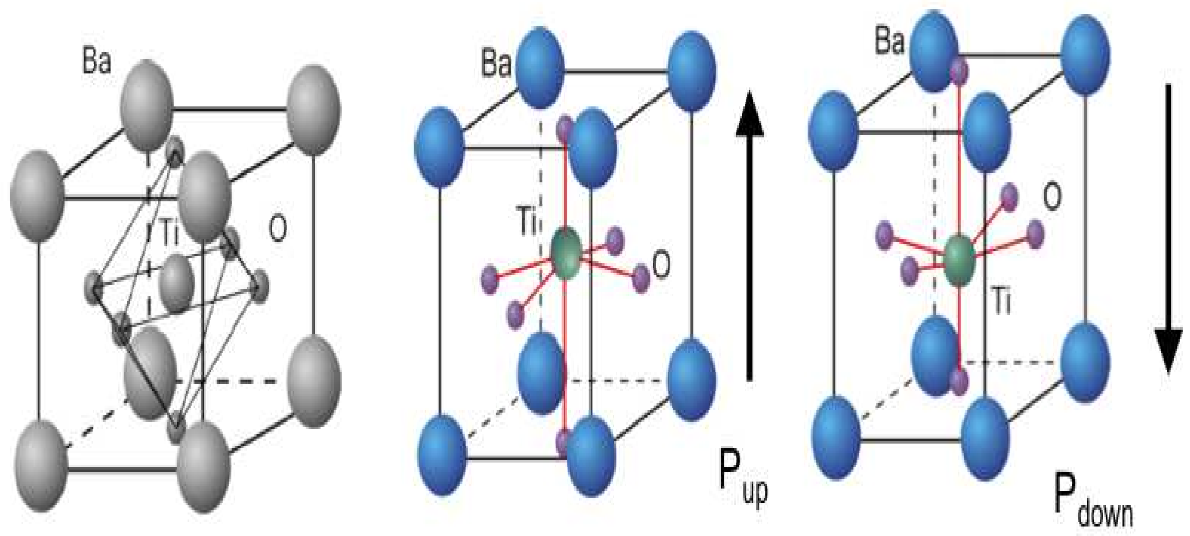

Figure 5.07 Crystal structure of Barium Titanate

We have experimentally investigated the effect of different applied electric field on the pulse width and measured it across the load. The breakdown voltage of sparkgap was varied and the composite dielectric PFL was charged at different voltage and discharged in to resistive load. The duration of pulse width across the load depends on relative permittivity (ε_r) of the dielectric being used in PFL and the length of the PFL (5.02). The pulse width was measured experimentally with different applied electric field and is shown in Table 5.01.

Applied Electric field (kV/ cm)	Measured pulse duration (ns)
4	20 ± 1
8	21 ± 1
12	20 ± 1
16	21 ± 1
20	21 ± 1

Table 5.01 Measured pulse width at different applied electric field

The length of the PFL was fixed and we found no variation in the value of relative permittivity of the composite mixture up to the electric field strength of 20 kV/cm. The pulse width measured at different applied electric fields is shown in Figure 5.08. We see that the non-linear phenomenon of composite ceramic material does not effects the pulse duration under the high voltage stress being reported here.

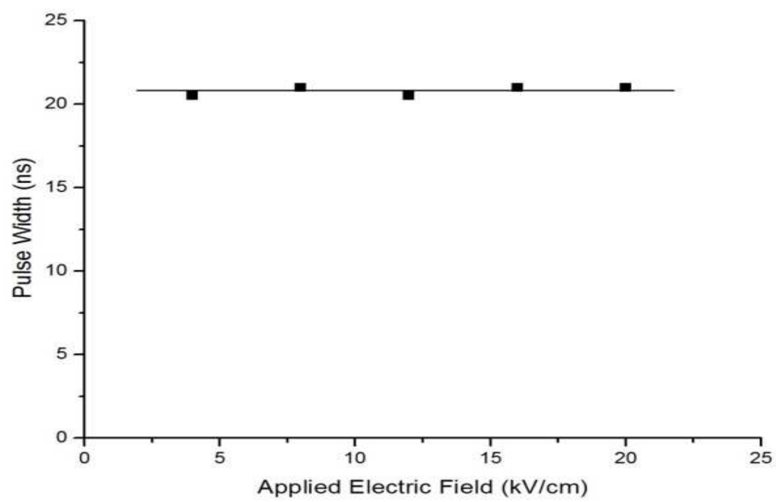

Figure 5.08 Experimentally pulse width measured at different applied electric field

The relative permittivity of the composite mixture remains unchanged under high voltage since the field in the barium titanate ceramic was lower than the threshold field for non-linearity.

5.4 Salient feature of solid composite dielectric pulse forming line development

Replacing the conventional liquid dielectrics with the solid dielectrics with high energy storage density is a promising way to realize an all-solid-state pulsed power system with high stability and compactness. Solid dielectric is generally considered to be non-recoverable in the event of dielectric breakdown but there are single shot pulsed power applications where it is useful. This can increase system capacitance with the possibility of operating at increased energy levels or reduced system volumes. A pulse forming line was made using a composite mixture of barium titanate and neoprene rubber which is compact in size as it has high relative permittivity, but due to porosity, high field stresses are developed, so it has not been used at higher voltages. The voltage breakdown strength of composite mixture has been tested up to 35 kV/cm. This PFL does not require maintenance compared to oil, water line as it is of all solid material. The pulse duration can be increased by increasing the length of the PFL. The compactness in the PFL was achieved by mixing of barium titanate in neoprene rubber which reduces the length of the PFL by a factor of 3.8. The PFL was charged and discharged for few shots (~ 10) and no significant effect on its performance degradation was seen. It was also found that the non linear phenomenon of composite ceramic material does not affect the pulse duration up to the electrical field strength of 20 kV/cm.

5.5 Testing of water helical pulse forming line

A compact pulsed power system was made using helical pulse forming line and its performance was evaluated. The block diagram of the experimental arrangement for testing of water helical pulse forming line is shown in Figure 5.09. The subsystems of these experimental arrangements are discussed in chapter 3.

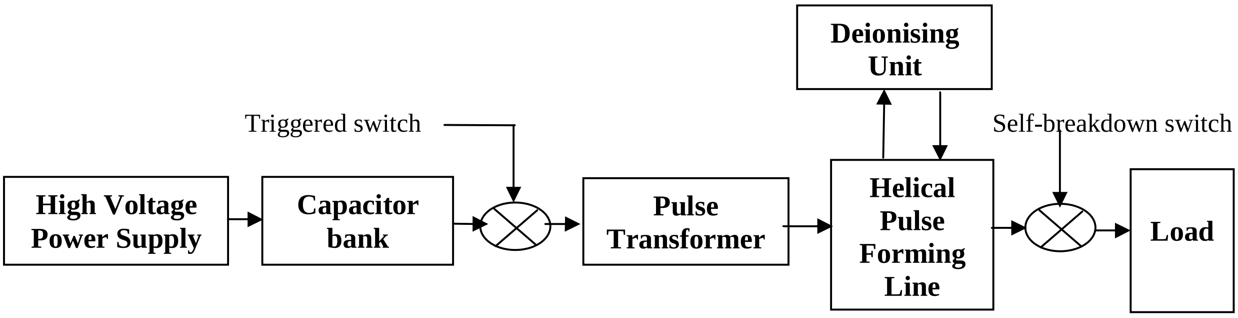

Figure 5.09 Block diagram of experimental setup

The experimental set for testing of helical PFL is shown in Figure 5.10. The capacitor bank was charged with a high voltage power supply to the rated voltage, it discharges into the primary of

Figure 5.10 Compact pulsed power system using helical PFL

the pulse transformer through a triggered sparkgap switch. The secondary of the pulse transformer charges the helical pulse forming line. The self breakdown switch after the helical PFL breaks at the set voltage and it discharges into the matched 22 Ω resistive load. The distance between the electrodes of the sparkgap switch was 15 mm and it was pressurized to 4.5 kg/cm^2. Deionised water was circulated from deionising unit at the rate of 2 litres per minute inside the helical PFL. The helical PFL charging voltage at the input end is measured with voltage divider (VD 100) and the voltage after the switch across the 22Ω load is measured using voltage divider (PVM 5). The accuracy of VD-100 and PVM 5 above 1 MHz signal frequency is < 4% and < 2% respectively. The specifications of these voltage dividers are mentioned in Appendix-2.

5.51 Experimental results

The performance of the compact pulsed power system using water helical PFL was tested and evaluated with matched 22Ω resistive load (Figure 5.10). The primary energy storage capacitor bank was charged to 20 kV and discharged into the primary of pulse transformer through a triggered sparkgap switch. The high voltage generated across the secondary of the pulse transformer charges the water helical pulse forming line to 200 kV peak. The pressure inside the self breakdown switch was kept at 4.5 kg/cm^2 and it breaks at 200 kV. The helical PFL was discharged into the matched resistive load of 22 Ω through a self breakdown spark-gap switch. The high voltage pulse was measured across the helical PFL and the load using standard voltage dividers VD-100 and PVM 5 (Figure 5.11). The compact pulse power system produces 100 kV, 260 ns pulse across the matched load (Figure5.12). So, we generate 260 ns pulse with 800 mm length of the helical PFL, as compared to coaxial PFL which generates 50 ns pulse with 800 mm length of the PFL.

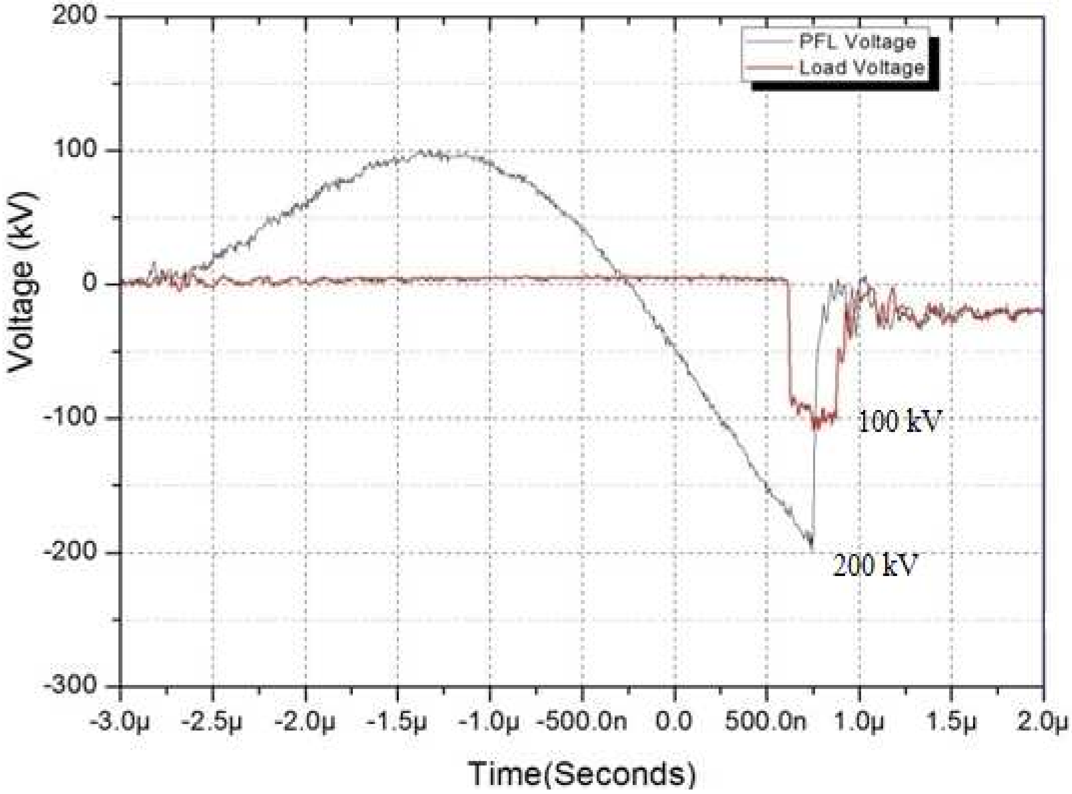

Figure 5.11 PFL charging voltage and load voltage

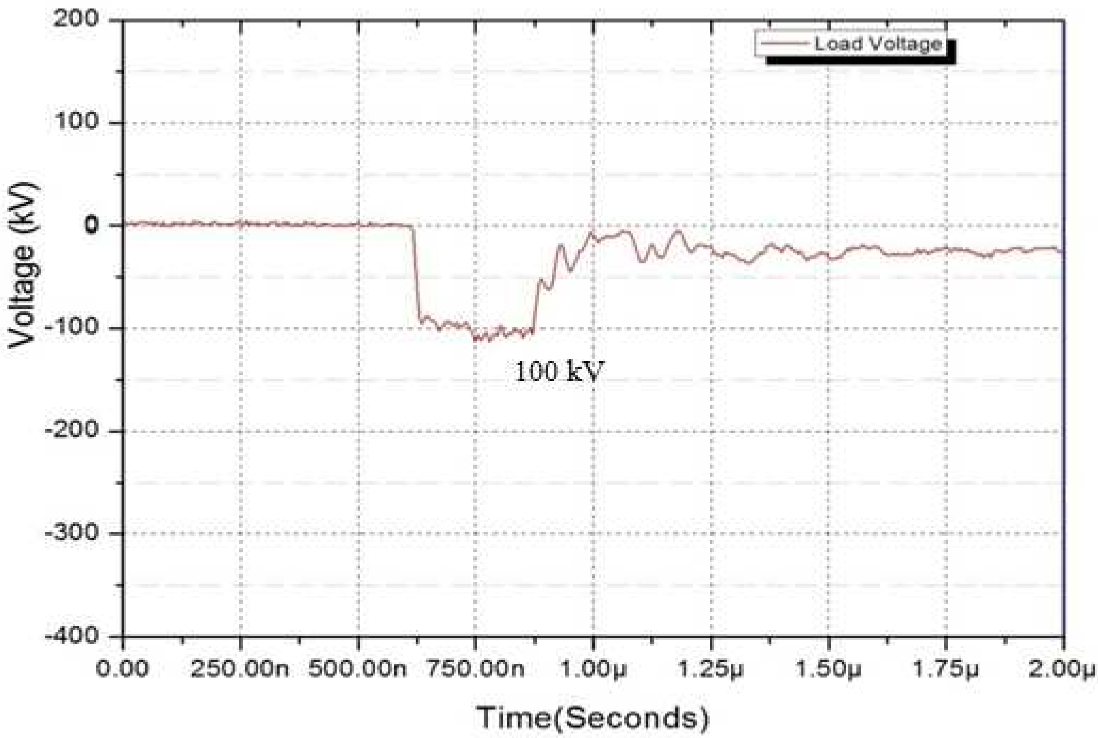

Figure 5.12 Pulse width generated across the match load

5.6 Modelling of the compact pulsed power system using helical PFL

The modelling of compact pulsed power system was done with student version of PSpice simulation software (Figure 5.13).

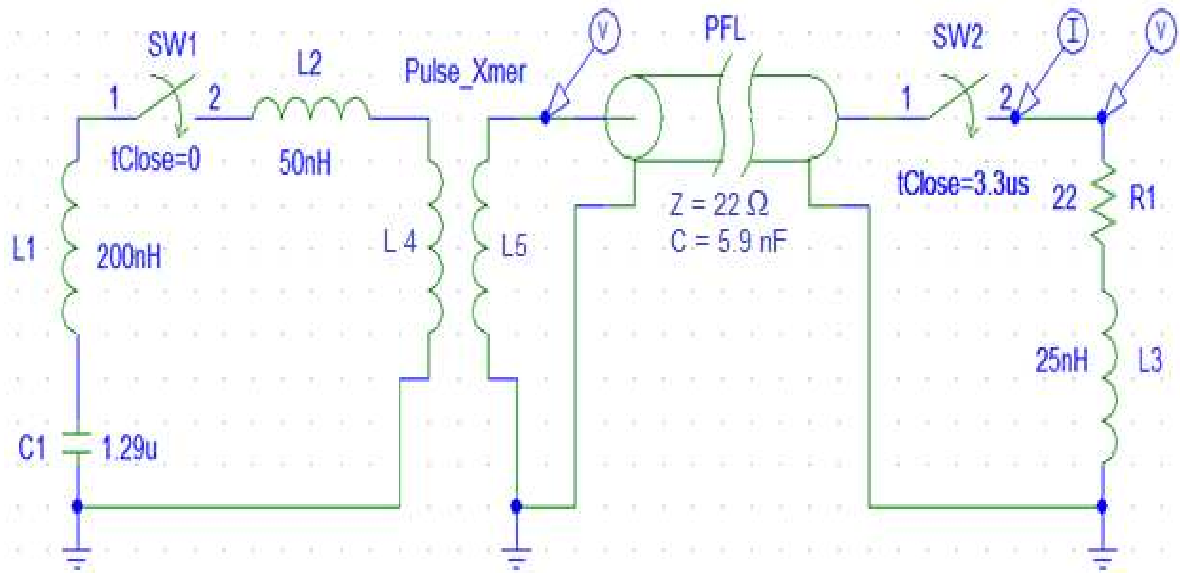

Figure 5.13 Modelling of compact pulsed power system

The pulse transformer was modelled as an equivalent air core pulse transformer (Pulse_Xmer) with primary and secondary inductances of 200 nH (L4) and 110 μH (L5) respectively and the coupling coefficient of 0.73. Water helical pulse forming line (PFL) was modeled as ideal transmission line with characteristic impedance of 22 Ω and one-way transit time of 130 ns. For simulating practical condition inductance of 25 nH (L3) is included on load side and 200 nH (L1) inductance in the primary circuit of capacitor bank, capacitor bank to pulse transformer connecting cable and switch inductance of 50 nH (L2) is added in the primary circuit. The capacitor bank (C1) was charged to 20 kV and the triggered sparkgap switch (SW1) closes at t=0, the secondary of the pulse transformer charges the PFL to 200 kV in 3.3μs and then self breakdown switch (SW2) closes and the PFL discharges into a matched 22Ω resistive load (R1).

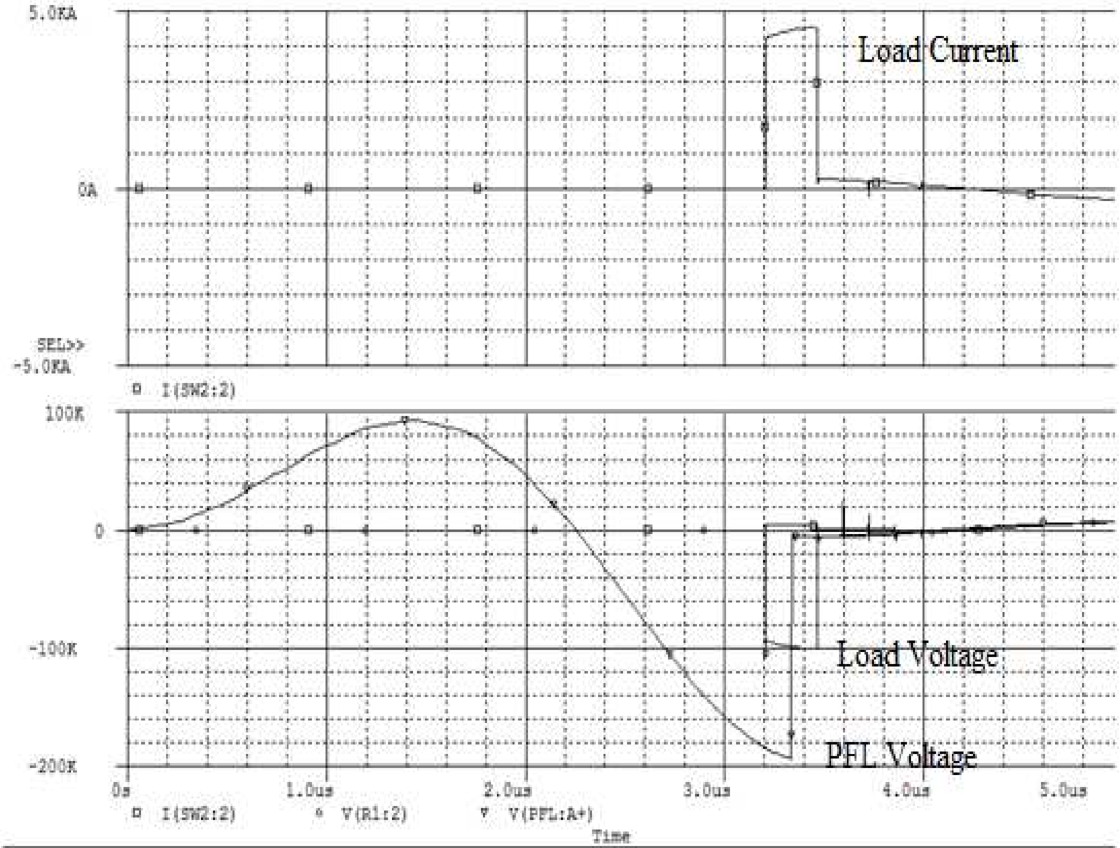

Figure 5.14 PFL voltage and voltage and current across load

The simulation result when the capacitor bank (C1) was charged with 20 kV is shown for helical pulse forming voltage, load current and voltage across the load (Figure 5.14).

5.7 Electrostatic modelling of the helical pulse forming line

The electrostatic modelling of the helical pulse forming line was done using Ansoft Maxwell 2DSV simulation software to simulate the electric field and potential distribution inside the helical PFL and also at its edge. A cross-section of the helical PFL having rotational symmetry in cylindrical geometry was modeled to simulate the electric field and the potential distribution inside the PFL (Figure 5.15).

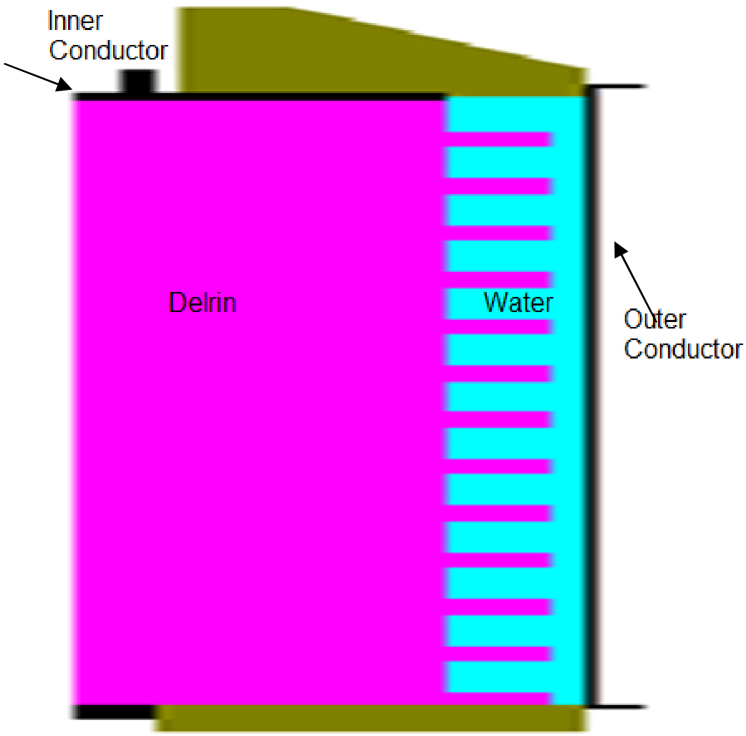

Figure 5.15 Electrostatic modelling of helical PFL

The feed through end of the helical PFL was also modelled to examine the magnitude of the electric field and potential at the triple points (Figure 5.16).

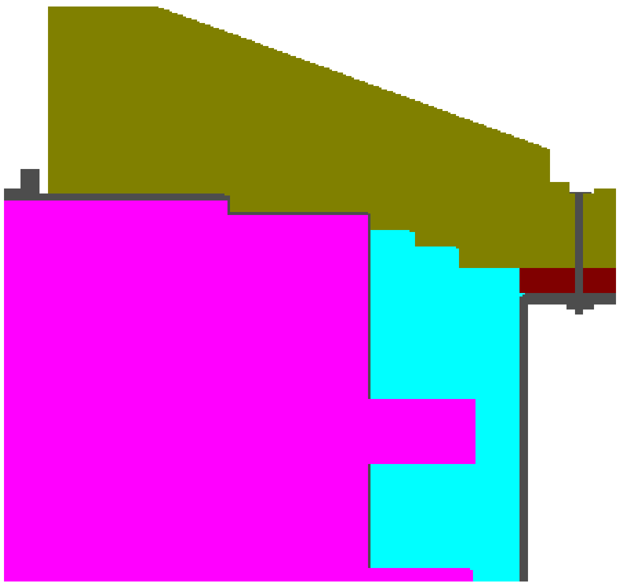

Figure 5.16 Electrostatic modelling at input end

5.71Electric field simulation inside helical PFL

The electric field inside the helical PFL was simulated when the inner conductor was charged to 200 kV and the outer cylinder was grounded. Figure 5.17 shows the electric field distribution inside the PFL and Figure 5.18 shows the electric field distribution at the input edge of the PFL. The electric field stress was maximum on the surface of the inner conductor and it should not be more than the breakdown strength of the medium. The maximum electrical field was 61kV/cm on inner conductor, when the PFL was charged up to 200 kV, which is less than the breakdown strength of the water.

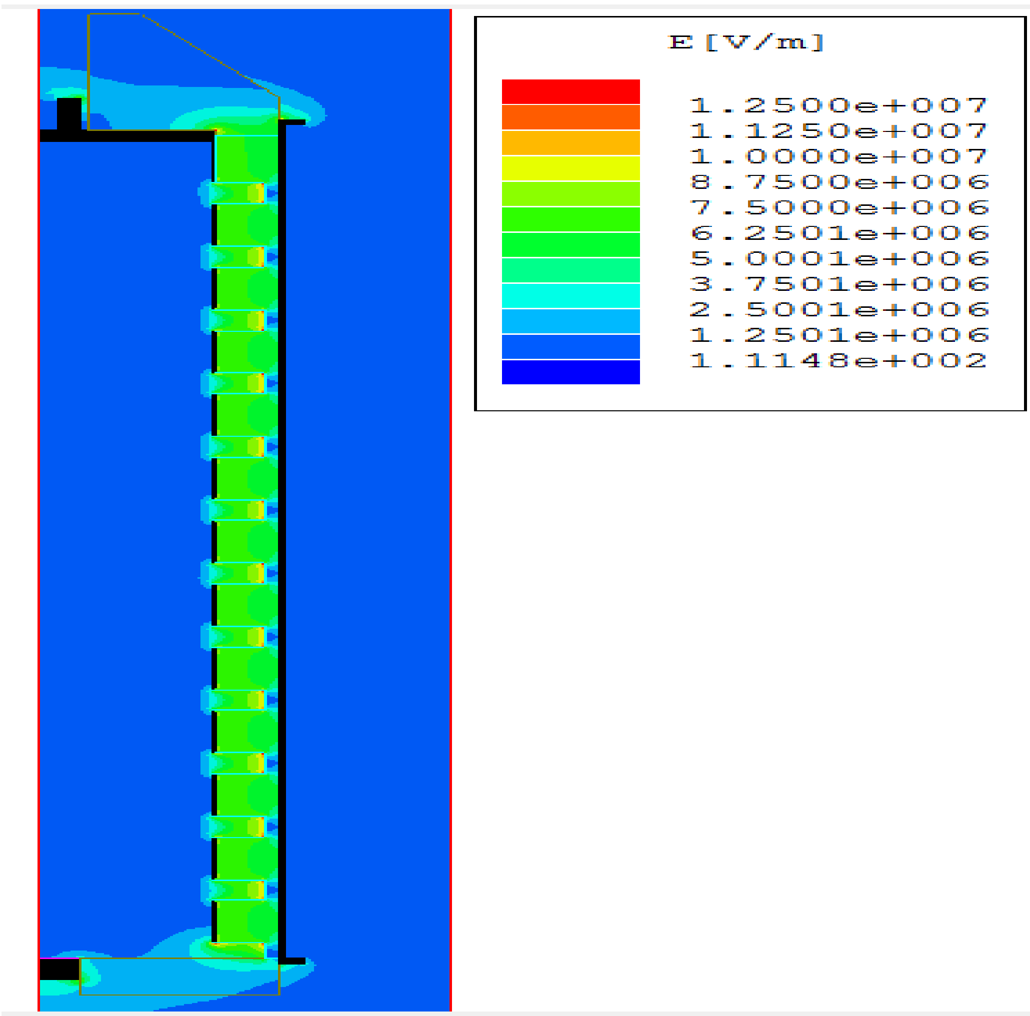

Figure 5.17 Electric field inside helical PFL

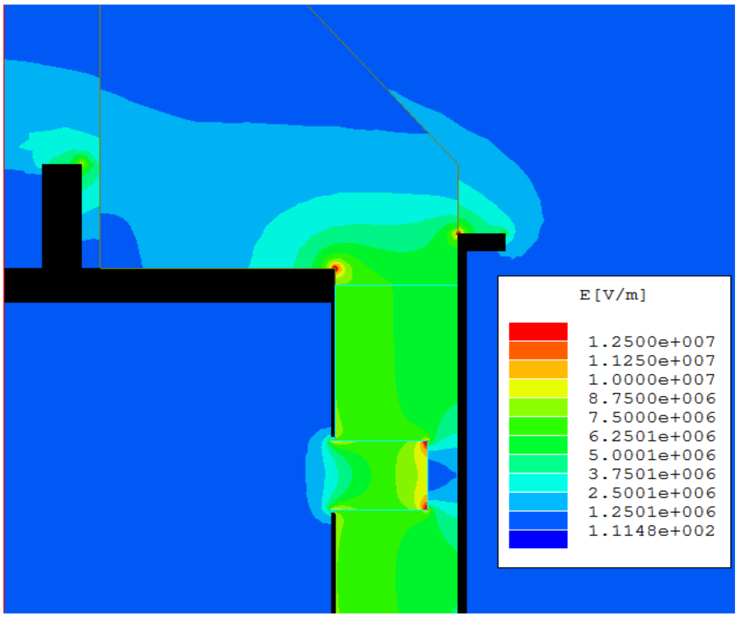

Figure 5.18 Electric field at the input end

5.72 Potential distribution simulation inside helical PFL

The potential distribution inside the helical PFL was also simulated. Figure 5.19 shows the potential distribution inside the PFL when the inner conductor is charged to 200 kV and Figure 5.20 shows the potential distribution at the edge of the PFL.

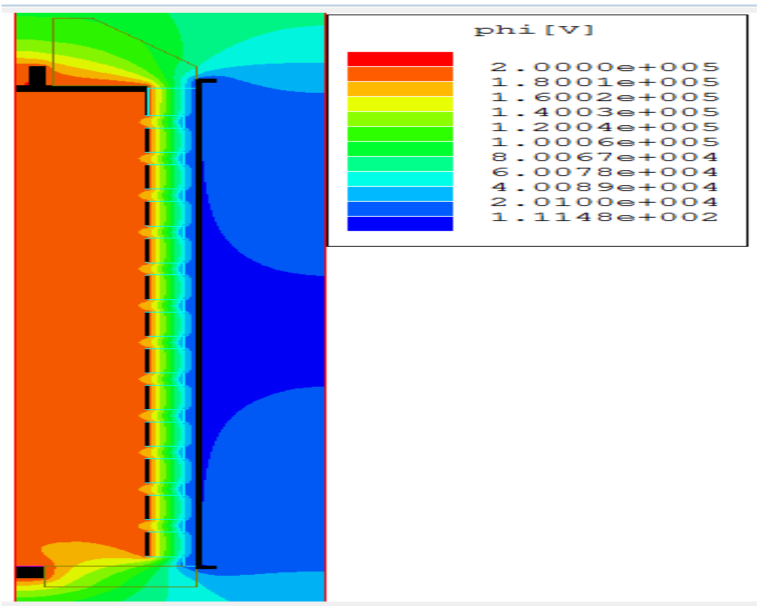

Figure 5.19 Potential inside the helical PFL

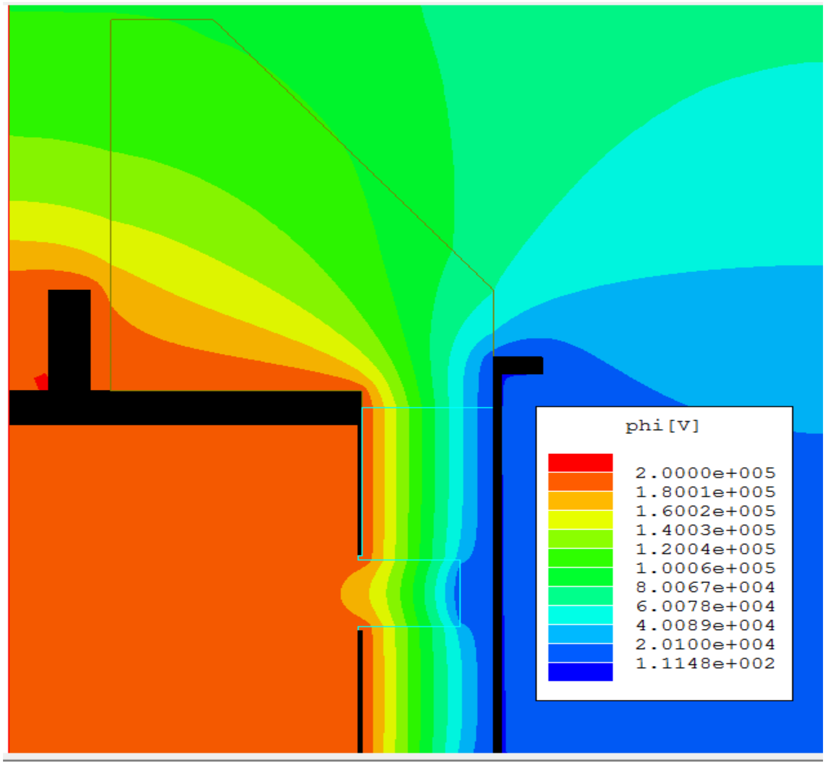

Figure 5.20 Potential inside the input end

5.8 Study on the effect of reduction in water temperature on the pulse width

The relative permittivity of water depends on temperature of water. The effect of reduction in temperature of deionised water on the pulse width generated across the load was investigated. The block diagram of experimental set up with chilled water circulation is shown in Figure 5.21.

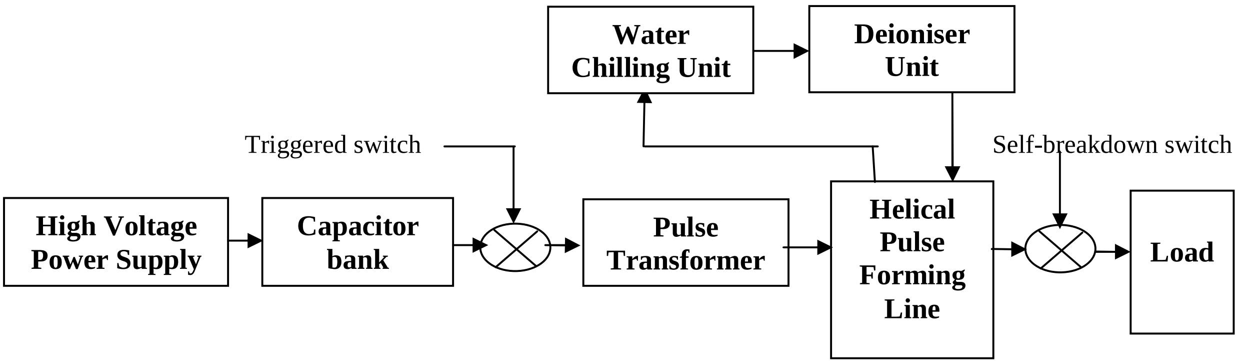

Figure 5.21 Block diagram of experimental setup

The capacitor bank was charged to 20 kV using high voltage power supply, and then discharged into the primary of the pulse transformer through a triggered sparkgap switch. The secondary of the pulse transformer charges the PFL. The deionised water was circulated through a 1.5 TR water chilling unit. The deionised water temperature was reduced from 25 ^{0}C to 5 ^{0}C and the pulse width was experimentally measured across the matched load at different temperature (Table 5.02).

Water Temperature in ^{0}C	Pulse width measured (FWHM) in ns
25	260 ± 1
20	265± 1
15	270 ± 1
10	275 ± 1
5	280 ± 1

Table 5.02 Experimentally pulse width measurement with different water temperature

The increase in pulse width was due to increase in the relative permittivity of the water with the reduction in temperature of water. The relative permittivity of the water increases with the reduction in the temperature of the water [71]. The relative permittivity of water was experimentally measured at different temperature (Figure 5.22). The dependence of relative permittivity of water on the temperature is given by (4.02)

$$\varepsilon_r = 78.54\,(1 - 4.579 \times 10^{-3}\, T_1) + 1.17 \times 10^{-5}\, T_1^2 - 2.8 \times 10^{-8} T_1^3$$

Where $T_1 = T_0 - 25$, T_0 is Temperature in (^{0}C)

The increase in relative permittivity with decreasing temperature is due to decrease in thermal agitation of molecular dipole of water.

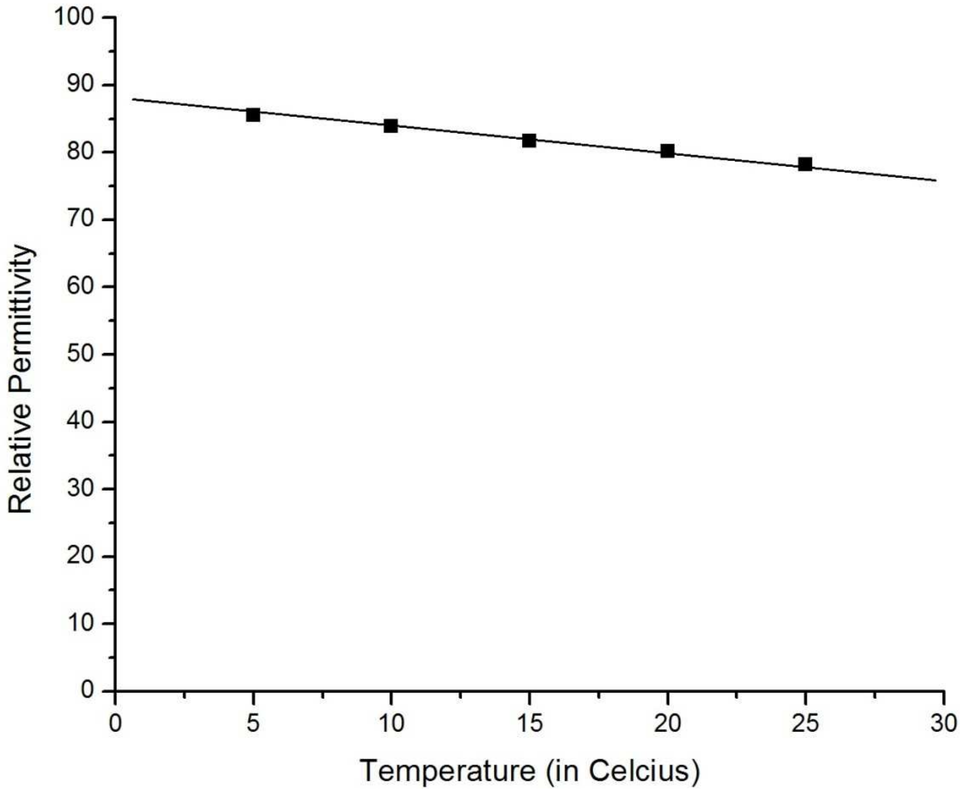

Figure 5.22 Experimentally relative permittivity measured at different temperature

We could see from Table 5.02 the increase in the pulse width generated across the load increases up to 6 % with the reduction in the temperature of the water from 25^0C to 5^0C. So the length of the PFL can further be reduced with the cold water circulation and the size of the PFL can be reduced.

5.9 Salient feature of helical pulse forming line development

An intermediate energy storage system for pulse compression using helical inner conductor was designed and investigated. A helical pulse forming line generates longer duration rectangular pulse as compared to coaxial pulse forming line. The helical conductor reduces the overall length of the PFL by packaging the length in compact geometry. The compactness was achieved in terms of reduction in its length by a factor of 5.5 times as compared to conventional water coaxial PFL of same length. Further the effect of reduction in deionised water temperature inside the pulse forming line on the pulse width was investigated. It was found that the pulse width generated across the load increases by 6%, so higher energy can be stored and more compact systems can be developed using chilled water circulation inside the PFL.

5.10 Conclusion

Compact pulse forming lines can be developed using high dielectric constant material, composite dielectric was made using high dielectric constant ceramic and evaluated for pulse compression of single shot pulsed power applications. The relative permittivity of water increases with reduction in the temperature, so this property was also investigated and used for developing compact systems as water is widely used for pulse compression in pulsed power system. A new technique for pulse conditioning was investigated and developed by using helical inner conductor inside the PFL and water as dielectric for generation of longer duration rectangular pulse in compact geometry.

CHAPTER 6

FAST REPETATIVE DOUBLE PULSE SYSTEM USING COMPACT PULSE FORMING LINE

6.1 Fast repetitive pulsed power system

Repetitive pulsed power generation by compact sources has enormous potential for military and industrial applications [37]. Laser induced breakdown spectroscopy is an analytical technique used for the analysis of solid, liquid and gaseous targets. It has lower sensitivity in comparison with other spectroscopic methods [104]; to overcome this limitation double pulse is used for the better coupling of laser energy to the targets and ablated material [105]. The numerical model for laser–solid interaction, vapour plume expansion, plasma formation and laser–plasma interaction is described for plume expansions times (~ 100 ns) and inter pulse delay of (~ few 10's of nanosecond) and found that laser ablation in double pulse configuration is more efficient [6]. Relativistic electron beam using double pulse have been generated in vacuum diode [106]. The electron beam generated by fast double pulse can be used to pump gases lasers [107]. A fast double pulse with extremely short interval can also be used to study the double pulse effect in nanosecond laser ablation for laser induced breakdown spectroscopy.

6.2 Development of fast repetitive double pulse system (FRDPS)

The repetition rate of the pulsed power system is determined by various factors such as the capacitance or inductance of electrical circuit, power supply, load characteristic and switch etc [108]. Transmission line characteristics of the pulse forming line (PFL) was investigated to develop a fast repetitive double pulse system (FRDPS) with extremely short inter pulse repetition interval. The FRDPS was developed that can generate two flat top rectangular pulses of desired pulse width (~ 100's of nano-seconds) and the desired interval between the pulses (few 10's of nano-seconds). The block diagram of the FRDPS is shown in Figure

6.01. The primary energy storage capacitor bank was charged at rated voltage and then it discharges into the primary of the pulse transformer through a triggered spark gap switch. The high voltage generated across the secondary of the pulse transformer charges the PFL, the self breakdown switch after the PFL closes at the set voltage and the PFL discharges into the load.

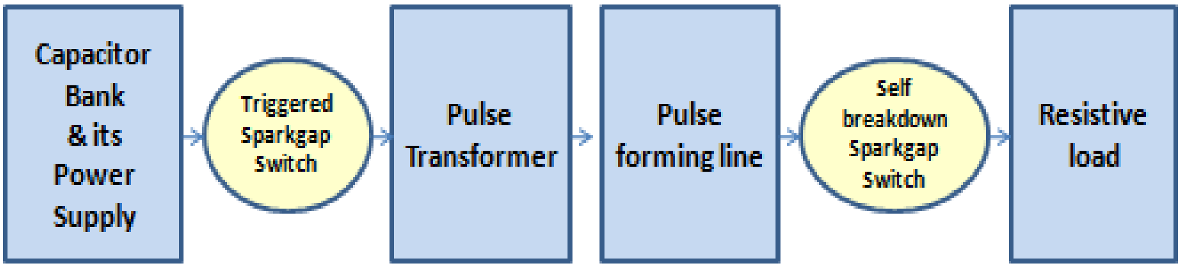

Figure 6.01 Block diagram of compact FRDPS

6.21 Capacitor bank and its power supply

The capacitor bank consists of eight number of 0.16µF / 50 kV capacitor connected in parallel. The capacitor bank was charged with unregulated 25 kV multiplier based power supply. The capacitor bank was discharged into the primary of pulse transformer through a triggered sparkgap switch. The details of the capacitor bank and its power supply are discussed in section 3.1 and 3.2.

6.22 Pulse Transformer

The air core pulse transformer was single turn primary made up of copper sheet and 28 turn secondary made of RG 213 cable with braid stripped. The primary inductance was 200 nH and the secondary inductance was 110 µH. The coefficient of coupling was 0.73. The secondary of the pulse transformer was connected to the input side of the inner conductor of the PFL to pulse charge it. The details of pulse transformer are discussed in section 3.3.

6.23 Pulse forming line

The helical pulse forming line was used as intermediate energy storage system. Water helical PFL was developed for the generation of longer duration rectangular pulse in smaller length and discussed in section 4.5. The helical PFL inner conductor was made up of SS-304 strip rolled on the delrin cylinder. The outer conductor was made up of SS-304 cylinder. The length of the PFL was 800 mm. The volume between the inner strip and outer cylinder was filled with deionised water. The deionised water was circulated through a pump and deionizer unit. The conductivity of the deionised water was kept very low (< 1 µS/cm) with a deionizer unit. 13 turns of SS strip are wounded on 168 mm diameter of delrin cylinder. The two turns at the input side of the PFL are covered with 3 mm of ethylene propylene rubber tape ($\varepsilon_r \sim 3$) on the SS strip (Figure 6.02). The input end of the helical PFL was connected to the secondary of pulse transformer to pulse charge it. The other end of the helical PFL was connected to the 22 Ω matched resistive load through a self breakdown sparkgap switch.

Figure 6.02 Input end of helical pulse forming line

6.24 Sparkgap switch

The self breakdown sparkgap switch was connected after the PFL to sharpen the pulse. The pressure inside the sparkgap switch was kept at 4.5 kg/cm^2 and it breaks at 200 kV. The schematic of sparkgap switch arrangement with the helical PFL is shown in Figure 6.03. The detail of the sparkgap switch was discussed in section 3.5.

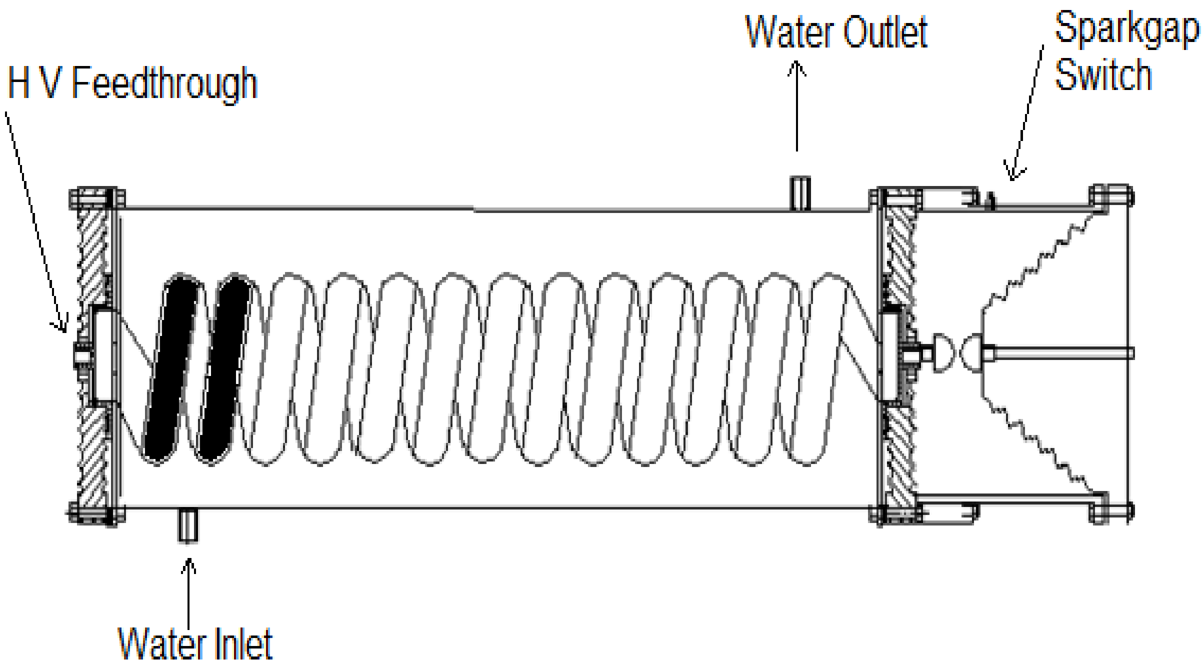

Figure 6.03 Schematic of sparkgap switch after helical PFL

6.3 Testing of the fast repetitive double pulse system

The testing of FRDPS was done by pulse charging the PFL to 200 kV and discharging it into the matched 22Ω load (Figure 6.04). The primary energy storage capacitor bank was charged to 20 kV. The sparkgap switch was triggered to discharge the capacitor bank in to the primary of the pulse transformer. The high voltage generated across the secondary of the pulse transformer charges the helical PFL to 200 kV, which then discharges through a self break down sparkgap switch to a 22 Ω load (Figure 6.04). The voltage across the PFL and the load was measured using dividers VD-100 and PVM -5. The accuracy of VD-100 and PVM 5 above 1 MHz signal frequency is < 4% and < 2% respectively.

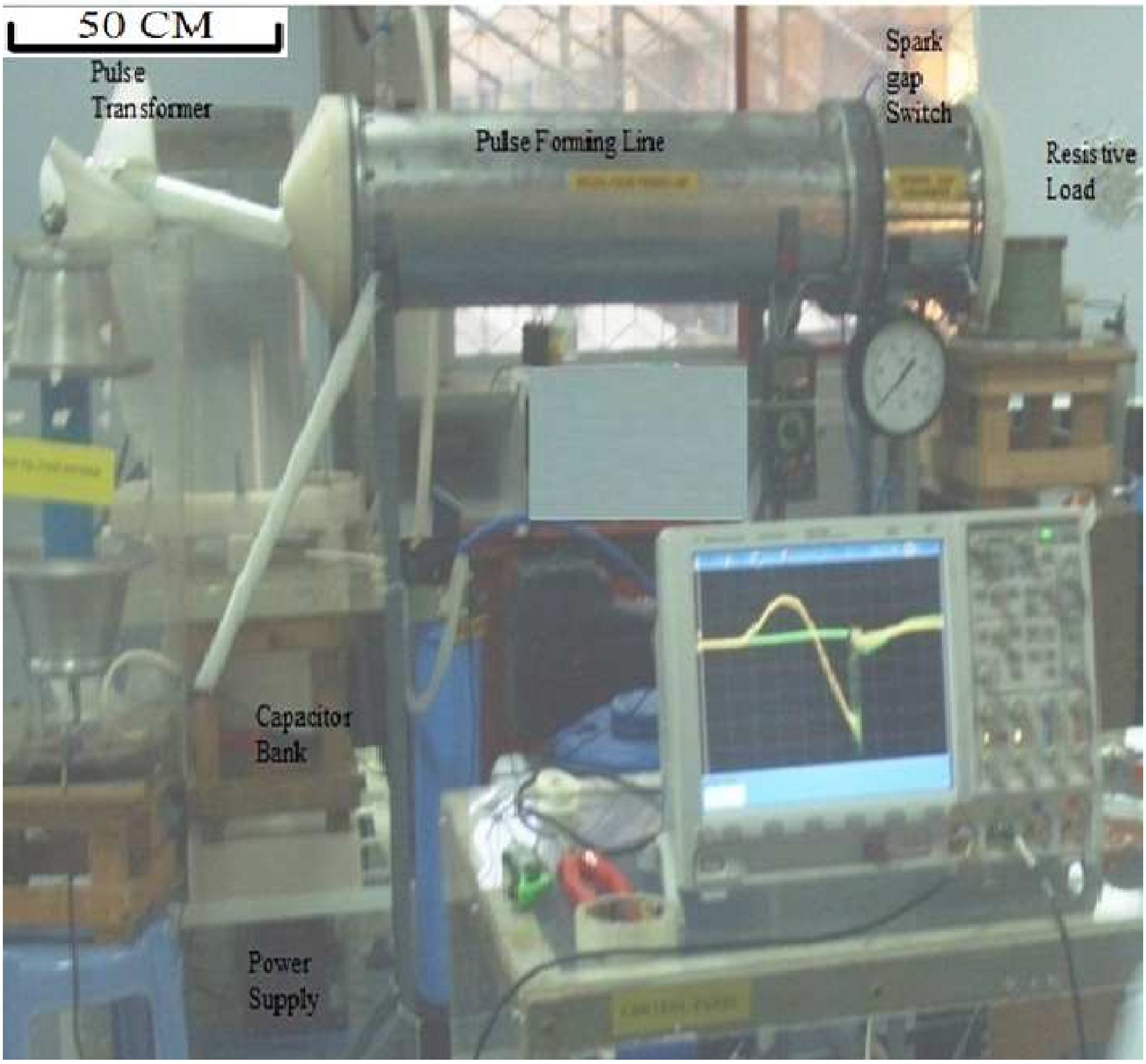

Figure 6.04 Experimental set up

6.31 Experimental results

The secondary of the pulse transformer charges the helical PFL to 200 kV in 3.5 μs (Figure 6.05). The pressurized sparkgap switch breaks and closes at 200 kV. It discharges the helical PFL to the matched load, while discharging it generates two fast pulses of 100 kV, 100 ns with 30 ns inter pulse interval across the load (Figure 6.06). 0.5 GW of peak power is delivered to load in each pulse. The double pulse generation from the system is explained in section 6.5.

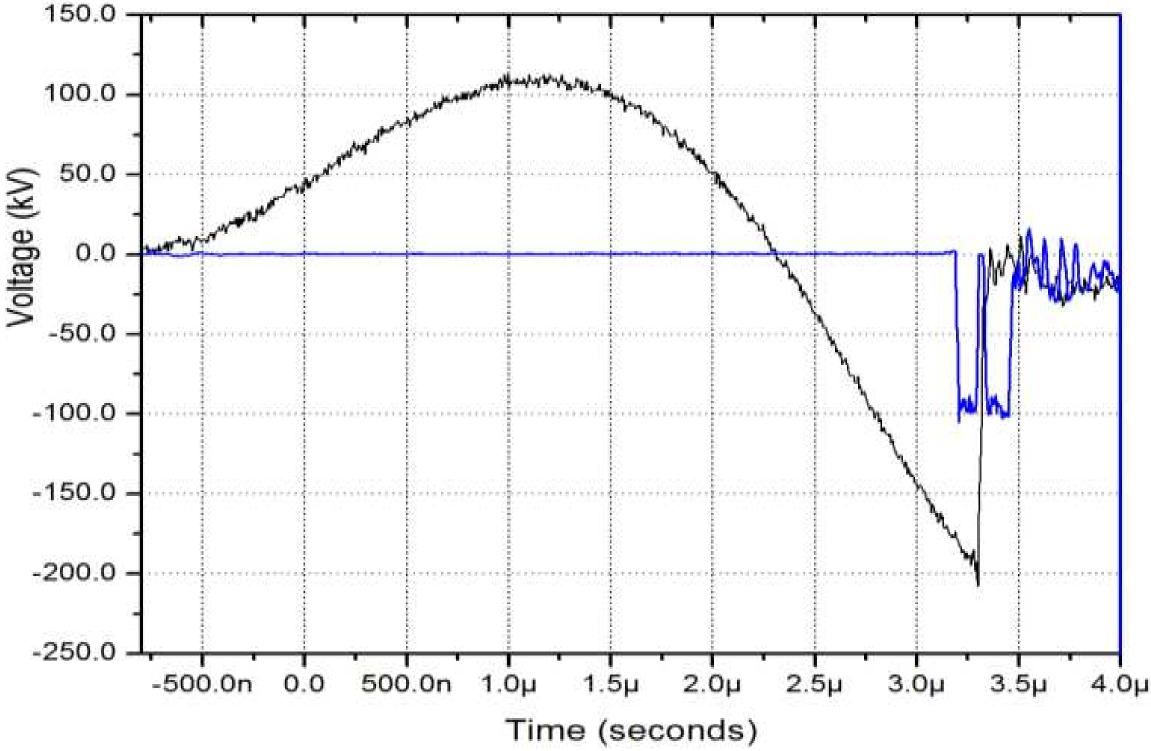

Figure 6.05 Voltage measured across PFL & load

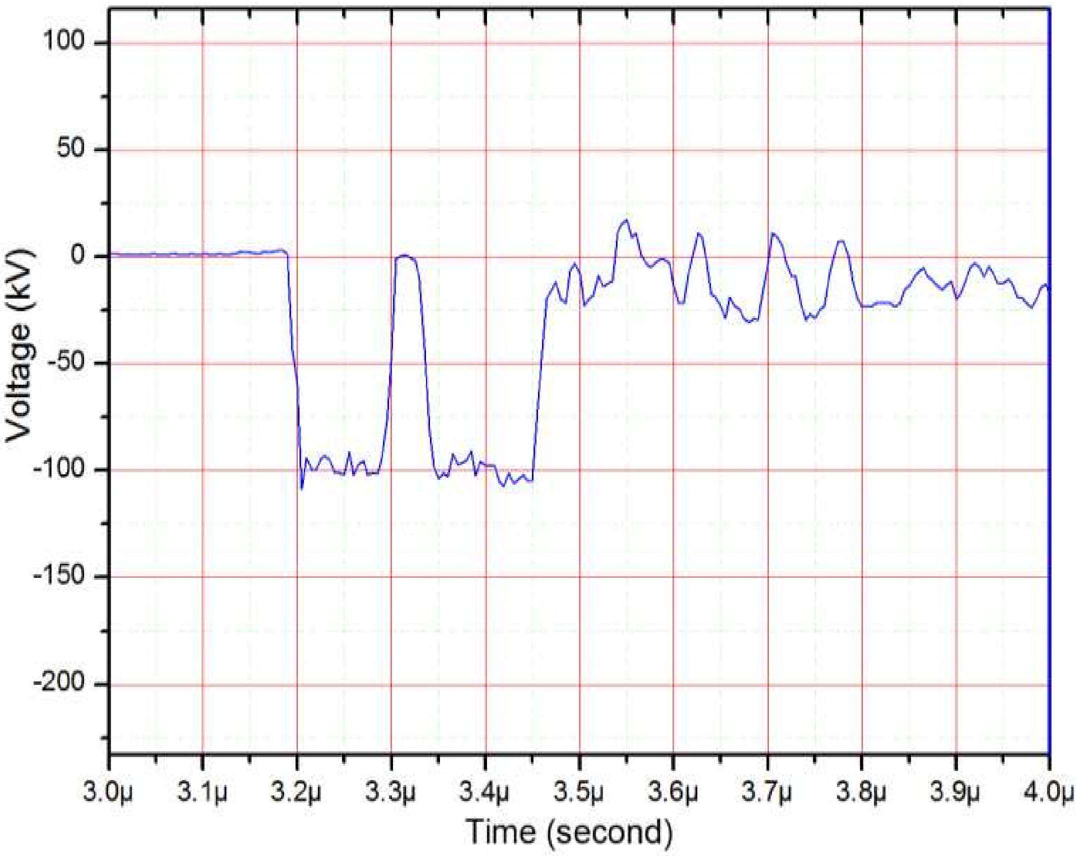

Figure 6.06 Voltage measured across load

6.4 Electrostatic modelling of the system

When more than one dielectric material is present in any region of an electric field, the boundary conditions satisfied by the electric field intensity $\bar{E}$ at dielectric boundary are [57],

$$E_{t1} = E_{t2} \tag{6.01}$$

$$E_{n1} = E_{n2} \tag{6.02}$$

$$\frac{\tan\alpha_1}{\tan\alpha_2} = \frac{\varepsilon_1}{\varepsilon_2} \tag{6.03}$$

Where,

E_{t1}, E_{t1} are the tangential and E_{n1}, E_{n2} are the normal components of the electric field in the dielectric 1 and 2.

α_1 and α_2 are the angle of incidence and the angle of refraction with the normal and ε_1 and ε_2 are the permittivity of the two dielectrics at the boundary.

Normally, all dielectrics are good insulators at lower magnitudes of field intensities. But as the electric field increases, the electrons bound to the molecules of dielectric will be subjected to higher forces, and some of them are freed from their molecular bonding. The electrons move in opposite direction to the electric field and thus create conduction current. This dissociation is temporary in gases in which a combination occurs when field is removed whereas it is a partial or permanent feature in liquids and solids results in dielectric breakdown. The magnitude of electric field that gives rise to the dielectric breakdown and destroys the property of insulation in dielectric materials is called the breakdown strength. The electrostatic modelling at the input side of helical pulse forming line is done using Ansoft Maxwell 2D-SV simulation software (Figure 6.07). The electric field and potential inside the ethylene propylene rubber and water at the input side of the PFL is simulated, when the inner conductor is charged to 200 kV.

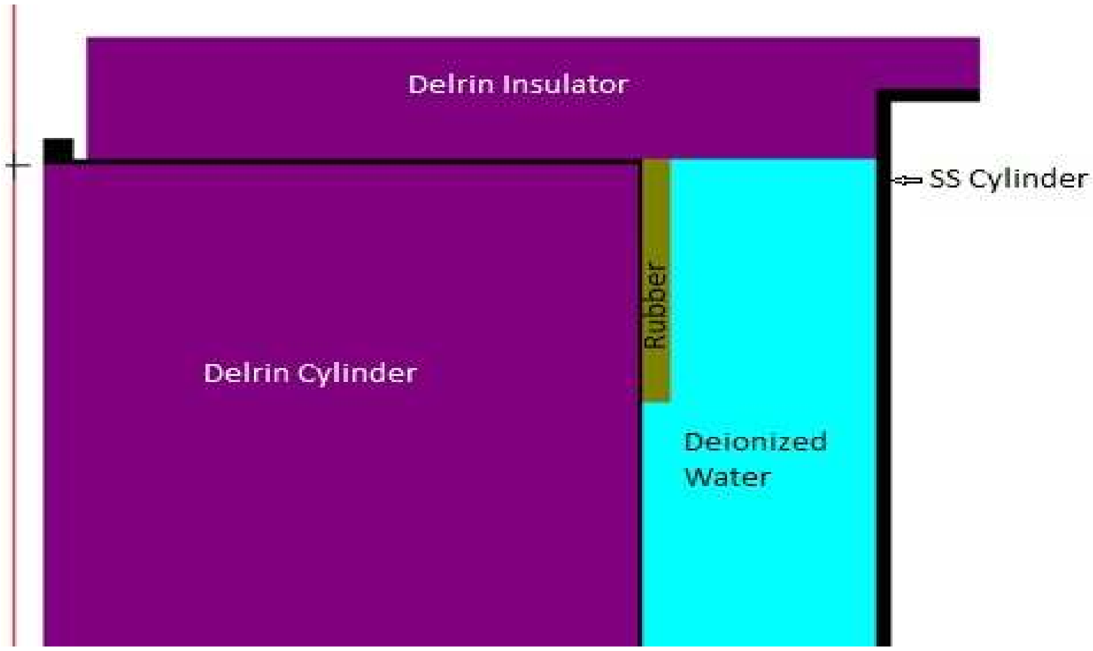

Figure 6.07 Electrostatic modelling of input side of helical PFL

6.41 Electric field simulated inside the PFL

The electric field was simulated inside the input side of the helical PFL when the inner conductor was charged to 200 kV, the maximum electric field appears across the ethylene propylene rubber ($\varepsilon_r \sim 3$) and electric field inside the water ($\varepsilon_r \sim 80$) capacitor above the ethylene propylene rubber was much less as simulated and shown in Figure 6.08.

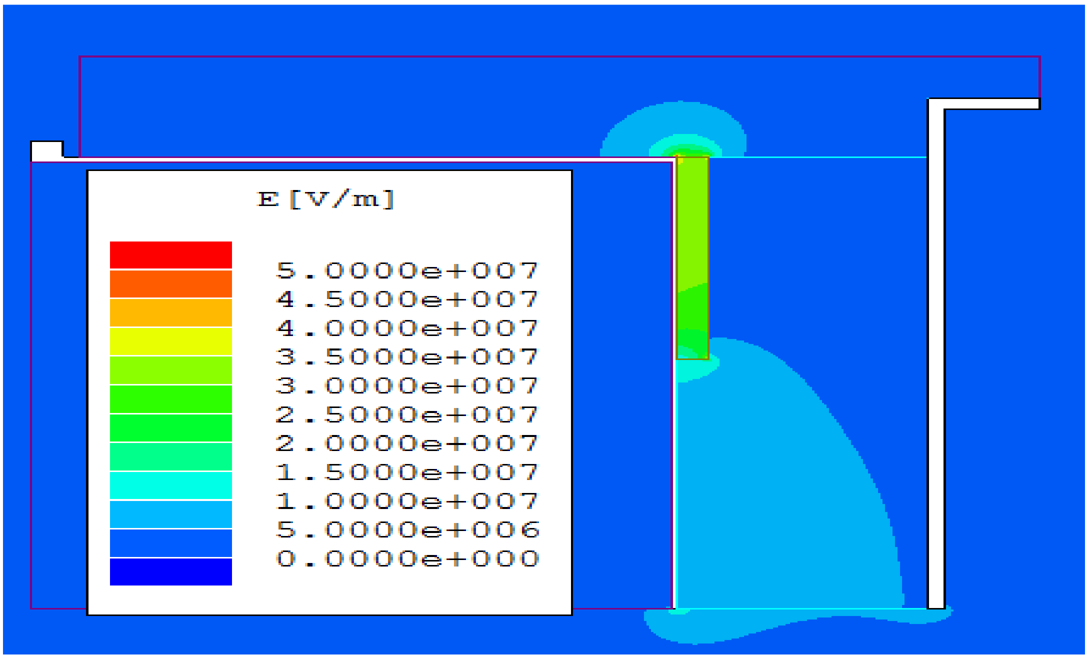

Figure 6.08 Electric field inside input side of helical PFL

6.42 Potential distribution simulated inside the PFL

The potential distribution inside the input side of helical PFL was simulated when the inner conductor was charged to 200 kV, the maximum potential appears across the ethylene propylene rubber and above that the water capacitor was charged to lesser extent (Figure 6.09). We see from the simulation of the potential distribution, the water capacitor was fully charged where there is no ethylene propylene rubber covered on the strip.

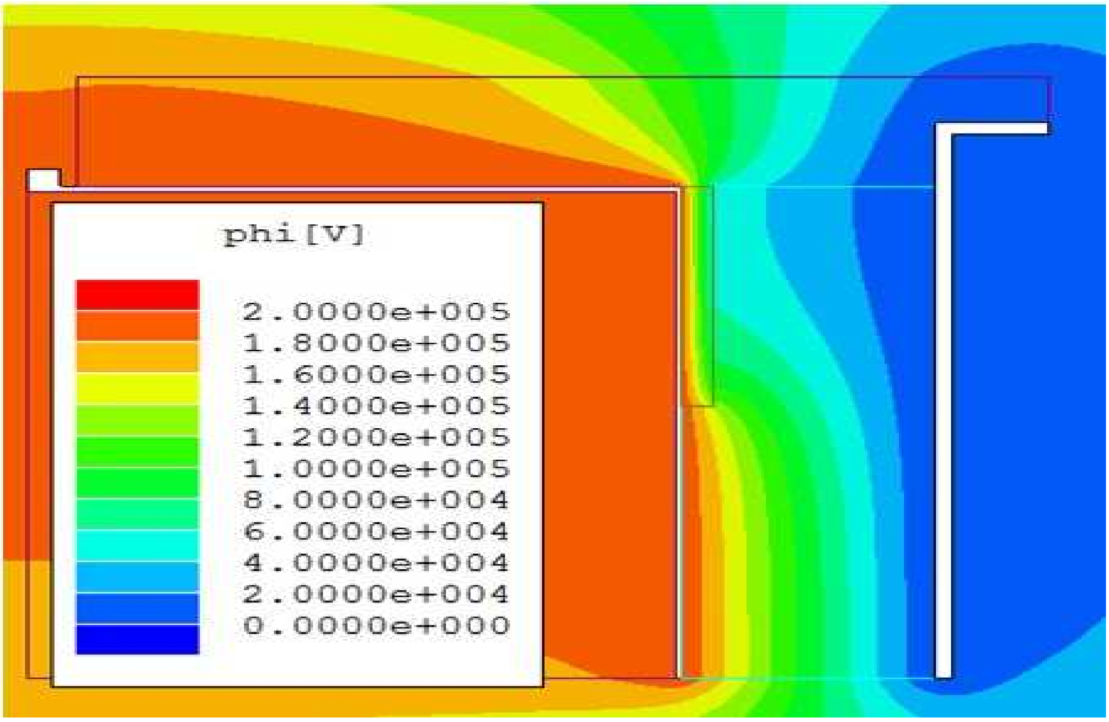

Figure 6.09 Potential inside input side of helical PFL

6.5 Results and Discussion

When the high voltage was applied to the inner conductor of the helical PFL and pulsed charged to 200 kV, the water capacitor was fully charged where there was no ethylene propylene rubber on the SS strip inner conductor. At the input side of the PFL maximum potential appears across the ethylene propylene rubber, and the water capacitor was charged to lesser extent due to its higher relative permittivity compared to that of ethylene propylene rubber. The self breakdown sparkgap switch closes at 200 kV and the PFL discharges into the load. While discharging the forward voltage wave travels towards the source and voltage appears across the load (Figure 6.10). The voltage across the load appears till it discharges up to the initial 2 turns. Then there was less voltage across the water capacitor above the ethylene propylene rubber, so no voltage appears across the load. When the wave is reflected from the input end due to the high impedance of pulse transformer it again appears across the load after the end of the 2 turns. So, the two pulses of 100 ns pulse width and interval of 30 ns between the pulses appears across the load (Figure 6.11).

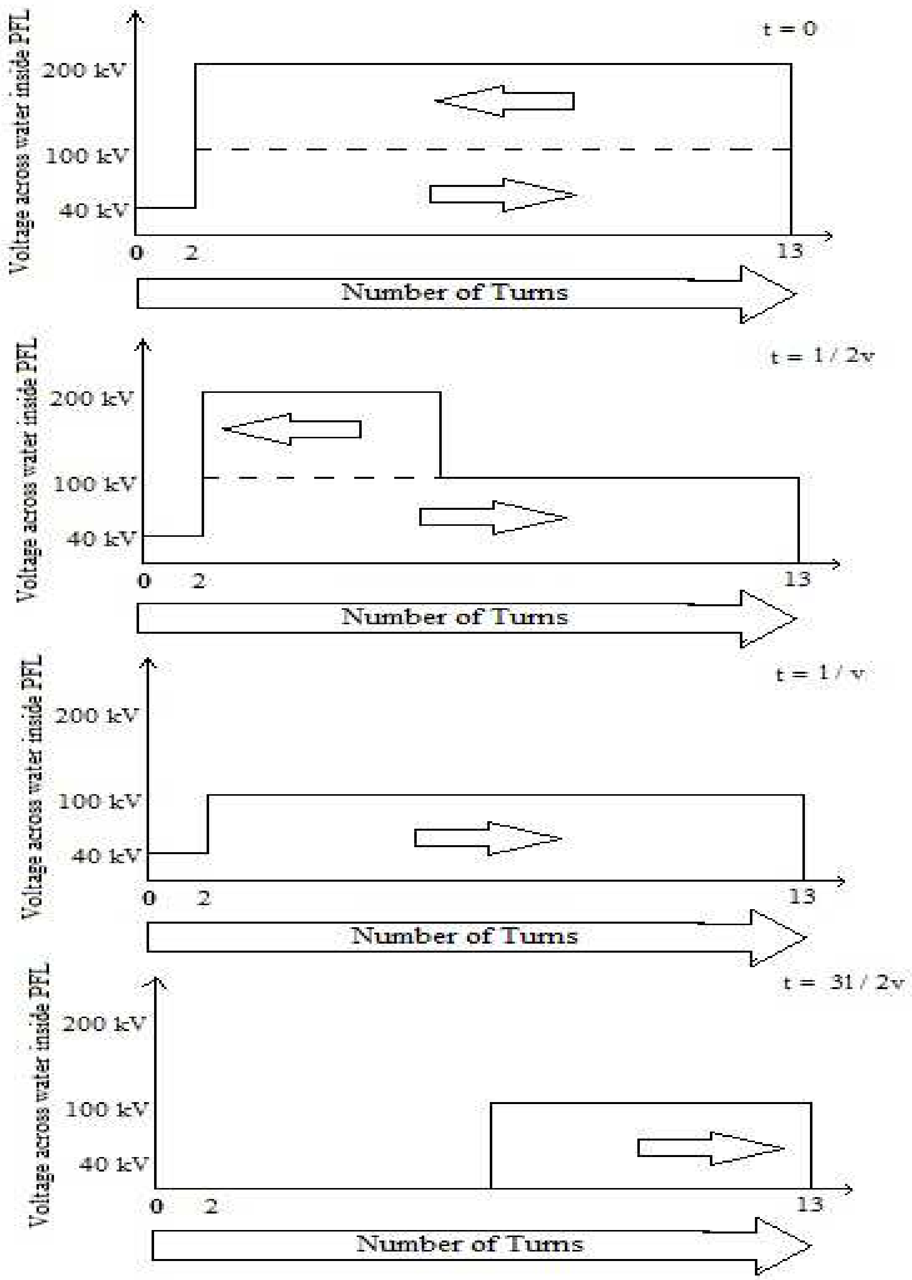

Figure 6.10 Schematic of voltage wave across PFL

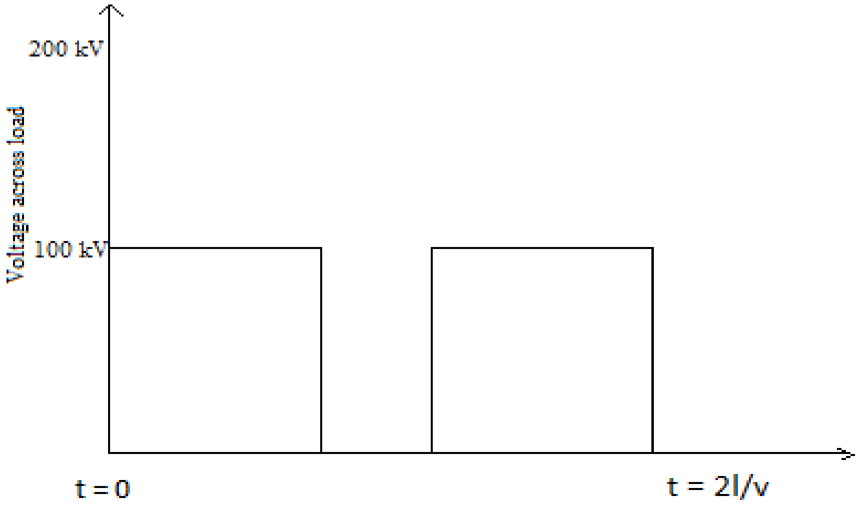

Figure 6.11 Schematic of voltage across the load

It is observed that increase in the length of the ethylene propylene rubber on the inner conductor reduces the pulse width and increases the interval between the pulses. When there was no ethylene propylene rubber on the inner conductor the helical PFL, it generates 100 kV, 260 ns pulse across the load when charged to 200 kV. This was also discussed in section 5.9.

6.6 Conclusion

A fast repetitive double pulse system (FRDPS) with extremely short interval was designed and developed using the transmission line characteristics of a pulse forming line. A novel technique was developed to generate fast repetitive double pulse. The system generates high voltage double pulse of 100 kV, 100ns with the interval of 30 ns between the two pulses, when the initial 2 turns on the helical PFL was wounded with ethylene propylene rubber tape. The pulse width and the interval between the pulses can be varied by changing the length of the ethylene propylene rubber insulation tape wounded on the SS strip of the helical PFL. It overcomes the limitation caused by circuit parameters, power supplies and switch to generate fast repetitive pulse with extremely small repetition interval. The system can be used for applications requiring fast repetitive pulse with very small inter pulse interval.

CHAPTER - 7

CONCLUSION AND FUTURE PERSPECTIVE

7.1 Conclusion

The fundamental study on the development of compact pulse forming line are done at component level using composite dielectric material with ceramic, and at the system level using alternative engineering topology for single and fast repetitive pulse generation. The following conclusions were made:

1. The composite dielectric with ceramic has higher dielectric constant and it can increase system capacitance with the possibility of operating at reduced system volumes for few shot applications. Compact PFL was developed using composite material of barium titanate and neoprene rubber and tested up to 120 kV. It was also found that the dielectric constant of the composite mixture remains unchanged under high electric field (< 20 kV/cm).
2. An alternative technique was investigated and developed using helical inner conductor inside the PFL. The helical conductor increases the transit time, so longer duration pulse can be generated in compact geometry. A 200 kV, 0.5 GW, 260 ns pulsed power system was designed and developed using helical PFL and was tested on matched load.
3. It was found that higher energy can be stored and more compact systems can be developed using chilled water circulation inside the PFL, it increases the pulse width by a factor of 6%, when the temperature of water was reduced from 25 ^{0}C to 5 ^{0}C. The pulse width can also be changed in existing water PFLs by accordingly changing the temperature of water.
4. A novel technique was developed using the transmission line characteristic of PFL and by using different dielectric constant material to store energy inside the PFL, to generate fast repetitive double pulse with small repetition interval.

In many cases novel propositions have been made for better understanding to solve the difficulties encountered for developing compact pulsed power system.

7.2 Future perspective

Further research issues are open on studying and utilizing new materials, dielectrics, insulators, metals and interface in the design of components of the compact pulsed power systems. Finally some future work is being outlined:

- New materials with high dielectric constant, high breakdown strength should be developed and investigated. The processing technique to reproduce sinter large quantities of ceramics has to be investigated for high dielectric constant ceramic development.
- Dielectric constant of the medium also depends on temperature, pressure and stress on the material. These properties of the materials can further be used and explored for compact system.
- Compact repetitive pulsed power systems will pose a significant challenge with respect to the heat dissipation in the system. Micro channel heat sinks and high fluence convective cooling aided thermal management will be used in developing the compact system. The advanced component technologies and application specific integrated circuits to replace the discrete circuits can be applied to pulsed power systems using a suite of integrated design tools and micromachining techniques.
- Continuous attention is required to address issues such as locally breakdown, ground noise, heat removal, when more components are integrated into a small space.

The new developments in materials, combined with electromagnetic and thermal design tools, will set a pathway for revolutionary advancements in compact pulsed power technology.

8. REFERENCES

[1] P. W. Smith, “Pulsed Power for Particle Accelerators,” The CERN Accelerator School, May 12th- 18th, 2004.

[2] D. Durga Praveen Kumar, S. Mitra, K. Senthil, Archana Sharma, K. V. Nagesh, S. K.Singh, J. Mondal, Amitava Roy, and D. P. Chakravarthy, “Characterization and analysis of a pulse power system based on Marx generator and Blumlein,” Rev. Sci. Instrum. 78, pp 115107, 2007.

[3] “U.S Department of defence fiscal year 2001 Multidisciplinary Research Program of the University Research Initiative (MURI) competition announcement”, Washington DC, FY2001 MURI Topic 30, 2000”

[4] I.R Smith, B. M Novac, “An Introduction to the Physics and Technology of Pulsed Power”, Taylor and Francis Publisher (2010)

[5] Hansjoachim Bluhm, “Pulsed Power Systems: Principles and Applications’, Springer- Verlag Berlin Heidelberg, Germany (2006).

[6] Annemie Bogaerts, Zhaoyang Chen, David Autrique, “Double pulse laser ablation and laser induced breakdown spectroscopy: A modelling investigation”, Spectrochimica Acta Part B 63 (2008) 746–754

[7] Roy A, Menon R., Mitra S, Kumar S, Sharma V, Sharma A, Nagesh K.V, Chakravorthy D.P, “ High power microwave generation from KALI 5000 pulse power system”, IEEE Pulsed Power Conference -2011, Chicago, 387-390 (2011)

[8] Archana Sharma, Senthil Kumar et. al., “Development and Characterization of Repetitive 1-kJ Marx- Generator-Driven Reflex Triode System for High- Power Microwave Generation,” IEEE Trans. Plasma Sci. 39, (2011): 1262- 1267.

[9] Bailey M.R., Cleveland R.O., Colonius T., Crum L.A, Evan A.P., Lingeman J.E., McAteer

J.A., Sapozhnikov O.A., Williams J.C. “Cavitation in shock wave lithotripsy: the critical role of bubble activity in stone breakage and kidney trauma “IEEE Symposium on Ultrasonics, Vol 1, pp 724 - 727 (Oct 2003)

[10]] R Shukla, S.K.Sharma, P.Banerjee, R.Das, P.Deb, B.K. Das, B.Adhikary and A.Shyam, “Low voltage operation of plasma focus” Review of Scientific Instruments. 81, Issue 8, (2010)

[11] S K Sharma, SC Jakhar, R Shukla, CVS Rao and A Shyam “Explosive detection system using pulsed 14 MeV neutron source”, Fusion Engineering and Design, Volume 85, pp 1562-1564 (Nov 2010.)

[12] Rakhee Menon, Amitava Roy, S. Mitra, A. Sharma, J. Mondal, K. C. Mittal, K. V. Nagesh, and D. P. Chakravarthy, “Generation and dose distribution measurement of flash x-ray in KALI-5000 system,” Rev. Sci. Instrum. 79, (2008):103301.

[13] Bloomquist D D et. al.,“SaTPro: the system assessment test program for ZR” 26th International Power Modulator Symposium 2004 and High Voltage Workshop. 106– 110 (2004)

[14] R Aymar, P Barabaschi and Y Shimomura,“The ITER design” Plasma Phys. Control. Fusion 44, 519 (2002)

[15] C. Manssion, “Pulsed power technology and applications – Scandinavia”, EPRI, Palo Alto, CA: 1999. TR – 112566

[16] P.R. Chalise, S. Perni, G. Shama, B. Novac, I.R. Smith and M.G. Kong, "Lethality Mechanisms in Escherichia coli Induced by Intense Sub-microsecond Electrical Pulses", Appl. Phys. Lett., 89, pp 153902 (2006).

[17] Akira Mizuno, Yuji Hori, “Destruction of living cells by pulsed high voltage application,” IEEE Trans. on Industry Applications, vol. 24, pp. 387-394, 1988.

[18] Y. Sun, P.T. Vernier, M. Behrend, L. Marcu and M.A. Gundersen, "Electrode Microchamber for Non-Invasive Perturbation of Mammalian Cells with Nanosecond Pulsed Electric Fields," IEEE Transactions on Nanobioscience, Vol. 4, No. 4, pp. 277-283, Dec 2005.

[19] S. J. Beebe, P. M. Fox, L. J. Rec, K. Somers, R. H. Stark, and K. H. Schoenbach, "Nanosecond pulsed electric field (nsPEF) effects on cells and tissues: apoptosis induction and tumor growth inhibition." IEEE Trans.Plasma Sci., 30:286-292, 2002.

[20] I. R. McNab, "Developments in battlefield power technology," in Proc. 12th IEEE Int. Pulsed Power Conf., 1999, pp. 359–363.

[21] Nunnally W. C., "Critical component requirements for compact pulse power system architectures", IEEE Trans. on Plasma Sci, Vol 33, pp 1262-1267, 2005

[22] J.R. MacDonald, M.A. Schneider, J.B. Ennis,F.W. MacDougall, X.H. Yang "High Energy density capacitors" IEEE Electrical insulation conference, Canada (2009)

[23] Michael V. Fazio and Hugh C Kirbie, "Ultracompact Pulsed Power", Proceedings of IEEE, 92, 7, pp 1197 (2004)

[24] D. Bhasavanich, D. F. Strachan et. al., "Compact high current, high energy closing switches for electric gun applications," in Proc. 9th IEEE Int. Pulsed Power Conf., 1993, pp. 356–359.

[25] J. D. Sethian, "A compact parallel plate water capacitor," in Proc. 8th IEEE Int. Pulsed Power Conf., 1991, pp. 170–172.

[26] G. J. Rohwein, R. N. Lawson, and M. C. Clark, "A compact 200kV pulse transformer system," in Proc. 8th IEEE Int. Pulsed Power Conf., 1991, pp. 968–970.

[27] C. R.Wilson, G. A. Erickson, and P.W. Smith, "Compact, repetitive, pulsed power generators based on transmission line transformers," in Proc. 7th IEEE Int. Pulsed Power Conf., 1989, pp. 108–112.

[28] P. Winsor *et al.*, “Pulse power capability of high energy density capacitors based on a new dielectric material,” in Proc. 12th IEEE Int. Pulsed Power Conf., 1999, pp. 102–105.

[29] M. Bramoulle *et al.*, “Ultimate properties of the polypropylene film for energy storage capacitors,” in Proc. 13th IEEE Int. Pulsed Power Conf., 2001, pp. 413–416.

[30] W J Sarjeant, Capacitors, IEEE Trans. on Electrical Insulation, 25, (5), Oct 1990

[31] F. W. MacDougall, J. B. Ennis, R. A. Cooper, J. Bates, and K. Seal, “High energy density pulsed power capacitors,” in Proc. 14th IEEE Int. Pulsed Power Conf., 2003

[32] E. Schamiloglu, J. Buchenauer, J. Gaudet, and P. Castro, "Studies of Dielectric Breakdown Under Pulsed Power Conditions," 31st IEEE Intemational Conference On plasma Science, June 28-July 1, 2004, Baltimore, Maryland.

[33] Luis S. Caballero Bendixsen and Paul W Smith, “Very low impedance pulse forming line built from ferroelectric tiles” IEEE Pulsed Power Conference, pp 1333- 1336, Monterey (2005)

[34] J. Qian, R. P. Joshi, J. Kolb, and K. H. Schoenbach, J. Dickens, A. Neuber, M. Butcher, M. Cevallos, and H. Krompholz, E. Schamiloglu and J. Gaudet, "Microbubble-based model analysis of liquid breakdown initiation by a submicrosecond pulse" J. Appl. Phys. 97, 113304, 2005.

[35] P. Wijetunga, X. Gu, P. T. Vernier, A. Kuthi, M. Behrend, and M. A. Gundersen, "Electrical Modeling of Pulsed Power Systems for Biometical Applications," In Proc. of 14th IEEE International Pulsed Power Conference, 2003.

[36] M. Joler, C. Christodoulou, E. Schamiloglu, and J. Gaudet, “Modeling of a compact, portable transmission line for pulsed-power applications,” in Proc. 14th IEEE Int. Pulsed Power Conf., 2003, pp.253–256.

[37] Buttram M, “Some future directions for repetitive pulsed power”, IEEE Trans. Plasma Sci. 30 262 (2002)

[38] A. Guenther, M. Kristiansen and T. Martin, “Opening switches” Plenum, 1987.

[39] S T Pai, Qi Zhang “Introduction to High Power Pulse Technology” World Sci. press, 1995

[40] R A Cooper, J.B Ennis, F.W MacDougall and J F Bates, Progress in the reduction of Inductance in the standard 100 kV energy storage capacitor, in Proc. IEEE Pulsed power Conference, pp 409 - 412, (2001)

[41] Holystone, Capacitor Dielectric Comparison, Tecnical Note 3(http://www.holystonecaps. com /PDF/TechNotes/200712181125470.Capdielectriccomp3.pdf)

[42].WIMA, Characteristics of Metallized Film Capacitors in Comparison with Other Dielectrics (http://www.wima.de/EN/characteristics.htm)

[43] AVX, Dielectric Comparison Chart (http://www.avx.com/docs/techinfo/dielectr.pdf)

[44] S. P. Murarka, Moshe Eizenberg, A. K. Sinha: Interlayer dielectrics for semiconductor technologies. Academic Press, 2003,

[45] Marin S. Halper, James C. Ellenbogen (March 2006). "Supercapacitors: A Brief Overview" http://www.mitre.org/work/tech_papers/tech_papers_06/06_0667/06_0667.pdf)

[46] B.E. Conway,“ Electrochemical Supercapacitors: Scientific Fundamentals and Technological Applications. Springer, Berlin 1999

[47] Matthews, E.J., Kristiansen, M., Neuber, A.A, “Capacitor Evaluation for Compact Pulsed Power” IEEE Trans. Plasma Science, Vol 38, Issue 3, pp 500-508, Mar 2010

[48] S K Sharma, P Deb, R Shukla, P Banerjee, T Prabaharan, R Das, B Das, B Adhikary & A Shyam, “Design and modeling of capacitor bank power supply for fast charging”, Journal of Korean Physical Society, Volume 59, No. 6, 3468 (Dec 2011)

[49] T.Prabaharan, A Shyam, R Shukla, P Banerjee, S K Sharma, P Deb, R Verma, R Kumar, R Das, B Das & B Adhikary, “Development of 2.4ns rise time, 300kV, ~500MW compact co-axial

marx Generator", Indian Journal of Pure & Applied Physics Volume 49(1) pp 64-72 (Jan 2011).

[50] B Adhikary, A Shyam, R Shukla, S K Sharma, P Deb, P Banerjee, T Prabaharan, R Das, "Fast Marx generator for direct driving a Virtual Cathode Oscillator", Journal of Korean Physical Society, Volume 59, No. 6, 3476 (Dec 2011)

[51] K. K. Jain, D. Chennareddy, P. I. Jhon and Y. C. Saxena, "Design and performance of a Tesla transformer type relativistic electron beam generator ", Sadhana, 9, 19 (1986).

[52] I. Boscolo, M. Leo, A. Luches and L. Provenzano, "Electron beam production by a Tesla transformer accelerator", Review of Scientific Instruments, 48, 747 (1977).

[53] E.A Abramyan, V.V Borobev, A.A Egorov, V.A Elkin and A.G Ponomarenko, Initiation of discharge in a Mega Volts gas sparkgap by an electron beam, Instru. And Expt. Techn, pp130 (Jan-Feb 1971)

[54] E.A Abramyan, Transformer type accelerators for intense electron beam, IEEE Trans. on Nuclear Science, NS-18, 3, pp 447 (June 1971)

[55] P Sarkar, S W Braidwood, I R Smith, B M Novac, R A Miller and R M Craven, A compact battery powered half Megavolt transformer system for EMP generation, IEEE Trans. on Plasma Science, 34 (5), pp 1832 (2006)

[56] P. H. Ron, Proc. Workshop on Pulsed Power Technology, BARC, Mumbai, August 17-19 (1993).

[57] E. Kuffel and W.S. Zaengl, High Voltage Engineering-Fundamentals, Pergamon Press, 1984.

[58] Ravindra Arora & W. Mosch, High Voltage Insulation Engineering, New Age International, 2005.

[59] M.M Morcos, K. D Srivastava, "On the statistical testing of solid dielectrics", Proc. of IEEE

6th International Conference on Conduction and Breakdown in Solid Dielectrics, pp-514 (1998)

[60] D B Watson, W Heyes, K C Kao, J H Calderwood, Some aspects of dielectric breakdown of solids, IEEE Trans. on Electrical Insulation 1 (2) 1965

[61] Mario Cacciari, G Mazzanti and G C Montanari, Weibull statistics in short term dielectric breakdown of thin polyethylene films, IEEE Trans on Dielectric and Insulation, 1 pp 153-159 (1994)

[62] C Laurent, C Chauvet and J Berdala, The significance of the weibull threshold in short term breakdown statistics, IEEE Trans on Dielectric and Insulation, 1 pp 160-162 (1994)

[63] Hideo Hirose, Maximum likelihood estimation in the 3 parameter weibull distribution, IEEE Trans. on Dielectric and Insulation 3, (1), pp 43-55 (1996)

[64] R.Shukla. S.K.Sharma et. al. "Microwave emission from an AXIAL-Virtual Cathode Oscillator driven by a compact pulsed power source", Journal of Physics: Conference Series 390 (2012) 012033

[65] V. Y. Ushakov, "Insulation of High-Voltage Equipment", Berlin/Heidelberg: Springer-Verlag, 2004.

[66] M. Zahn, Y. Ohki, D. B. Fenneman, R. J. Gripshover, and V. J. Gehman, Jr., "Dielectric Properties of Water and Water/Ethylene Glycol Mixtures for Use in Pulsed Power System Design," Proc. of the IEEE, V. 74, pp. 1182-1221, 1986.

[67] R. E. Hebner, "Measurements of Electrical Breakdown in Liquids" Plenum,New York, 1988, pp. 519–537.

[68] J. C. Devins, S. J. Rzad, and R. J. Schwabe, "Breakdown and pre-breakdown phenomena in liquids," J. Appl. Phys., vol. 52, pp. 4531-4545, 1981

[69] T.H Martin, A nominal one megavolt pulsed power generator, IEEE Trans. NS-16, No.3, 59 (June, 1969)

[70] Y.P Singhal, B.S Narayan, K Nanu and P.H Ron, Development of a Blumlein based helical line storage elements, Rev. Sci. Instrum. 72, 1862 (2001)

[71] A.I Gerasimov,“Water as insulator in pulsed facilities”, Instruments and Experimental Techniques, Vol 48. No. 2, pp 141 – 167 (2005)

[72] Fennman D.B & Gripshover R.J, “Experiments on electrical breakdown in water in the microsecond regime” IEEE Trans. Plasma Sci. 8, 209–213. (1980)

[73] G J J Winands, Z. Liu, A. J M. Pemen, E J M. Heesch, and K. Yan,"Long lifetime, triggered, spark-gap switch for repetitive pulsed power applications", Rev.Sci.Inst.76, 85107 (2005)

[74] K. V. Nagesh, P. H. Ron, G. R. Nagabhushana, and R. S. Nema, “Over Recovery in Low Pressure Sparkgaps—Confirmation of Pressure Reduction in Over Recovery”, IEEE Trans. Plasma Sci, 27,6, 1159-1565 (1999)

[75] F Sabath, D V Giri, F Rachidi, A Kaelin. “Ultra-Wideband Short Pulse Electromagnetics 9”, Springer (2010)

[76] S.L Moran and L.W Hardsty, High repetation rate hydrogen spargap, IEEE Trans. On Electron Devices, Vol 38, No. 4, 1991, pp 726

[77] S.L Moran, M.G Grothaus and L.W Hardsy, Hydrogen spark switches for rep-rated accelerator, Proc. Inter. Conf. on High Power Particle Beams, Part,III, May 25-29, 1992, pp 726

[78] David Finkelstein, Philip Goldberg and Joshua Shuchatowitz, “High voltage impulse system”, Review of Scientific Instruments, vol. 37, no. 2, pp. 159-162, 1966.

[79] C.R.J. Hoffmann, “A Tesla transformer high-voltage generator”, Review of scientific instruments, vol. 46, no. 1, pp. 1-4, 1975.

[80] Marco Denicolai, “Tesla transformer for experimentation and research”, Thesis, Helsinki University of Technology, Finland, May 2001

[81] P. W. Smith, Transient Electronics: Pulsed Circuit Technology, ISBN: 978-0-471- 97773-5, John Wiley and Sons Ltd., England (2002).

[82] Rajesh Kumar, “High power Tesla driven miniaturized plasma opening switch” PhD Thesis, Loughborough University, U.K (2009)

[83] Noboru Miura and Koichi Nakao, “Computer analysis of mega gauss field generation by condenser bank discharge”, Japanese journal of applied physics, vol. 29, no. 8, 1580-1599, 1990.

[84] J. Luo “Novel insulation techniques for high-voltage pulse transformers”, PhD thesis, Loughborough University (2007)

[85] F.W Grover, Inductance calculation book, Dover Phoenix Edition (2004)

[86] T.H Martin, A.H Guenther and M. Kristiansen, “Overview -J.C Martin on pulsed power”, Springer-Verlag, New York (1996)

[87] School on Pulsed Power Technology (SPPT-2010), BARC, Mumbai (May 2011)

[88] David R. Linde, CRC Handbook of Chemistry and Physics (2009)

[89] Songsong Wang, Ting Shu, and Hanwu Yang, “A modularized pulse forming line using glass-ceramic slabs” Rev. Sci. Instrum. 83, 084703 (2012)

[90] L. Xia, H. Zhang, J. Shi, L. Zhang, J. Deng, H. Liu, and M. Cao, “A compact portable pulse forming line”, Rev. Sci. Instrum. 79, 086113 (2008).

[91] G. Zhao, R. Joshi, V. Lakdawala, E. Schamiloglu, and H. Hjalmarson, “TiO_2 breakdown under pulsed condition”J. Appl. Phys. 101, 026110 (2007).

[92] M. T. Domonkos, P. J. Turchi, J. V. Parker, T. C. Grabowski, C. W. Gregg, C. E. Roth, and K. Slenes, “A modularized pulse forming line using glass ceramic slabs”, in Proceedings of the

15th IEEE International Pulsed Power Conference, Monterey, CA, 2005, p. 1322.

[93] Junjie Gao, Zhuo Xu, Fei Li, Changhui Zhang, Yi Liu, Gaomin Liu and Hongliang He, "The hydrostatic pressure dependence of the piezoelectric properties for the barium titanate and lead titanate crystals: Thermodynamic analysis" Journal of Applied Physics, 109, 114111 (2011)

[94] L. L. Hench and L. K. West, "Principles of Electronic Ceramics", (John Wiley & Sons Inc., 1990),

[95] ASTM D 1418-79

[96] A. R. Von Hippel, "Dielectric Materials and Applications", Cambridge, MA: MIT Press, 1954, pp. 361-362.

[97] H. Yamada, 5. Sakamoto, and Y. Nakao, "Studies of the breakdown processes in dielectric liquids using high speed photography," Journal of Electrostatics, vol. 7, pp. 155-1 68, 1979.

[98] LIU Zhenxiang, Z HANG Jiande, "Investigation of Helical Pulse Forming Line", Plasma Science & Technology, Vo1.8, No.5, pp 596 - 599 (Sept. 2006)

[99] Morcos, M.M.; Cherukupalli, S.E. "Review of statistical testing of solid insulating materials", Proceedings of the 3rd International Conference on Conduction and Breakdown in Solid Dielectrics, 574 – 581 (1989)

[100] R Shukla, P Banerjee, S K Sharma, R Das, P Deb, T Prabaharan, B Das, B Adhikary, R Verma & A Shyam, "Compact high voltage pulse transformer made using a capacitor bank assembled in the shape of primary", Review of Scientific Instruments, 82, 106103 (2011)

[101] C.R Wilson, M. M Turner and P W smith, "Electromagnetic shock-wave generation in a lumped element delay line containing nonlinear ferroelectric capacitors" IEEE Trans. Electron Devices 38, 767 (1991)

[102] Xiaodong Chen, Guiqin Wang, Yuping, Duan and Shunhua Liu, "Electromagnetic characteristics of barium titanate/epoxide resin composites in X and Ku bands",Journal of Alloys and Compounds 453, 433 (2008)

[103] J.C.Burfoot and G.W.Taylor, "Polar dielectrics and their applications" Macmillan, 1979.

[104] J.D. Winefordner, I.B. Gornushkin, T. Correll et. al., "Comparing several atomic spectrometric methods to the super stars: special emphasis on laser induced breakdown spectrometry, LIBS, a future super star", J. Anal. At. Spectrom. 19 (2004) 1061–1083.

[105] P.A. Benedetti, G. Cristoforetti, S. Legnaioli et. al. "Effect of laser pulse energies in laser induced breakdown spectroscopy in double-pulse configuration", Spectrochim. Acta Part B 60 (2005) 1392–1401.

[106] XIA Lian-Sheng, LI Jin, ZHANG Huang et. al. "Experimental Research on Double Pulsed Relativistic Electron Beams Emission from Velvet", high energy physics and nuclear physics, Vol 31, Issue 7, 674-677, July 2007

[107] M H R Hutchinson and C D P Levy, "A modified, scalable, coaxial diode for electron-beam pumped gas lasers" J. Phys. D: Appl. Phys. 15 431(1982)

[108] Schneider L, Reed K, Harjes H, Pena G, Martinez L, Harden M, presented at 12th IEEE International Pulsed Power Conference, Volume 1, pp 523 - 527 (1999)

9. Appendix - 1

1.1 Self inductance of circular sheet of finite thickness

The self inductance of a circular sheet with finite thickness, and assuming that the current is flowing along the circular ribbon of radius “a” and axial length “t” as shown in Figure 1.

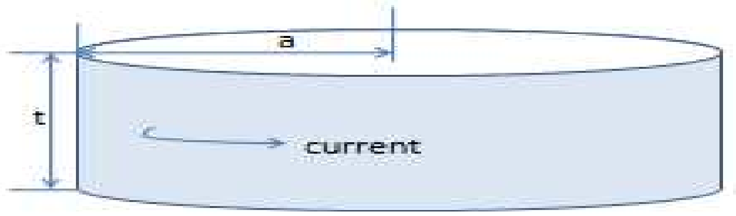

Figure 1. Circular sheet of finite thickness

and t << a

$$L = a\mu_0(0.3862944 + 0.17308q^2 - \ln q - 0{,}253863q^2 \ln q) \quad (1)$$

Where

$$q = {}^{t}/_{2a} \quad (2)$$

1.2 Self Inductance of circular section of finite radius

The self inductance of a single loop with a circular cross section of finite radius r_c (Figure 2) is

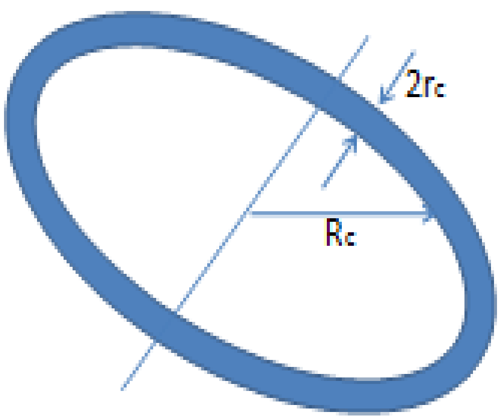

Figure 2 Circular cross section wire with finite radius

$$L_c = \mu_0 R_c \left(ln \frac{4\pi R_c}{2r_c} \right) - \frac{3}{4} \quad (3)$$

1.3 Mutual Inductance between two parallel and coaxial loops

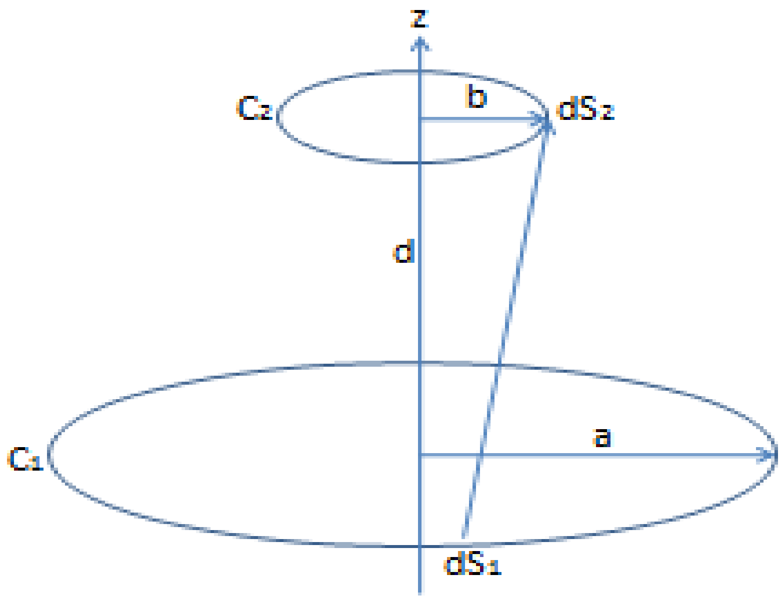

Figure 3 Schematic representations of two loops

The mutual inductance M between the two loops C_1 and C_2 shown in Figure 3 having radii of a and b respectively can be written

$$M = \frac{\mu_0}{4\pi}\iint \frac{dS_1 dS_2}{r}$$

Where dS_1 and dS_2 are the differential vectors for each loop and r is the vector shown in figure then M may be expresses in the form

$$M = \mu_0 \left\{-\sqrt{(a+b)^2 + d^2}E\left(\frac{4ab}{(a+b)^2 + d^2}\right) + \frac{a^2+b^2+d^2}{\sqrt{(a+b)^2+d^2}}K\left(\frac{4ab}{(a+b)^2+d^2}\right)\right\} \tag{4}$$

Where d is the axial distance between the two loops and E and K are the elliptical integrals defined as

$$E(k^2) = \int_0^{\frac{\pi}{2}} \sqrt{1 - k^2 sin^2\theta}\, d\theta \tag{5}$$

$$K(k^2) = \int_0^{\frac{\pi}{2}} \frac{d\theta}{\sqrt{1-k^2 sin^2\theta}} \tag{6}$$

The above equations will be used to calculate the inductances and mutual inductance of the transformer.

1.4 Equation used in filamentary modelling of conical pulse transformer

The primary sheet and conical secondary winding is shown in Figure 4 and the pulse transformer parameters are defined in Table 1. The primary sheet and secondary turns of the transformer are divided into filaments in the direction of current path to calculate their self inductances and mutual inductance.

Table 1: Parameters defined for pulse transformer

Thickness of primary sheet	tp
Length of primary sheet	lp
Internal radius of primary	rps
Secondary wire diameter	ts
Lowest radius of secondary	rsNI
Highest radius of secondary	rsNO
Pitch of secondary	P
Total numbers of secondary turns	ns

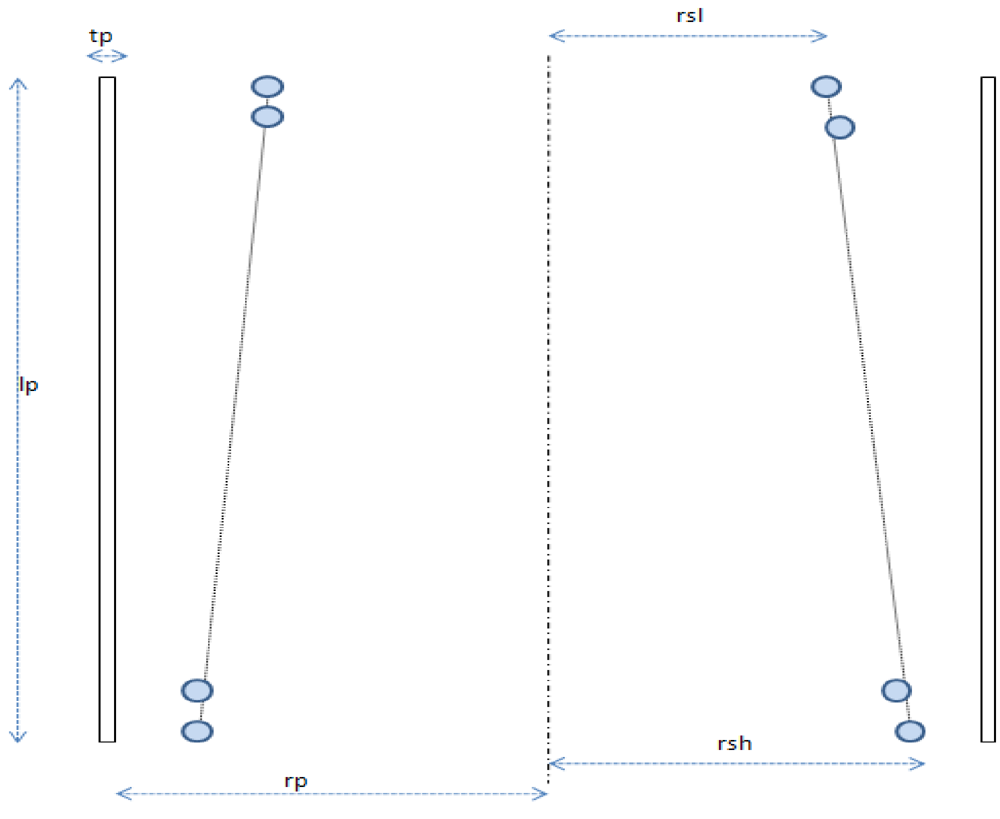

Figure 4. Constants defined for calculation

The primary and secondary windings are divided into the filament as shown in Figure 5. The primary winding is divided into *np x mp* parts (*np* rows and *mp* columns) and each secondary winding is treated as a separate single turn winding for simplicity.

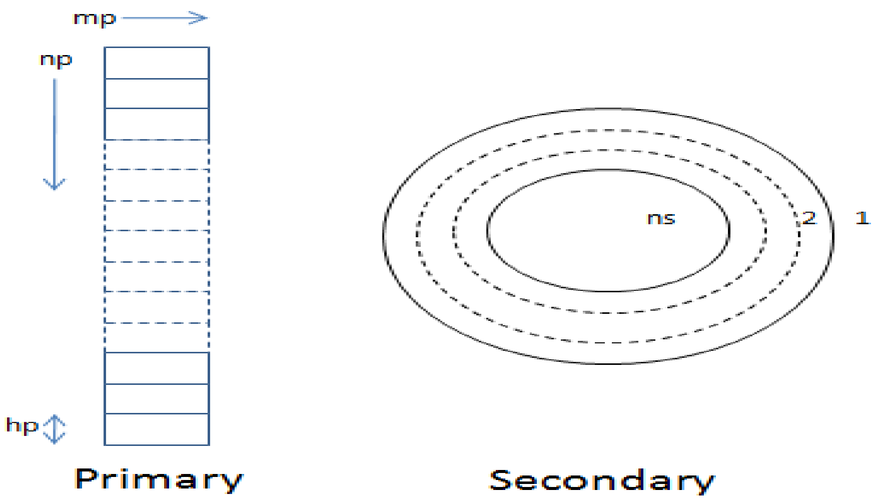

Figure 5 Filaments used to calculate pulse transformer inductance

The primary is divided into the np x mp filaments shown in Figure 5, where np=100 and *mp = 1* for simplicity.

The total no of filaments in the primary is therefore

N p = np x mp

The secondary is divided into 28 parts (each turns is as one filament), *ns = 28*

Total numbers of secondary filament is

Ns = ns

The total no of filaments is

Nt =N p+N s

The following equations are used in matlab programming for the calculation of the self and mutual inductances and the parameters are defined in Table 1.

The taper ratio (*t_ratio*) of the secondary is defined as

$$t\_ratio = \frac{rsNO - rsNI}{ns - a}$$

where rsh and rsl are defined in the Figure 4 and Table 1.

The radius of any secondary turn can be defined as

rsN(nsind): = rsNO –*t_ratio*(nsind - 1)

The following expressions are defined for the filaments positions in the primary and secondary. If the filaments are described as columns and rows, then any filament position of column in primary is defined as

$$wchcolp(i) \coloneqq floor\left(\frac{i-1}{n_p}\right) + 1$$

any filament position of column in secondary is defined as

$$wchcols(i) := floor\left(\frac{i-1}{n_s}\right)+1$$

any filament position of rows in primary is defined as

$$wchrwp(i) := mod(i-1, np)+1$$

any filament position of rows in secondary is defined as

$$wchrws(i) := mod(i-1, ns)+1$$

The distance between any two primary filaments defined as

$$distp(i,j) := wchrwp(i) - wchrwp(j) . hp$$

The distance between any two secondary filaments are defined as

$$dists(i,j) := wchrws(i) - wchrws(j) . p$$

The distance between any primary and any secondary filaments is defined as.

$$distps(i,j) := \left[\left|wchrwp(i-1).hp+\frac{hp}{2}-(wchrws(j-1).p+1.5\ x\ 10^{-3})\right|\right]$$

The radius of any primary filament is given by

$$rp(i) := rpr+\frac{tp.wchcolp(i)}{2.mp}$$

The following variables are defined as required by the equation (1) to get the inductance of the coil. Values of q as in equation (2)

For the primary

$$qp(i) := \frac{hp}{2.rp(i)}$$

For the secondary

$$qs(i) := \frac{p}{2.rsN(i)}$$

Variables for the elliptical function defined as in equation (4)

For the primary only

$$kp(i,j) := \sqrt{\frac{4.rp(i).rp(j)}{(rp(i)+rp(j))^2+distp(i,j)^2}}$$

For the primary and secondary (combined to provide the mutual inductance between them)

$$kps(i,j) := \sqrt{\frac{4.rp(i).rsN(j)}{(rp(i)+rsN(j))^2+distps(i,j)^2}}$$

For the secondary only

$$ks(i,j) := \sqrt{\frac{4.rsN(i).rsN(j)}{(rsN(i) + rsN(j))^2 + dists(i,j)^2}}$$

Inductance formed by the primary filaments as from equation (1)

$$Lp(i) := \mu_0.rp(i).(0.3862944 + 0.17308qp(i)^2 - \ln(qp(i)) - 0.253863qp(i)^2\ln(qp(i)))$$

Inductance formed by the secondary filaments as from equation (1)

$$Lsjj(i) := \mu_0.rsN(i).(0.3862944 + 0.17308qs(i)^2 - \ln(qs(i)) - 0.253863qs(i)^2\ln(qs(i)))$$

Inductance of any secondary winding as from equation (3)

$$Ls(i) := \mu_0 rsN(i)\left(ln\frac{4\pi rsN(i)}{ts}\right) - \frac{3}{4}$$

Inductance of different filaments of primary and their interaction as from equation (4)

$$Mp(i,j) := \begin{cases} \left[2.\mu_0.kpi,j^{-1}\sqrt{rp(i).rp(j)}\left[\left(1-\frac{1}{2}kp(i,j)^2\right)LegendreKc\big(kp(i,j)\big) - LegendreEc(kp(i,j))\right]\right] & if\ i \neq j \\ Lp(i) & \end{cases}$$

Inductance of different filaments of secondary and their interaction as from equation (4)

$$Ms(i,j) := \begin{cases} \left[2.\mu_0.ks(i,j)^{-1}\sqrt{rsN(i).rsN(j)}\left[\left(1-\frac{1}{2}ks(i,j)^2\right)LegendreKc\big(ks(i,j)\big) - LegendreEc(ks(i,j))\right]\right] & if\ i \neq j \\ Ls(i) & \end{cases}$$

Mutual inductance between primary and secondary filaments

$$Mps(i,j) := 2.\mu_0.kps(i,j)^{-1}\sqrt{rp(i).rsN(j)}\left[\left(1-\frac{1}{2}kps(i,j)^2\right)LegendreKc\big(kps(i,j)\big) - LegendreEc(kps(i,j))\right]$$

The above parameters are used in solving equations (3.16, 3.17 and 3.18) for calculation of primary inductance, secondary inductance and mutual inductance between the winding.

10. Appendix – 2

Specification of standard voltage divider

Model Number	**PVM-5**	**VD-100**
Max DC/Pulsed Voltage (kV)	60 / 100	100 / 200
Max Frequency (MHz)	90	20
Cable Impedance (ohms)	50	50
DC – 2 Hz Accuracy	< 0.1%	< 0.1%
2 Hz – 200 Hz Accuracy	< 1.5%	1%
200 Hz – 1 MHz	< 2.5%	1%
> 1 MHz Accuracy	< 4%	2%
Input R/C (Megohm/pf)	600 / 8	1400 / 20
Cable length (ft/m)	30 / 9	30 / 9
Standard Divider ratio	1000 : 1	10000 : 1
Length (inches/cm)	19 / 45	23 / 59